UNIVERSITY OF SOUTHAMPTON

FACULTY OF NATURAL AND ENVIRONMENTAL SCIENCES

School of Ocean and Earth Science

Fluorescence on Coral Reefs

by

Elena Bollati

Thesis for the degree of Doctor of Philosophy

April 2018

A Claudia e Gabriella,

Che mi hanno insegnato ad imparare

E a non temere le alghe ballerine

To Claudia and Gabriella,

Who taught me to learn

And not to fear the dancing seaweeds

UNIVERSITY OF SOUTHAMPTON

ABSTRACT

FACULTY OF NATURAL AND ENVIRONMENTAL SCIENCES

Ocean and Earth Sciences

Thesis for the degree of Doctor of Philosophy

FLUORESCENCE ON CORAL REEFS

by Elena Bollati

Coral reefs are highly biodiverse ecosystems and provide vital resources for the human population. Due to increasing pressure by climate change and local stressors, these ecosystems currently face a global crisis. The development of tools to monitor how coral reefs respond to environmental change is a key aspect of the conservation of their biodiversity and resources. A number of reef organisms produce fluorescent molecules, including photosynthetic pigments and green fluorescent protein (GFP)-like pigments found in Anthozoa. These pigments are responsive to environmental conditions and can be optically monitored *in vivo*, making them a promising tool to investigate organism- and community-level processes on coral reefs. In this thesis, the fundamental principles and technological developments necessary for the application of fluorescence as a biomarker are explored. First, the mechanisms regulating coral fluorescence are considered for two functionally and biochemically distinct groups of GFP-like proteins. In mesophotic and depth-generalist symbiotic corals, incomplete light-driven maturation of the red GFP-like protein pool is shown to determine the spectrum of fluorescence emission. A role of this mechanism in adaptation to the reduced mesophotic light spectrum is discussed. In corals from shallow water environments, enhancement of internal light fluxes due to reduced absorption by symbiont pigments during bleaching is shown to induce expression of GFP-like proteins. High-level expression of these pigments in bleached tissue is shown to promote recovery of the symbiotic algae complement after a stress event. Second, a novel approach to fluorescence imaging for coral reef surveys is presented. The method enables automatic classification of reef benthic organisms based on the intensity of fluorescent signal in different excitation and emission bands. These findings demonstrate the potential of fluorescence as an *in vivo* marker for physiological and ecological studies of coral reef organisms, contributing to ongoing efforts to monitor and preserve the health of these ecosystems.

Table of Contents

Table of Tables

Table of Figures

Academic Thesis: Declaration Of Authorship

I, Elena Bollati

declare that this thesis and the work presented in it are my own and has been generated by me as the result of my own original research.

Fluorescence on Coral Reefs

I confirm that:

1. This work was done wholly or mainly while in candidature for a research degree at this University;
2. Where any part of this thesis has previously been submitted for a degree or any other qualification at this University or any other institution, this has been clearly stated;
3. Where I have consulted the published work of others, this is always clearly attributed;
4. Where I have quoted from the work of others, the source is always given. With the exception of such quotations, this thesis is entirely my own work;
5. I have acknowledged all main sources of help;
6. Where the thesis is based on work done by myself jointly with others, I have made clear exactly what was done by others and what I have contributed myself;
7. Parts of this work have been published as:

   Bollati, E., Plimmer, D., D'Angelo, C. and Wiedenmann, J, 2017. FRET-mediated long-range wavelength transformation by photoconvertible fluorescent proteins as an efficient mechanism to generate orange-red light in symbiotic deep water corals. *International Journal of Molecular Sciences* **18**(7):1174.

Signed: .....

Date: .....

Acknowledgements

First and foremost, I would like to thank Jörg for being my main supervisor and mentor all these years. I have learnt an incredible amount from you, about how to be a good scientist and a good teacher. Thank you for always being so patient, and for encouraging me to do better and think bigger. Cecilia, thank you for everything you have taught me, in the lab and out. Your knowledge and hard work have been a great source of inspiration for me every day.

Thank you to all the fellow CRL students and postdocs who shared this experience with me over the years. I am especially grateful to Nina, Cath, Adam and Ben, whose help, knowledge and support got me through the long lab days, and to Rachel, whose incredibly hard work contributed to this thesis. I would like to thank Robbie Robinson for always fixing my aquarium problems, John Gittins for his help in the lab, and Graham Blythe and Neil Jenkinson for assisting me with electrical work. I also thank Michael Barrett for his role in my CASE studentship.

I thank Davey Kline and Greg Mitchell for welcoming me in their labs at SIO and making sure I had an amazing experience during my placement, and Natalie for welcoming me into her home.

I would also like to acknowledge Mark Moore for being supportive and helpful as my panel chair, and Lawrence Hawkins for his advice and support since I was a first-year undergraduate student.

To Clarke and his office friends Abbie, Charlotte, Claire, Clare, Cobain, David, Katie and Maarten, thanks for going through this PhD together. It would have been impossible without your help, the laughs, and the endless supply of caffeine and chocolate digestives.

I would like to thank my family, especially my mum, for always believing in me and supporting me from far away.

Finally, during my time as a PhD student I had to face a great personal challenge. I am grateful to all the people who have helped and supported me through it. Above all, Katie, I never would have made it without you. Thank you for your friendship, your wisdom, and for always holding my hand while I dealt with the unicorns and dragons of life.

Definitions and Abbreviations

abs	Absorbance
a.u.	Arbitrary units
ANOVA	Analysis of variance
B	Bleached
BCA	Bicinchoninic acid assay
BSA	Bovine serum albumine
c.i.	Confidence intervals
CCA	Crustose coralline algae
CCD	Charge-coupled device
CFP	Cyan fluorescent protein
CMOS	Complementary metal-oxide-semiconductor
conc	Concentration
CP	Chromoprotein
DIN	Dissolved inorganic nitrogen
em	Emission
ex	Excitation
FP	Fluorescent protein
FRET	Förster Resonance Energy Transfer
FWHM	Full width at half maximum
GFP	Green fluorescent protein
H	Healthy
HI	Healthy inner region
HM	Healthy margin
HN/HP	High nitrate / high phosphate
HN/LP	High nitrate / low phosphate
HSD	Honestly significant difference
IMAC	Immobilised metal ion affinity chromatography
LED	Light-emitting diode

MH	Metal halide
PAR	Photosynthetically active radiation
PBS	Phosphate buffered saline
pcRFP	Photoconvertible red fluorescent protein
PE	Phycoerythrin
PSII	Photosystem II
R	Reflectance
RFP	Red fluorescent protein
RI	Recovering inner region
RM	Repeated measures
ROS	Reactive oxygen species
s.d.	Standard deviation
UV	Ultra-violet

Chapter 1 Introduction

1.1 Background

1.1.1 Coral reefs in the Anthropocene

Coral reefs are one of the most productive ecosystems on Earth. The biodiversity inhabiting the three-dimensional reef structure, built by scleractinian corals and other calcifying organisms over geological timescales, is greater than anywhere else in the ocean (Knowlton, 2010). Such abundance of life is a vital resource for the human population, particularly in developing coastal and island nations (Burke *et al.*, 2011). Coral reefs host about a quarter of all marine fish species (Spalding *et al.*, 2001); the fisheries they support, largely small scale or subsistence activities, provide the primary income for six million fishers and their families (Teh *et al.*, 2013; Kittinger *et al.*, 2015). Reefs provide a surface for human settlement by building atolls and islands, and they protect coastal communities from waves, storms and erosion (Ferrario *et al.*, 2014). Reef organisms are a source of valuable biological compounds, such as toxins and fluorophores, which are widely employed in biomedical research (Gayler *et al.*, 2005; Wiedenmann *et al.*, 2009; Mehbub *et al.*, 2014). In 2017, the revenue derived from coral reefs via tourism alone was estimated at US$ 36 billion (Spalding *et al.*, 2017).

This thriving ecosystem is built on the symbiotic association between coral polyps and *Symbiodinium* sp. dinoflagellates, or zooxanthellae (Dubinsky and Jokiel, 1994), which supply part of the host's metabolic requirements through translocation of photosynthates (Muscatine, 1990). This relationship allows the coral holobiont to survive in nutrient-depleted waters, and to build the structural foundation of the ecosystem through biological deposition of the calcium carbonate skeleton. The geographical distribution of warm water coral reefs is determined by the environmental parameters required to support this symbiotic relationship, including availability of a hard substrate for polyp settlement, sufficient aragonite saturation, and light to sustain photosynthesis (Kleypas *et al.*, 1999a; Muir *et al.*, 2015); coral reefs are thus predominantly found in shallow, coastal, tropical waters, where centuries of human activity have placed these ecosystems under great pressure (Jackson *et al.*, 2001; Pandolfi *et al.*, 2003). Anthropogenic pressure has increased dramatically over the past century, when the industrial release of CO_2 into the atmosphere has caused ocean temperatures to rise. Positive temperature anomalies are known to trigger the breakdown of the coral symbiosis, a process known as coral bleaching. Bleaching occurs as a response to the increased production of reactive oxygen species (ROS) by symbionts under stress (Lesser, 1997). The exact mechanism through

which heat stress disrupts symbiont photosynthesis has not been fully elucidated; the D1 protein of photosystem II (PSII), the thylakoid membranes and the enzyme Rubisco have been indicated as sites of primary damage (Jones *et al.*, 1998; Warner *et al.*, 1999; Tchernov *et al.*, 2004). In order to prevent the accumulation of ROS and consequent host cellular damage, symbiont cells are degraded or expelled from the holobiont (Weis, 2008). The symbiont complement can be restored after bleaching, however mortality results from reduced translocation if the stress is prolonged (Williams and Bunkley-Williams, 1990). As a result of anthropogenic climate change, the incidence of bleaching on a global scale is on the rise, and the most severe series of mass bleaching events on record was reported in 2016-2017 (Hughes *et al.*, 2017, 2018).

Repeated mass bleaching events, combined with continued overexploitation, have induced dramatic changes in the ecology of coral reefs; phase shifts towards macroalgae-dominated systems (Hughes *et al.*, 2007), changes in the size structure of fish communities (Graham *et al.*, 2007), and shortening of the food webs (Hempson *et al.*, 2017) have been documented. Eutrophication of coastal regions caused by human activity further exacerbates these processes, increasing the susceptibility of reefs to bleaching events and phase shifts (Fabricius, 2005; Wiedenmann *et al.*, 2013; D'Angelo and Wiedenmann, 2014). Other threats to the structural integrity and ecological viability of reefs include destructive fishing methods (McManus *et al.*, 1997), introduction of invasive species (Albins and Hixon, 2011), and the decrease in calcification caused by ocean acidification (Kleypas *et al.*, 1999b; Orr *et al.*, 2005; De'ath *et al.*, 2009). As a result of these combined stressors, coral cover in the world's oceans is in decline (Gardner *et al.*, 2003; Bruno and Selig, 2007; De'ath *et al.*, 2012).

In the years to come, it is predicted that coral reefs will undergo an extreme transformation. Even under milder climate change scenarios, it has been suggested that most coral reefs could be eliminated by 2050 (Hoegh-Guldberg *et al.*, 2017). Evolutionary evidence shows that the coral holobiont has the potential to adapt, but that present-day biodiversity is key for future adaptation (Hume *et al.*, 2016). The preservation of biodiversity and of the benefits we derive from reefs will rely heavily on the actions of the global community. The role of scientific research during this process is to provide the tools to understand, monitor and manage these changing ecosystems and their valuable resources. Despite attracting considerable scientific attention, many processes underlying the response of reefs to environmental pressure remain poorly understood. In guiding conservation and restoration efforts, knowledge of what mechanisms enable reef-building corals to adapt to a changing environment, and of how the environment in turn affects these mechanisms, is paramount.

1.1.2 Biomarkers of change

Environmental change affects coral reefs on all levels of biological complexity. Ecosystem and community-level indicators have long been employed to study coral reefs, and to monitor their response to change through time (Jameson *et al.*, 1998; Fisher *et al.*, 2008; Bradley *et al.*, 2009). Early techniques based on *in situ* assessments of community composition (Risk, 1972) have evolved into global endeavours, also thanks to the contribution of citizen science (Hodgson, 1999). Advances in remote sensing technology have enabled monitoring of environmental stress and of change at the ecosystem level with global coverage and fine temporal resolution (Mumby *et al.*, 2004; Liu *et al.*, 2014). These methods rely on knowledge of the optical properties of the water column, atmosphere and reef organisms to provide data on both abiotic parameters and community composition (Hedley and Mumby, 2002; Mumby *et al.*, 2004). Other tools to understand and monitor change rely on particular taxa in order to identify processes that might be underway for the entire ecosystem. For example, abundance and diversity of groups that are sensitive to change (Crosby and Reese, 1996) or that vary along gradients of disturbance (Fabricius *et al.*, 2005) have been employed to assess reef health and detect environmental pressure. Processes such as coral bleaching, disease, or recruitment, which directly affect ecosystem function, are also used as indicators for monitoring purposes (Jameson *et al.*, 1998; Cooper *et al.*, 2009).

As well as monitoring the ecological effects of environmental change, however, it is important to consider how change affects the physiology of organisms or groups of organisms. Organism-level physiological responses precede and underlie community or ecosystem-level change; knowledge of these processes is not only necessary to fully understand ecosystem-level indicators, it is also likely to yield new tools for the assessment of change on coral reefs (Downs *et al.*, 2005). Physiological responses of organisms to environmental change can in some cases be detected almost immediately (Cooper *et al.*, 2009), and at sublethal levels of stress (Downs *et al.*, 2012). Indicators of organism-level response range from parameters of overall physiological functioning, such as photosynthetic efficiency or respiration rates, to measurements of cellular-level mechanisms that involve assaying particular proteins or probing gene expression (Edge *et al.*, 2005; Van Oppen and Gates, 2006; Cooper *et al.*, 2009). One great power of these biomarkers is that, differently from many ecosystem-level indicators, they are based on a mechanistic relationship between the environmental condition and the measured response, thus allowing the application of diagnostic approaches to environmental monitoring (Downs *et al.*, 2005). However, measurements at this level often require destructive sampling and specialised equipment, with the result that the scale of application is limited.

As well as being a tool in environmental monitoring, biomarkers of different levels of physiological response are also required for use in experimental studies that aim to understand the mechanisms of adaptation and acclimation of reef organisms; these studies are key to predict how future change will affect organisms, and indirectly communities and ecosystems. The development of tools to study organism response to environmental change is thus an integral part of coral reef research.

1.1.3 Fluorescence as a biomarker

In the search for biomarkers of the coral host response to environmental change, some attention has been given to a group of proteins homologous to the Green Fluorescent Protein (GFP) first described from the jellyfish *Aequorea victoria* (Shimomura *et al.*, 1962; D'Angelo *et al.*, 2008; Smith-Keune and Dove, 2008). Many GFP-like proteins found in reef-building corals emit bright cyan, green or orange fluorescence when illuminated by light in the blue or green range (Alieva *et al.*, 2008). The fluorescence signal can be easily monitored *in vivo* with spectroscopic or imaging techniques; therefore, GFP-like proteins expressed in recombinant organisms have become invaluable markers in biomedical imaging of living cells (Chishima *et al.*, 1997; Giepmans *et al.*, 2006; Wiedenmann *et al.*, 2009). In reef-building corals, the expression of these proteins has been shown to vary with light intensity (D'Angelo *et al.*, 2008), during heat stress (Smith-Keune and Dove, 2008; Hume *et al.*, 2013), and with immune response (D'Angelo *et al.*, 2012). Thus, it has been suggested that GFP-like proteins could provide a non-invasive biomarker of physiological processes in corals (Zawada and Jaffe, 2003; D'Angelo *et al.*, 2008; Smith-Keune and Dove, 2008), allowing fine temporal resolution monitoring without the need for a large sample size. However, practical application of naturally-occurring GFP-like proteins as biomarkers has been hindered by a number of issues. First, although studies have shown an important ecophysiological role of these proteins in regulating light fluxes inside coral colonies (Salih *et al.*, 2000; Smith *et al.*, 2013, 2017; Lyndby *et al.*, 2016), the mechanisms involved are diverse and not yet fully understood. Second, their regulation in response to environmental conditions exhibits variability within the group (Leutenegger *et al.*, 2007a; D'Angelo *et al.*, 2008). Third, corals exhibit a great degree of intraspecific polymorphism regarding the complement of GFP-like proteins expressed and the maximum expression level (Wiedenmann *et al.*, 1999; Gittins *et al.*, 2015). A more comprehensive understanding of the mechanisms underlying the function and regulation of GFP-like proteins is thus a pre-requisite to any further development of host fluorescence-based biomarkers in corals.

While Anthozoa are the main group of reef organisms expressing GFP-like proteins, the photosynthetic pigments found in algae, including coral symbionts, also emit fluorescence

under violet, blue or green light (Kautsky and Hirsch, 1931; French and Young, 1952). Application of a coral fluorescence biomarker approach *in situ* thus relies on the ability to discriminate GFP-like proteins from other fluorescent pigments. Chlorophyll fluorescence is already widely applied as a tool to study the physiological response of photosynthetic organisms to environmental conditions, including on coral reefs (Falkowski and Kiefer, 1985; Warner *et al.*, 2010). As well as organism-level response, the fluorescence signatures produced by different pigments can be used to characterise the composition of marine communities (Seppala and Balode, 1998; Suggett *et al.*, 2009; Beijbom *et al.*, 2016). Advances in the application of coral host fluorescence as a biomarker will therefore not only facilitate physiological studies and organism-level environmental monitoring, but will also be of use in community-level ecosystem assessment.

1.2 Thesis overview

1.2.1 Thesis aims

The aim of this thesis is to develop the use of fluorescence as a tool to monitor coral reef organisms and communities. Downs *et al.* (2005) describe the process required for the development of assessment tools to be used in diagnostic approaches to coral reef monitoring as follows:

> "Advancing a new paradigm for assessing coral-reef condition that includes organismal- and environmental-based metrics will require progress in three areas: (1) knowledge of fundamental processes, (2) technology development and application, and (3) validation of the concepts and technologies […] for real world situations."

Advancing areas 1 and 2 in the context of coral reef fluorescence is thus the focus of this thesis. More specifically, this thesis aims to advance our *(1) knowledge of fundamental processes* by exploring the function and regulation of two biochemically and ecologically distinct groups of coral GFP-like proteins. In order to complement the concise background information provided in each research chapter, a summary of the current literature regarding the biochemical basis, the environmental regulation and the ecophysiological role of GFP-like proteins in reef building corals is provided in Chapter 2.

Chapter 3 explores the function and regulation of a group of red fluorescent proteins that are often found in corals from low-light environments, including mesophotic reefs (Alieva *et al.*, 2008; Eyal *et al.*, 2015). Expression of these proteins is independent of light intensity (Leutenegger *et al.*, 2007a), but maturation of the red-emitting chromophore from an immature green form is dependent on the presence of wavelengths ~400 nm (Ando *et al.*, 2002). However, the mesophotic light spectrum is predominantly blue-green, and the ~400 nm band reduces with depth. Chapter 3 therefore addresses the following research question:

> **Q1. How do corals maintain red fluorescence in the mesophotic light environment?**

Next, the chapter examines the ecophysiological relevance of the green-to-red photoconversion mechanism. In solution, partially converted tetramers of these proteins exhibit efficient Förster Resonance Energy Transfer (FRET) between green and red subunits (Wiedenmann *et al.*, 2004a); however, this mechanism has not been studied in live corals. The following research question is therefore addressed:

Q2. Is intratetrameric FRET part of the function of GFP-like proteins in mesophotic corals?

Chapter 4 considers a second group of GFP-like proteins, which are found in corals from shallow water environments and are transcriptionally regulated by light intensity in the blue spectral range (D'Angelo *et al.*, 2008). As these protein are responsive to changes in environmental conditions, they have been considered as a potential non-invasive biomarker of coral health (D'Angelo *et al.*, 2008, 2012; Smith-Keune and Dove, 2008). However, the relationship between protein concentration and optical measurements of fluorescence has been observed to decouple during bleaching (Roth and Deheyn, 2013), thus hindering biomarker application. The following research question is therefore addressed:

Q3. How does bleaching affect the regulation of GFP-like proteins?

The chapter then explores the function of these proteins during coral bleaching and recovery, posing the following research question:

Q4. Are GFP-like proteins involved in coral recovery after bleaching?

This thesis also aims to contribute to *(2) technology development and application* of fluorescence as a tool to survey coral reefs at the community level. Fluorescence imaging has been shown to facilitate automatic annotation of survey images, particularly discrimination between coral, algae and abiotic substrates (Mazel *et al.*, 2003a; Beijbom *et al.*, 2016). Chapter 5 presents the conceptual development of a novel underwater imaging system, which uses excitation of fluorescent pigments in two distinct bands in order to classify benthic organisms. This approach aims to provide discrimination between functionally distinct groups of algae, which often present a challenge to automatic and manual annotation (Beijbom *et al.*, 2015). The following research question is therefore addressed:

Q5. Is multi-excitation fluorescence imaging a suitable approach to automatic classification of coral reef communities?

1.2.2 Thesis structure

The experimental work undertaken for this thesis is presented in chapters 3-5, which are written as research manuscripts and are at different stages of the publication process at the time of writing. For each chapter, the sections below provide an outline of the experimental approach, the author contributions, and the publication status.

1.2.2.1 Chapter 3. FRET-mediated long-range wavelength transformation by photoconvertible fluorescent proteins as an efficient mechanism to generate orange-red light in symbiotic deep water corals

This study used an *in vivo* and *in vitro* spectroscopic approach to investigate the function and regulation of red fluorescence in deep-water corals.

To address **Q1**, red and green fluorescence of live coral colonies was monitored during long-term acclimation to different spectral light regimes, equivalent to the photon irradiance in the photoconversion action spectrum experienced i) in the euphotic reef zone ii) in the mesophotic reef zone iii) beyond the lower depth distribution limit of symbiotic corals. Recombinantly produced proteins were then exposed to a spectral gradient equivalent to what measured in the Red Sea, in order to investigate how the attenuation of ~400 nm light by the water column affects the photoconversion rate.

To address **Q2**, measurements of red and green fluorescence were used to calculate the FRET-derived fluorescence emission in a colony undergoing photoconversion, and to establish the existence of FRET *in vivo*. The role of FRET in adaptation to the mesophotic light spectrum was then assessed in comparative spectroscopic analysis of recombinant proteins, where the potential to transform blue-green wavelengths into orange-red ones was assessed for proteins with partially converted, fully green or fully red tetramers.

This chapter has been published as:

> Bollati, E., Plimmer, D., D'Angelo, C. and Wiedenmann, J, 2017. FRET-mediated long-range wavelength transformation by photoconvertible fluorescent proteins as an efficient mechanism to generate orange-red light in symbiotic deep water corals. *International Journal of Molecular Sciences* **18**(7):1174.

E.B., C.D.A., and J.W. designed the study and developed the methodology. D.P. collected the *in vivo* fluorescence data as part of a MSci research project supervised by E.B. and J.W.. Plasmids used in recombinant expression were provided by C.D.A., J.W., and M. Matz (University of Texas at Austin). E.B. performed all other experimental work, performed the analysis and wrote the initial manuscript draft. C.D.A and J.W. supervised the experimental work, commented on the analysis and edited the manuscript.

1.2.2.2 Chapter 4. Bleaching corals express bright colours to facilitate recovery

In this study, the regulation of GFP-like proteins in shallow water corals during bleaching was explored using an *in vivo* optical biomarker approach.

To address **Q3**, multiple mesocosm experiments of up to 100 days were performed on live colonies of coral species able to express light-induced GFP-like proteins. To induce bleaching, the colonies were exposed to either a gradual heating regime (up to 32°C) or to an imbalance in macronutrient ratios (high nitrate, low phosphate). Measurements of *in vivo* fluorescence were used to monitor changes in host and symbiont pigments, and end-point tissue sampling was used to ground-truth the optical data.

To address **Q4**, GFP-like protein expression during bleaching was compared to the expression in colony growth areas, where these proteins are thought to promote colonisation with symbionts (D'Angelo *et al.*, 2012; Smith *et al.*, 2013). In addition, spectral light was used to induce or prevent the upregulation of GFP-like proteins in bleached corals, in order to assess the ability of corals to recover their pre-bleaching symbiont complement.

This chapter has been prepared for submission as a *Science* report, and as such it follows the length and structuring guidelines of the journal. Additional background information is provided in chapter 2. The submitted manuscript title and author list is:

> Bollati, E., D'Angelo, C., Alderdice, R., Pratchett, M. and Wiedenmann, J. Bleaching corals express bright colours to facilitate recovery.

E.B., C.D.A., and J.W. designed the study and developed the methodology. M.P. and R. Goehrung (University of Washington) provided field images of colourful bleaching. C.D.A. performed the *M. foliosa* bleaching experiment. R.A. performed the spectral light experiments as part of a MSci research project supervised by E.B. and J.W.. A. Thomson (Scottish Association for Marine Science) collected the *P. lichen* high light acclimation data. E.B. performed all other experimental work, performed the analysis and wrote the initial manuscript draft. C.D.A. and J.W. commented on the analysis and edited the manuscript. M.P. also commented on the manuscript.

1.2.2.3 Chapter 5. A multi-excitation fluorescence imaging method to improve detection of coralline algae in benthic surveys

This study develops the concept for a multi-excitation approach to underwater fluorescence imaging. A prototype illumination system was built with off-the-shelf components, and combined with either a microscope CCD camera or a compact

underwater camera to obtain images of representative purified fluorescent pigments and of live reef organisms.

To address **Q5**, an *a priori* classification algorithm was developed using spectral data and fluorescence images collected from purified pigments. The algorithm was then applied to classify images of live coral reef organisms collected with the prototype imaging system.

This chapter is in preparation for submission. The authors involved in the project are:

Bollati, E., Kline, D.I., D'Angelo, C., Mitchell, B.G. and Wiedenmann, J.

E.B., C.D.A, and J.W. developed the initial concept. B.G.M. and D.I.K advised on the concept and provided materials. C.D.A. produced the recombinant proteins. C. Quick (Coral Reef Laboratory) collected seaweed samples. E.B. developed the system, designed the study, collected the data, performed the analysis and wrote the manuscript. G. Blythe (National Oceanography Centre) assisted with design and assembly of the illumination system.

Chapter 2 Fluorescent proteins and chromoproteins in reef corals

The following sections provide background information on the biochemistry, the environmental regulation and the function of GFP-like proteins in corals, aimed at complementing the literature review presented in chapters 3 and 4. As much of the work undertaken in this thesis is based on the optical detection of fluorescence *in vivo*, relevant information on biological fluorescence and on the optical microenvironment of coral colonies is also provided.

2.1 Fluorescence of living organisms

Fluorescence is the emission of light by a molecule upon absorption of energy (Stokes, 1852). It is characteristic of chemical structures with delocalised electrons, which are able to generate an excited singlet state upon absorption of a photon energy; the energy absorbed is then released in two steps, first by internal conversion to the lowest vibrational level of the excited singlet state, then by fluorescence emission to a vibrational level of the ground state (Fig. 2.1) (Valeur and Berberan-Santos, 2013). Due to the non-radiative energy loss during internal conversion, the photon emitted is of lower energy, hence longer wavelength, than the one absorbed; this difference is known as Stokes shift. The Stokes shift is one of the characterising features of a fluorescence event, together with the quantum yield of fluorescence, which is the ratio of emitted to absorbed photons, and the lifetime, which is the duration of the existence of the excited state before relaxation (Valeur and Berberan-Santos, 2013).

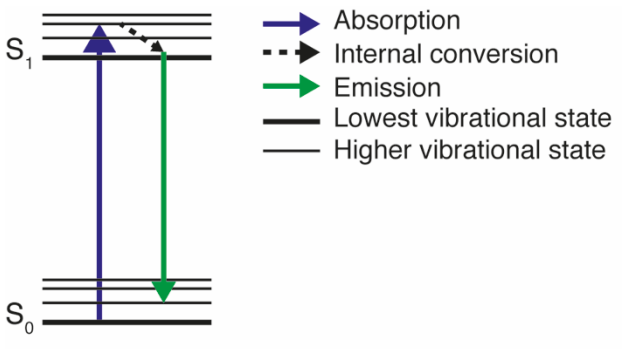

Figure 2.1 Jablonski energy diagram of a fluorescence event

S_0 = electronic ground state; S_1 = excited singlet state.

Fluorescence of biological molecules often arises from a chromophore, a structure containing a system of conjugated π bonds able to absorb light energy. The energy

transition between the ground state and excited state decreases with increasing number of π bonds; hence, chromophores with larger conjugated systems generally absorb longer wavelengths (Rabinowitch, 1944). Chromophores that are able to release this energy via fluorescence are also known as fluorophores. As well as fluorescence emission and internal conversion, excitation of a fluorophore can result in a number of other events that are relevant to biological processes, including intersystem crossing, Förster Resonance Energy Transfer (FRET), and photo-oxidation (Hochstrasser and Porter, 1960). Transition to a triplet state via intersystem crossing can result in covalent modifications and generation of reactive oxygen species (ROS) via singlet oxygen; this can impair the ability of a molecule to fluoresce, a phenomenon known as photobleaching (Kasha, 1950). FRET occurs when two molecules with overlapping excitation/emission spectra are positioned at a distance of typically >10 nm, enabling the excitation energy to be transferred from one fluorophore to the other without emission; the distance at which transfer efficiency is 50%, known as Förster radius, is characteristic of each pair of fluorophores (Förster, 1960). Lastly, photo-oxidation or photochemical quenching is the transfer of the excited electron to a nearby molecule, as observed during the light reactions of photosynthesis (Hochstrasser and Porter, 1960).

2.2 Biochemistry of coral fluorescent proteins

In reef-building corals, fluorescence is due to a family of proteins expressed by the coral host (Dove *et al.*, 2001). These pigments are homologous to the green fluorescent protein (GFP) first described from the bioluminescent hydromedusa *Aequorea victoria* (Shimomura *et al.*, 1962). The *A. victoria* GFP (avGFP) acts as an acceptor of FRET from aequorin, a blue-emitting bioluminescent protein, causing the live jellyfish to appear green (Morin and Hastings, 1971; Morise *et al.*, 1974). The GFP chromophore is a 4-(*p*-hydroxybenzylidine)-5-imidazolinone (Shimomura, 1979), formed autocatalitically by cyclisation and oxidation of a Ser-Tyr-Gly tripeptide (Prasher *et al.*, 1992; Heim *et al.*, 1994). The chromophore is surrounded by an 11-stranded β-can (Fig. 2.2), which includes a number of residues involved in determining the fluorescence properties of the molecule (Orm *et al.*, 1996; Yang *et al.*, 1996). Under native conditions, the avGFP chromophore exists in a neutral (hydroxyl Tyr66) and an anionic (phenolate Tyr66) form, with absorption maxima in the UV and blue range, respectively (Ward *et al.*, 1982). As well as from excitation of the anionic form, green fluorescence emission of avGFP also results from excitation of the neutral chromophore due to excited state proton transfer (ESPT) (Chattoraj *et al.*, 1996). The discovery of the GFP represents a milestone of 20th century molecular biology. As no enzymes or cofactors other than molecular oxygen are required for chromophore formation (Heim *et al.*, 1994), cloning of the avGFP gene (Prasher *et al.*,

1992) allowed heterologous expression of functional protein in bacteria and eukaryotic organisms (Chalfie *et al.*, 1994; Inouye and Tsuji, 1994). This revolutionised the fields of cell biology and biomedical imaging, eventually leading to the 2008 Nobel Prize in Chemistry being awarded to Osamu Shimomura, Martin Chalfie and Roger Tsien for their discovery.

The search for fluorescent proteins (FPs) with different spectral properties for use in live imaging led to the discovery and cloning of a diversity of FPs from Anthozoa (Wiedenmann, 1997; Matz *et al.*, 1999) and Scleractinia (Alieva *et al.*, 2008). Anthozoan FPs are structurally similar to the avGFP, with the notable difference that they mostly arrange in homotetramers (Baird *et al.*, 2000; Wiedenmann *et al.*, 2004a) instead of monomers or dimers (Orm *et al.*, 1996; Yang *et al.*, 1996) (Fig. 2.2). Furthermore, modifications of the chromophore and chromophore environment result in a variety of spectral properties (Nienhaus and Wiedenmann, 2009). The following sections provide an overview of the biochemical properties of some groups of anthozoan FPs that are of relevance for the work presented in this thesis.

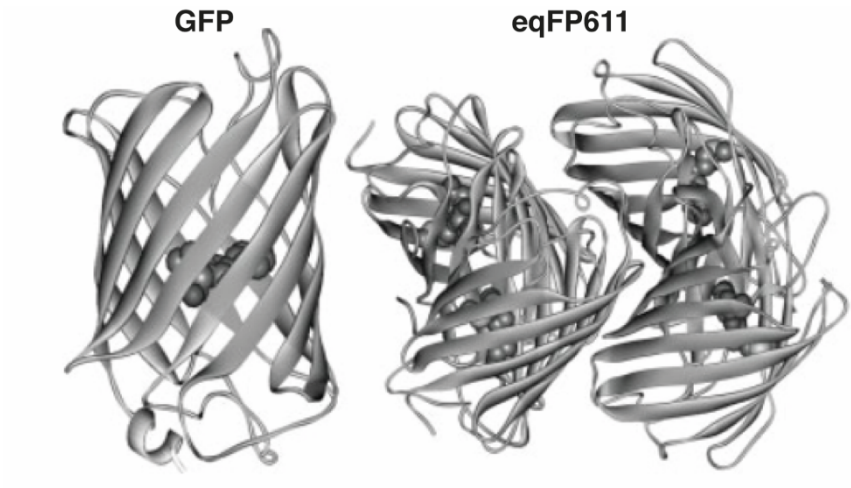

Figure 2.2 Tertiary and quaternary structure of GFP-like proteins

Ribbon diagram showing the 11-stranded β-can and the chromophore of monomeric GFP and of a tetrameric Anthozoa FP (eqFP611). Reproduced with permission of the authors (Wiedenmann *et al.*, 2009).

2.2.1 GFPs

Anthozoa GFP present a 4-(*p*-hydroxybenzylidine)-5-imidazolinone chromophore, as described for avGFP (Nienhaus and Wiedenmann, 2009). While the Tyr and Gly residues of the chromophore-forming tripeptide are conserved, the first residue is variable (Alieva *et al.*, 2008). The chromophore of Anthozoa GFP is predominantly found in the anionic form under physiological conditions, therefore the excitation maxima of these proteins are

in the blue-green range rather than in the UV (Alieva *et al.*, 2008; Nienhaus and Wiedenmann, 2009).

2.2.2 CFPs

Cyan FPs (CFPs) are characterised by blue-shifted excitation and emission maxima and broader spectra compared to GFPs (Alieva *et al.*, 2008). These spectral differences are due to residues found adjacently to the chromophore, which affect the chromophore environment by modifying charge density localisation (Henderson and Remington, 2005; Nienhaus *et al.*, 2006a); the chromophore structure is the same as that of GFPs (Henderson and Remington, 2005). CFPs are extremely widespread among the Scleractinia (Alieva *et al.*, 2008) and their evolution appears to have been driven by positive selection (Field *et al.*, 2006).

2.2.3 RFPs

Cloning of the first red fluorescent protein (RFP) (Matz *et al.*, 1999) from the corallimorpharian *Discosoma* sp. was another milestone in biochemistry, as it allowed multi-colour labelling of cellular components for *in vivo* imaging. The Anthozoa RFP chromophore is also referred to as DsRed-type, from the name the *Discosoma* RFP was later commercialised with. The red chromophore primary structure is a Gln-Tyr-Gly tripeptide; red fluorescence arises from extension of π-conjugation to include the oxidised Cα-Nα bond of Gln66 (Baird *et al.*, 2000; Gross *et al.*, 2000; Wall *et al.*, 2000) (Fig. 2.3). For this group of FPs, maturation of the red chromophore occurs spontaneously in presence of molecular oxygen (Gross *et al.*, 2000). Under native conditions, the red chromophore is commonly found together with a green-emitting form (Baird *et al.*, 2000; Gross *et al.*, 2000); the green chromophore is either a precursor of the red-emitting form (Baird *et al.*, 2000), or it was suggested that both forms mature in parallel from a non-fluorescent precursor (Strack *et al.*, 2010). As well as from direct excitation of the red chromophore, red emission also results from excitation of the green form via FRET when the two are present within the same tetramer; green emission only arises from all-green tetramers (Heikal *et al.*, 2000; Schüttrigkeit *et al.*, 2001). A particular type of RFP chromophore with planar *trans* conformation is found in the anemone protein eqFP611 (Wiedenmann *et al.*, 2002; Nienhaus and Wiedenmann, 2009) (Fig. 2.3). This protein differs markedly from other RFPs also due to the ability of the red chromophore to mature rapidly and almost completely, with less than 1% green emission observed in the mature form (Wiedenmann *et al.*, 2002).

2.2.4 pcRFPs

A second category of red chromophore found in Anthozoa FPs is that of photoconvertible RFPs (pcRFPs), also known as Kaede-type from the first protein of this group to be characterised (Ando *et al.*, 2002). The pcRFP chromophore is formed from a His-Tyr-Gly tripeptide, producing a structure analogous to that of GFP with a neutral form absorbing at ~400 nm and an anionic, green-absorbing form (Ando *et al.*, 2002; Wiedenmann *et al.*, 2004a). Excitation of the pcRFP neutral chromophore results in cleavage of the peptide backbone between Cα and Nα of His62 and extension of π-conjugation to the His62 imidazole (Mizuno *et al.*, 2003; Nienhaus *et al.*, 2005). This irreversible reaction, which differently from other FP maturation pathways does not require oxygen, produces a red-emitting chromophore (Fig. 2.3). Photo-induced backbone cleavage occurs via β-elimination, and involvement of a number of mechanisms such as ESPT and intersystem crossing has been hypothesised (Mizuno *et al.*, 2003; Nienhaus *et al.*, 2005; Lelimousin *et al.*, 2009). Similarly to what observed in DsRed, intratetrameric FRET from green to red subunits is the dominant de-excitation mechanism of the anionic green chromophore (Wiedenmann *et al.*, 2004a). Excitation of the neutral form of the converted pcRFP chromophore can also produce red fluorescence, mainly via intratetrameric FRET to the anionic red chromophore rather than via ESPT (Hosoi *et al.*, 2006).

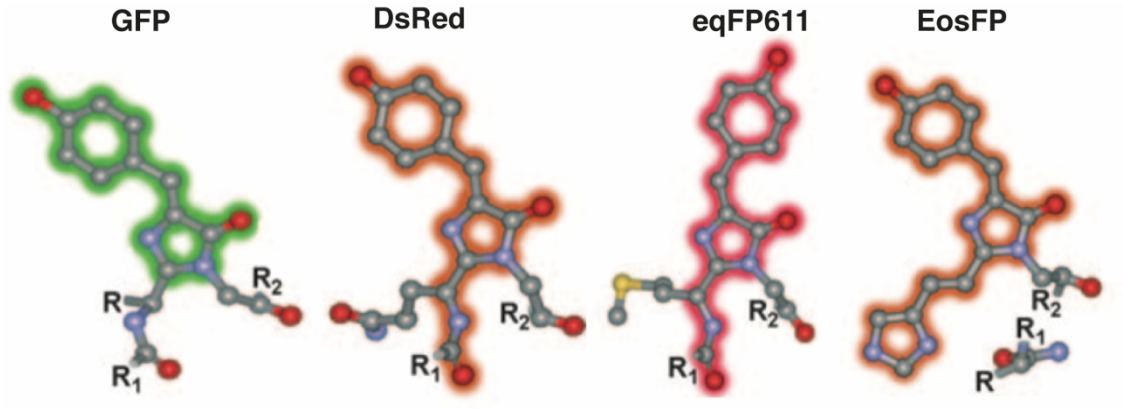

Figure 2.3 Chromophore structures of GFP-like proteins

Chromophore structures of GFP, of the RFPs DsRed from *Discosoma* sp. and eqFP611 from *Entacmaea quadricolor*, and of the red form of the pcRFP EosFP from *Lobophyllia hemprichii*. Adapted with permission of the authors (Nienhaus and Wiedenmann, 2009).

2.2.5 CPs

The GFP-like protein family also includes a group of non-fluorescent chromoproteins (CPs), which absorb visible wavelengths with high extinction coefficients but present no or little emission, thus appearing blue, purple or pink (Dove *et al.*, 2001; Alieva *et al.*, 2008).

The CP chromophore consists of a non-coplanar isomer of the RFP chromophore (Prescott *et al.*, 2003). In some cases, fluorescence of CPs can be induced by light (Lukyanov *et al.*, 2000) due to *trans-cis* isomerisation of the excited chromophore (Chudakov *et al.*, 2003).

2.3 GFP-like proteins in reef-building corals

Extensive research has focussed on the biochemical and optical properties of coral GFP-like proteins, with the aim of improving existing fluorophores or creating novel ones for use in fluorescent imaging. However, comparatively fewer studies have addressed the role of this protein group in the context of coral ecophysiology. The following sections summarise the current knowledge on GFP-like proteins function and regulation within the coral holobiont.

2.3.1 Distribution of GFP-like proteins in coral tissue

Like other Cnidaria, scleractinian polyps are diploblastic organisms composed of an outer epidermis and an inner gastrodermis, which lines the gastrovascular cavity; the two cellular layers are separated by an acellular mesoglea (Fig. 2.4). The aboral region of the polyp, which is the site of substrate attachment, is characterised by a modified ectodermal layer known as calicoblastic epithelium, which secretes the aragonite skeleton and provides the attachment between the skeleton and the cellular layers (Vandermeulen, 1975) (Fig. 2.4). In symbiotic (or zooxanthellate) corals, symbiont cells are localised within host gastrodermal cells and surrounded by a membrane of host origin, the symbiosome (Trench, 1993). The localisation and arrangement of GFP-like proteins in host tissue can vary between species and between proteins within a species (Salih *et al.*, 2000). Many FPs and CPs are found in the ectoderm, localised either inter- or intracellularly, or arranged in granules (Schlichter *et al.* 1986, Salih *et al.*, 2000) (Fig. 2.4). On some occasions, GFP-like proteins can be found in the gastrodermis, either below the symbiont cells or in association with them (Schlichter *et al.*, 1986; Salih *et al.*, 2000; Oswald *et al.* 2007).

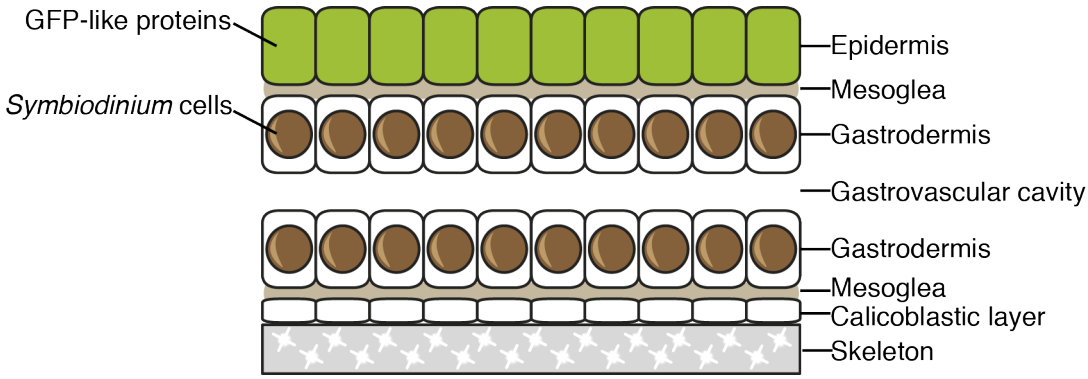

Figure 2.4 Tissue organisation of reef corals.

Schematic representation of the oral and aboral tissue regions of a coral polyp, separated by the gastrovascular cavity. Symbiont cells are contained within gastrodermal host cells, while GFP-like proteins are often highly expressed in ectodermal cells.

2.3.2 Regulation of coral GFP-like proteins

One of the traits that make GFP-like proteins a promising biomarker of coral physiology is their sensitivity to a number of environmental conditions. The following sections describe the regulation of GFP-like proteins in relation to light and heat stress, as well as considering the intraspecific variability observed in this response.

2.3.2.1 Light

Based on their regulation in relation to light intensity, coral GFP-like proteins can be classified into two broad groups: light induced proteins and constitutively expressed ones. Light-induced GFP-like proteins are typical of shallow water corals. This group includes a large number of CFPs, GFPs, RFPs and CPs which are regulated at the transcriptional level by the intensity of blue light (D'Angelo *et al.*, 2008). The specific regulation pathway that leads to this transcriptional response has not been elucidated. However, blue-light sensing cryptochromes have been identified in corals (Levy *et al.*, 2007), as have opsins, G-proteins and G-protein-coupled receptors (Mason *et al.*, 2012; Kaniewska *et al.*, 2015), all plausible components of a light-induced signalling cascade; cytoplasmic calcium has also been suggested to play a role in light signal transduction (Hilton *et al.*, 2012). Although all proteins belonging to this group are upregulated in response to blue light, the specifics of the relationship vary within the group; in particular, D'Angelo *et al.* (2008) identified low-threshold proteins, which are expressed under moderate light levels and become saturated at intermediate levels, and high-threshold proteins, which respond to stronger light and saturate at much higher intensities. Many CFPs belong to the low-threshold group, while GFPs, CPs and RFPs have a higher induction threshold (D'Angelo

et al., 2008); combinations of proteins from both groups are often found within the same individual or species (Alieva *et al.*, 2008; D'Angelo *et al.*, 2008). Light-induced GFP-like proteins are also highly expressed in the symbiont-free growth margins of colonies and in areas affected by wounding or epibionts (D'Angelo *et al.*, 2012).

Constitutively expressed GFP-like proteins are found in corals from all depths (Leutenegger *et al.*, 2007a; Eyal *et al.*, 2015; Roth *et al.*, 2015). Proteins in this group are expressed in the host tissue even in the dark (Leutenegger *et al.*, 2007a; Eyal *et al.*, 2015), and can make up a significant proportion of the host's total protein content (Oswald *et al.*, 2007). As their concentration is independent of light intensity, coral pcRFPs also fall into this category (Leutenegger *et al.*, 2007a). However, since post-translational maturation of the red chromophore requires ~400 nm light (Ando *et al.*, 2002; Wiedenmann *et al.*, 2004a), the spectral properties of these proteins *in vivo* are still affected by the light environment (Leutenegger *et al.*, 2007a). A single individual or species can express constitutive proteins and light-induced ones at the same time; pcRFPs have been observed in conjunction with other constitutive proteins (Oswald *et al.*, 2007), but not with light-induced ones.

2.3.2.2 Heat stress

A number of studies have reported a decrease in the concentration of GFP-like proteins from the tissue of corals undergoing heat stress (Dove *et al.*, 2006; Hume *et al.*, 2013; Roth and Deheyn, 2013). While some authors have suggested that this decrease could be caused by active degradation of the protein (Roth and Deheyn, 2013), other studies have shown that expression of genes coding for GFP-like proteins is downregulated during acute heat stress (Desalvo *et al.*, 2008; Smith-Keune and Dove, 2008). Roth and Deheyn (2013) also reported that the concentration of GFP-like proteins decreases in corals undergoing heat stress, but that after the onset of bleaching fluorescence measured optically *in vivo* increases, resulting in the uncoupling of the two parameters; the authors attributed this result to enhanced skeletal scattering of excitation light and of emission signal caused by the reduced symbiont pigment absorption (Enríquez *et al.*, 2005; Roth *et al.*, 2010; Roth and Deheyn, 2013). Not many studies have explored the regulation of GFP-like proteins in the context of bleaching events; in the field, concentration of GFP-like proteins was shown to decrease in the Mediterranean anemone *Anemonia sulcata* during a bleaching event (Leutenegger *et al.*, 2007b), while upregulation of the gene coding for a CP was measured in the tropical coral *Acropora millepora* (Seneca *et al.*, 2010).

2.3.2.3 Colour polymorphism

The expression of GFP-like proteins in corals exhibits intraspecific polymorphism, which should be taken into account in the context of biomarker development. On the reef, conspecific colonies expressing widely different GFP-like protein complement can be found within similar environmental conditions, sometimes even side by side (Wiedenmann *et al.*, 1999; Kelmanson and Matz, 2003; Eyal *et al.*, 2015; Roth *et al.*, 2015). The maximum level of expression of GFP-like proteins by a particular morph is correlated with the number of actively expressed gene copies (Gittins *et al.*, 2015). The persistence of this genotypic and phenotypic diversity can be explained as the product of balancing selection, whereby the fitness advantage conferred by the ability to express high concentrations of GFP-like proteins is counteracted by the metabolic cost of expression (Gittins *et al.*, 2015; Quick *et al.*, 2018).

2.3.3 Functions of coral GFP-like proteins

Considered the diversity of optical properties, of distribution, and of regulation of GFP-like proteins on coral reefs, it is not surprising that attempts to pinpoint a single shared function of this protein group have been unsuccessful. Chapter 3 and chapter 4 of this thesis address two potential roles of GFP-like proteins in Scleractinia, furthering the notion that the group is functionally diverse. Early studies of coral fluorescence suggested both a photoprotective role in shallow water (Kawaguti, 1944) and a role in enhancement of symbiont photosynthesis in mesophotic corals (Schlichter *et al.*, 1986). This view was furthered by many after the discovery of GFP-like proteins in coral (Salih *et al.*, 2000; Dove *et al.*, 2001), but challenged by others after the observation that some GFP-like proteins had no effect on chlorophyll excitation (Mazel *et al.*, 2003b). The hypothesis that GFP-like proteins could have either a photoprotection or a light-enhancement function depending on their ecological context was supported by the different localisation of these pigments with respect to symbiont cells. It was suggested that when localised ectodermally, GFP-like proteins could reduce the amount of light reaching symbiont cells, while when localised around or below the symbionts in the gastrodermis they could act to enhance symbiont photosynthesis (Schlichter *et al.*, 1986; Salih *et al.*, 2000). A photoprotective function has now been experimentally demonstrated for CPs (Smith *et al.*, 2013), RFPs (Gittins *et al.*, 2015), and CFPs (Quick *et al.*, 2018), and a light-enhancement mechanism has been proposed for pcRFPs (Smith *et al.*, 2017, chapter 3 of this thesis). This indicates that the function of GFP-like proteins depends on the type of protein and on the environmental context. Recently, it was demonstrated that GFP-like proteins can reduce or enhance light absorption depending on their concentration (Lyndby *et al.*, 2016), confirming the ability of this protein group to modulate the internal light environment of

coral colonies at both ends of the scale of light intensity. In shallow water corals, it is proposed that photoprotection occurs via screening of symbionts from PAR wavelengths by the ectodermal layer of GFP-like proteins (Smith *et al.*, 2013); light penetration to the symbiont-harbouring gastrodermis is therefore regulated by blue light intensity, which controls the ectodermal concentration of these pigments (D'Angelo *et al.*, 2008). In deep-water and mesophotic corals, enhancement of photosynthesis has been proposed to occur via transformation of incident wavelengths into more penetrative ones (Smith *et al.*, 2017, Chapter 3 of this thesis), to overcome the inner filter effect resulting from the high photosynthetic pigment concentration observed in shade-adapted corals (Stambler and Dubinsky, 2005).

A second line of work has suggested a role of GFP-like proteins in scavenging reactive oxygen species (ROS) produced by symbiont photosynthesis (Bou-Abdallah *et al.*, 2006). Although some antioxidant activity has been shown for avGFP and for a coral RFP *in vitro* (Bou-Abdallah *et al.*, 2006; Shikina *et al.*, 2016), no direct *in vivo* evidence has yet been presented. Some authors have suggested scavenging of ROS as the reason for the observed decrease in protein concentration during heating (Roth and Deheyn, 2013); however, this is in contrast with studies reporting that GFP-like protein genes are downregulated under acute heat stress (Smith-Keune and Dove, 2008).

Finally, a function of GFP-like proteins associated with visual ecology of marine animals has been hypothesised, either as a means to increase or decrease the visibility of coral colonies to other reef organisms (Matz *et al.*, 2006; Gruber *et al.*, 2008).

2.4 Corals and light

The quality and quantity of incident light at the surface of coral colonies is a function of geographical and atmospheric factors, of attenuation of light by water, and of the interaction with phytoplankton and suspended particles. At the colony surface, however, measurements of spectral irradiance show that the incident spectrum is modified by the underlying tissue and skeletal structures (Kühl *et al.*, 1995; Wangpraseurt *et al.*, 2012). These structures play an important role in determining the internal light environment of colonies, affecting holobiont physiology.

The coral skeleton is composed of calcium carbonate in the form of aragonite, precipitated by cells in the aboral calicoblastic ectoderm (Vandermeulen, 1975). Multiple scattering by this biomineral has been shown to enhance the light environment experienced by symbionts inside the tissue, thus facilitating absorption (Enríquez *et al.*, 2005; Terán *et al.*, 2010). However, the morphology of coral skeleton exhibits a great degree of variability between taxa, and scattering properties vary with morphology (Marcelino *et al.*, 2013;

Wangpraseurt *et al.*, 2016; Enríquez *et al.*, 2017). Comparative studies have shown that, on the microscale, skeletons with low fractality are able to redistribute light within the colony more efficiently than skeletons with high fractality (Marcelino *et al.*, 2013); on the macroscale, plating and branching growth forms enhance light more than massive ones (Enríquez *et al.*, 2017). Skeletal morphology is also plastic intraspecifically; therefore, differences in growth form to optimise light absorption are commonly encountered in conspecific colonies along depth gradients, or in areas of the reef with different exposure (Muko *et al.*, 2000; Anthony *et al.*, 2005; Einbinder *et al.*, 2009; Kaniewska *et al.*, 2009). As well as the skeleton, the optical properties of the overlying tissue have been shown to play an important role in modulating the internal light environment of coral colonies (Wangpraseurt *et al.*, 2014, 2016, 2017); these properties include the ability to enhance and transfer light directionally, and are particularly important in corals with thicker tissue, such as faviids (Wangpraseurt *et al.*, 2014, 2016, 2017).

An optical mechanism that is highly relevant to the work presented in this thesis is the optical feedback loop associated with bleaching (Marcelino *et al.*, 2013; Swain *et al.*, 2016; Wangpraseurt *et al.*, 2017). When symbionts or symbiont pigments are lost, the decrease in photosynthetic pigment absorbance produces a dramatic enhancement of the light fluxes inside coral tissue (Enríquez *et al.*, 2005; Wangpraseurt *et al.*, 2012). This increase in light levels can exacerbate bleaching, particularly in corals with skeleton/tissue structures that are most efficient in redistributing light (Marcelino *et al.*, 2013; Swain *et al.*, 2016; Wangpraseurt *et al.*, 2017); corals with more heterogeneous internal light distribution on the other hand can maintain lower-light areas, which potentially confer some bleaching resistance (Wangpraseurt *et al.*, 2017). As well as causing photoinhibition in the residual symbiont population, the increase in internal light fluxes has been shown to induce proliferation of endolithic algae found in the coral skeleton (Rodríguez-Román *et al.*, 2006). A role of the optical feedback loop in the regulation of light-induced GFP-like proteins has been previously proposed for symbiont free growth margins (D'Angelo *et al.*, 2012; Smith *et al.*, 2013; Wiedenmann and D'Angelo, 2015). The investigation of this mechanism in bleached corals is the focus of chapter 4.

2.5 Conclusion

The literature reviewed in this chapter shows that from a biochemical, functional and ecological point of view, GFP-like proteins are a highly diverse group. This is directly reflected in the range of expression patterns observed in response to environmental conditions. Understanding the diversity of GFP-like protein function and regulation is therefore key for the development of biomarkers, and is the focus of the studies presented in the following two chapters.

Chapter 3 FRET-mediated long-range wavelength transformation by photoconvertible fluorescent proteins as an efficient mechanism to generate orange-red light in symbiotic deep water corals

3.1 Abstract

Photoconvertible fluorescent proteins (pcRFPs) are a group of fluorophores that undergo an irreversible green-to-red shift in emission colour upon irradiation with near-ultraviolet (near-UV) light. Despite their wide application in biotechnology, the high-level expression of pcRFPs in mesophotic and depth-generalist coral species currently lacks a biological explanation. Additionally, reduced penetration of near-UV wavelengths in water poses the question whether light-driven photoconversion is relevant in the mesophotic zone, or whether a different mechanism is involved in the post-translational pigment modification *in vivo*. Here, we show in a long-term mesocosm experiment that photoconversion *in vivo* is entirely dependent on near-UV wavelengths. However, a near-UV intensity equivalent to the mesophotic underwater light field at 80 m depth is sufficient to drive the process *in vitro*, suggesting that photoconversion can occur near the lower distribution limits of these corals. Furthermore, live coral colonies showed evidence of efficient Förster Resonance Energy Transfer (FRET). Our simulated mesophotic light field maintained the pcRFP pool in a partially photoconverted state *in vivo*, maximising intra-tetrameric FRET and creating a long-range wavelength conversion system with higher quantum yield than other native RFPs. We hypothesise that efficient conversion of blue wavelengths, abundant at depth, into orange-red light could constitute an adaptation of corals to life in light-limited environments.

3.2 Introduction

Reef corals owe a large proportion of their striking green, red, and purple-blue colouration to green fluorescent protein (GFP)-like host pigments (FPs) found in the coral host (Dove *et al.*, 2001; Oswald *et al.*, 2007; Alieva *et al.*, 2008; D'Angelo *et al.*, 2012). The pigment concentrations of up to 7% of the total soluble protein content in coral tissue (Oswald *et al.*, 2007) are achieved by high-level expression of the encoding multicopy genes (Gittins *et al.*, 2015). The first representative of this protein family, GFP, was described from the

jellyfish *Aequorea victoria* (Shimomura *et al.*, 1962) and more were subsequently isolated from other Anthozoa (Matz *et al.*, 1999; Wiedenmann *et al.*, 2000, 2002, 2004b) and Scleractinia (Oswald *et al.*, 2007; Alieva *et al.*, 2008). The GFP structure consists of an 11-stranded β-can (Yang *et al.*, 1996) surrounding a fluorescent chromophore (Shimomura, 1979), and is widely conserved across a variety of taxa including reef corals (Shagin *et al.*, 2004; Nienhaus *et al.*, 2005). Structural studies revealed that the majority of Anthozoan FPs, unlike the monomeric GFP (Yang *et al.*, 1996), is assembled in tetramers (Nienhaus and Wiedenmann, 2009).

The tripeptide chromophore is synthesised autocatalytically (Cody *et al.*, 1993) in a process that requires molecular oxygen but no enzymes or cofactors (Heim *et al.*, 1994). The colour diversity of FPs can be attributed to modifications of the GFP-type chromophore and altered interactions with the surrounding protein scaffold (Nienhaus *et al.*, 2006b; Nienhaus and Wiedenmann, 2009). Notably, an additional oxidation step modifying the GFP-type chromophore results in the emergence of red fluorescence, as observed in DsRed and eqFP611 (Matz *et al.*, 1999; Wiedenmann *et al.*, 2002). In photoconvertible red fluorescent reef coral pigments such as Kaede or EosFP, the post-translational modification of the GFP-type chromophore is driven by exposure to near-ultraviolet (near-UV) light around 390 nm (Ando *et al.*, 2002; Mizuno *et al.*, 2003; Wiedenmann *et al.*, 2004a; Nienhaus *et al.*, 2005). Protein pigments characterised by this photoconversion process can be found in a number of Anthozoa species (Ando *et al.*, 2002; Labas *et al.*, 2002; Wiedenmann *et al.*, 2004a; Oswald *et al.*, 2007) and have been termed “photoconvertible red fluorescent proteins” (pcRFPs). The photoconversion mechanism is associated with cleavage of the peptide backbone between the Cα and Nα of His62 (Mizuno *et al.*, 2003; Nienhaus *et al.*, 2005), the first residue of a His-Tyr-Gly tripeptide that forms the chromophore of all so far known pcRFPs (Oswald *et al.*, 2007). Although this mechanism has found wide biotechnological application (Ando *et al.*, 2002; Wiedenmann *et al.*, 2004a, 2009; Wacker *et al.*, 2007; Adam *et al.*, 2010), the biological function and ecological relevance of photoconversion in this pigment group remains unexplained.

A photoprotective role has been demonstrated for certain FPs and biochemically related non-fluorescent chromoproteins in sea anemones and corals living in symbiosis with dinoflagellate algae (Wiedenmann *et al.*, 1999; Salih *et al.*, 2000; Smith *et al.*, 2013; Gittins *et al.*, 2015). The predominant localisation of FPs and homologous non-fluorescent chromoproteins in the ectoderm above the symbiont-harbouring endoderm (Salih *et al.*, 2003; Smith *et al.*, 2013) supports the experimental observations. Furthermore, D’Angelo and co-workers (D’Angelo *et al.*, 2008) found that many cyan, green and DsRed-type red FPs are regulated at the transcriptional level by the intensity of incident light, particularly in

the blue spectral range (D'Angelo *et al.*, 2008; Smith *et al.*, 2013; Gittins *et al.*, 2015). High tissue concentrations of FPs are also found, however, in azooxanthellate Anthozoa in a range of habitats not prone to light stress, including the deep sea (Wiedenmann *et al.*, 2004b; Vogt *et al.*, 2008), and in zooxanthellate mesophotic corals (Oswald *et al.*, 2007; Kahng *et al.*, 2012; Eyal *et al.*, 2015; Roth *et al.*, 2015). In the latter group, FPs are constitutively expressed independently of the level of light exposure (Leutenegger *et al.*, 2007a; D'Angelo and Wiedenmann, 2012; Eyal *et al.*, 2015) and have been suggested to facilitate photosynthesis of symbiotic algae in low light conditions (Wiedenmann *et al.*, 1999; Salih *et al.*, 2000). pcRFPs are commonly found in corals of the Faviina suborder with a preference for lower light habitats (Field and Matz, 2010), they have been reported from mesophotic depths (Eyal *et al.*, 2015) and their regulation is independent of light (Leutenegger *et al.*, 2007a). Furthermore, pcRFPs exhibit efficient non-radiative energy transfer via FRET between green and red chromophores in subunits of partially converted tetramers (Wiedenmann *et al.*, 2004a). This is promoted by the strong overlap of the emission spectrum of the green precursor chromophore with the absorption/excitation spectrum of the photoconverted red form, and by the close proximity between the chromophores within the tetrameric assembly (Ando *et al.*, 2002; Wiedenmann *et al.*, 2004a; Nienhaus *et al.*, 2005; Wolf *et al.*, 2013). Therefore, the formation of the chromophore and the photophysical properties of pcRFPs are distinct from those of red-emitting FPs from shallow water corals.

Green-to-red photoconversion might thus represent an important part of the adaption of mesophotic corals to life in low light environments. However, the blue-green wavelengths that dominate these light fields fall mostly beyond the photoconversion action spectrum of pcRFPs measured *in vitro* using recombinantly produced proteins (Wiedenmann *et al.*, 2004a). Hence, the question arises whether photoconversion of coral pigments at greater depth is at all of ecological relevance. To investigate whether the unique photophysical properties of pcRFPs represent an adaptation to life in low light environments, we explored the effects of a simulated deep-water light field on corals containing pcRFPs. Specifically, we assessed whether the near-UV light levels prevailing within the depth range of such corals are sufficient to induce green-to-red photoconversion. Finally, we investigated the possibility of FRET as a mechanism to fine-tune the internal light environment of the colonies. Our findings help place the photoconversion mechanism in an ecological context, a prerequisite to understanding the function of pcRFPs in the coral holobiont.

3.3 Results

3.3.1 Effects of light quality on photoconvertible red fluorescent proteins (pcRFPs)

3.3.1.1 Changes in live tissue fluorescence over time

In order to investigate the spectral dependence of photoconversion in live corals, colonies of *Montastraea cavernosa* and *Echinophyllia* sp. were exposed to 412 nm, 448 nm and 476 nm light from light-emitting diodes (LEDs) for >120 days. Fluorescence emission and excitation from the colony coenosteum were monitored *in vivo* throughout the exposure period.

The intensity of the LEDs used for the light treatment was adjusted to levels at which the amount of photons efficient for photoconversion fell within the range that corals experience over a depth gradient in their natural habitat. Specifically, the 412 nm LED set to 60 μmol photons $m^{-2}s^{-1}$ has a photoconversion potential equivalent to that of our Red Sea irradiance data at ~26 m, while the 448 nm LED was equivalent to ~81 m; the 476 nm LED had no photoconversion potential. For comparison, the photoconversion potential of 200 μmol photons $m^{-2}s^{-1}$ of metal halide was equivalent to ~37 m in the Red Sea.

Under 476 nm light illumination, green (514 nm) fluorescence emission of *M. cavernosa* increased with time, reaching ~6x pre-treatment values; this was accompanied by a decrease in red (582 nm) emission down to ~30% of pre-treatment fluorescence (Fig. 3.1a). Values in the excitation maximum (571 nm) of red fluorescence also decreased over time to ~25% of initial values. In contrast, when red fluorescence emission was recorded, the excitation value at 507 nm corresponding to the excitation maximum of the green fluorescent chromophore showed only a slightly decreasing trend. *M. cavernosa* exposed to 448 nm light showed a smaller increase in green emission, while red emission, 507 nm red excitation and 571 nm red excitation showed only minor changes. Under 412 nm light illumination, green emission did not show pronounced changes, while an increase in red emission, 507 nm red excitation and 571 nm red excitation was observed (Fig. 3.1a).

Similar trends were observed for *Echinophyllia*, with green fluorescence emission (515 nm, ex = 450 nm) increasing under 476 nm light. Red fluorescence emission (581 nm, ex = 530 nm) and excitation (571 nm, em = 620 nm) decreased down to ~50% of the initial values. In contrast, red fluorescence appeared essentially unchanged in comparison to pre-treatment values when excited in the green excitation band (507 nm). Colonies

of *Echinophyllia* kept under 448 nm and 412 nm light, however, showed no major difference in the measured tissue fluorescence values during the experiment (Fig. 3.1b).

The ratio of red-to-green fluorescence emission values provides an indication of the relative proportions of unconverted (green) and converted (red) protein. For both *M. cavernosa* (Fig. 3.1a) and *Echinophyllia* (Fig. 3.1b), the ratio remained relatively stable over time when the corals were exposed to 412 nm light, with values comparable to those of colonies kept under metal halide, while it showed a decreasing trend under 448 nm light and an even larger decrease under 476 nm light. The ratio between the red fluorescence excitation values recorded at 571 and 506 nm was also constant under 412 nm light, while it stabilised at a lower value under 448 and 476 nm light Fig. 3.1a,b).

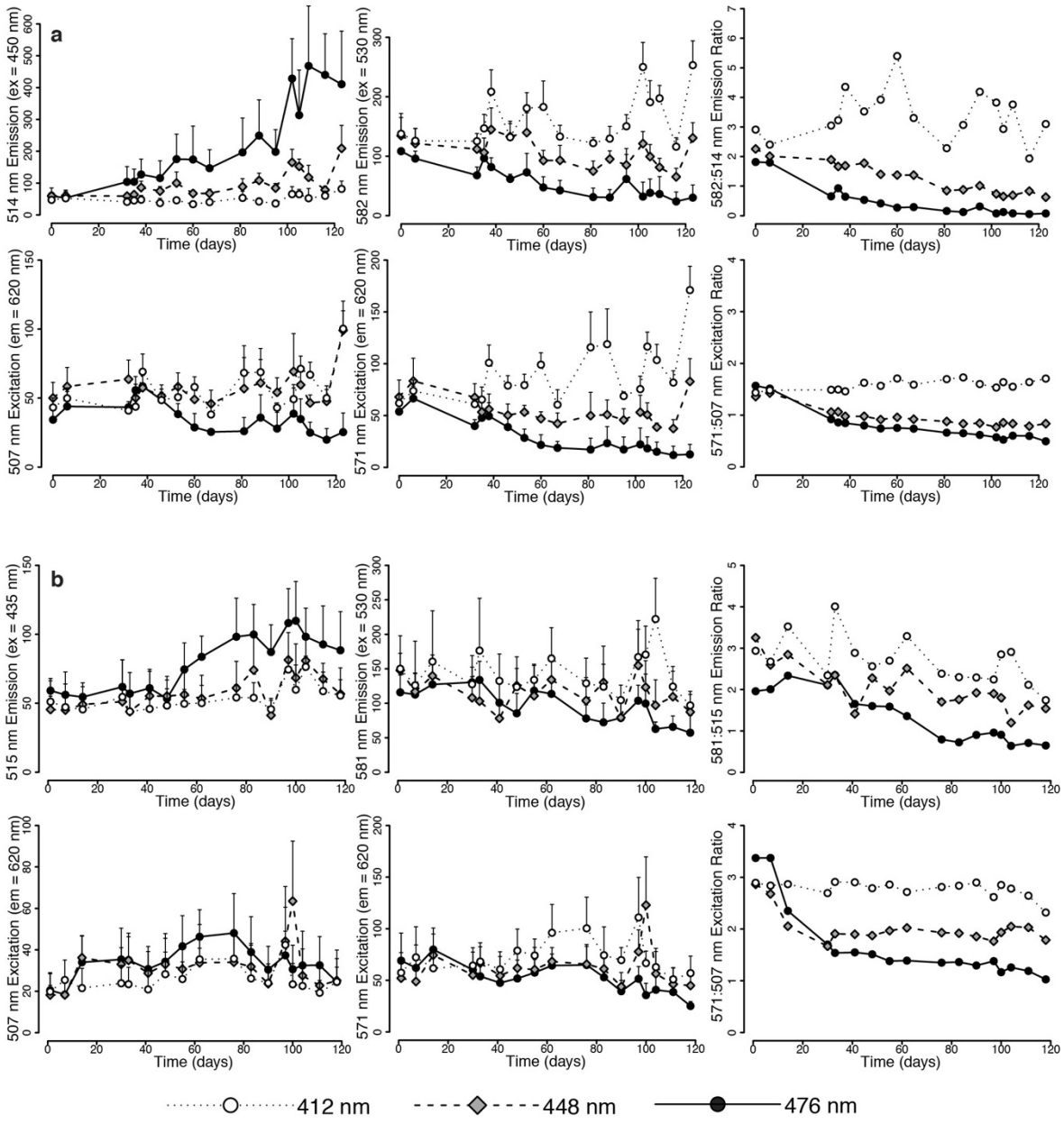

Figure 3.1 ***In vivo*** **fluorescence of** ***M. cavernosa*** **and** ***Echinophyllia*** **sp. during 123 days exposure to 476, 448 and 412 nm light**

(**a**) *M. cavernosa*: green emission (514 nm) measured with 450 nm excitation, red emission (582 nm) with 530 nm excitation, and 507 and 571 nm excitation measured for 620 nm emission; (**b**) *Echinophyllia* sp.: green emission (515 nm) measured with 435 nm excitation, red emission (581 nm) measured with 530 nm excitation, and 507 and 571 nm excitation measured for 620 nm emission. Mean + standard deviation (s.d.), n = 6.

3.3.1.2 Microscopic and spectroscopic characterization of tissue fluorescence

Microscopic imaging of the control colonies of *M. cavernosa* kept under white metal halide light revealed prevalent red fluorescence across the coenosteum, with green fluorescence of the tentacles (Oswald *et al.*, 2007) contributing to the fluorescence of the polyps (Fig. 3.2a). Spectroscopic measurements showed a red emission (excitation) peak at 582 (571) nm, along with a smaller green peak at 514 (507) nm (Fig. 3.2b). *M. cavernosa* kept under 412 nm light had retained red coenosteum fluorescence, while green fluorescence was still visible exclusively in the oral region of polyps (Fig. 3.2a); emission and excitation spectra matched those measured in the white light control colonies (Fig. 3.2b). When kept under 476 nm LED, on the other hand, the coenosteum showed dominant green fluorescence (Fig. 3.2a) and a corresponding increase in the green emission and excitation peak (Fig. 3.2b). The colony exposed to 448 nm light appeared as an intermediate stage, with both red and green fluorescence observable across the tissue (Fig. 3.2a); the emission and excitation spectrum were characterised by double peaks in the green and red regions (Fig. 3.2b).

Prevalence of red fluorescence was also observed for colonies of *Echinophyllia* kept under metal halide or 412 nm LED (Fig. 3.2c). The red emission (excitation) spectrum peaked at 581 (571) nm, and a small green excitation peak was detected at 507 nm. However, the emission spectrum showed a strong peak around 480 nm, indicating the contribution of cyan fluorescent pigments (Fig. 3.2d). Kept under the 476 nm LED, the coral tissue appeared yellow in fluorescence micrographs, indicating a mixture of red and green fluorescence (Fig. 3.2c). The emission spectrum showed an increase in the cyan peak relative to red emission values, as well as in the contribution of green fluorescence with a maximum around 507 nm visible as a pronounced shoulder on the 480 nm emission peak. The green excitation maximum was equal in magnitude to the red peak (Fig. 3.2d). *Echinophyllia* sp. kept under 448 nm light showed an intermediate appearance between those under 476 and 412 nm.

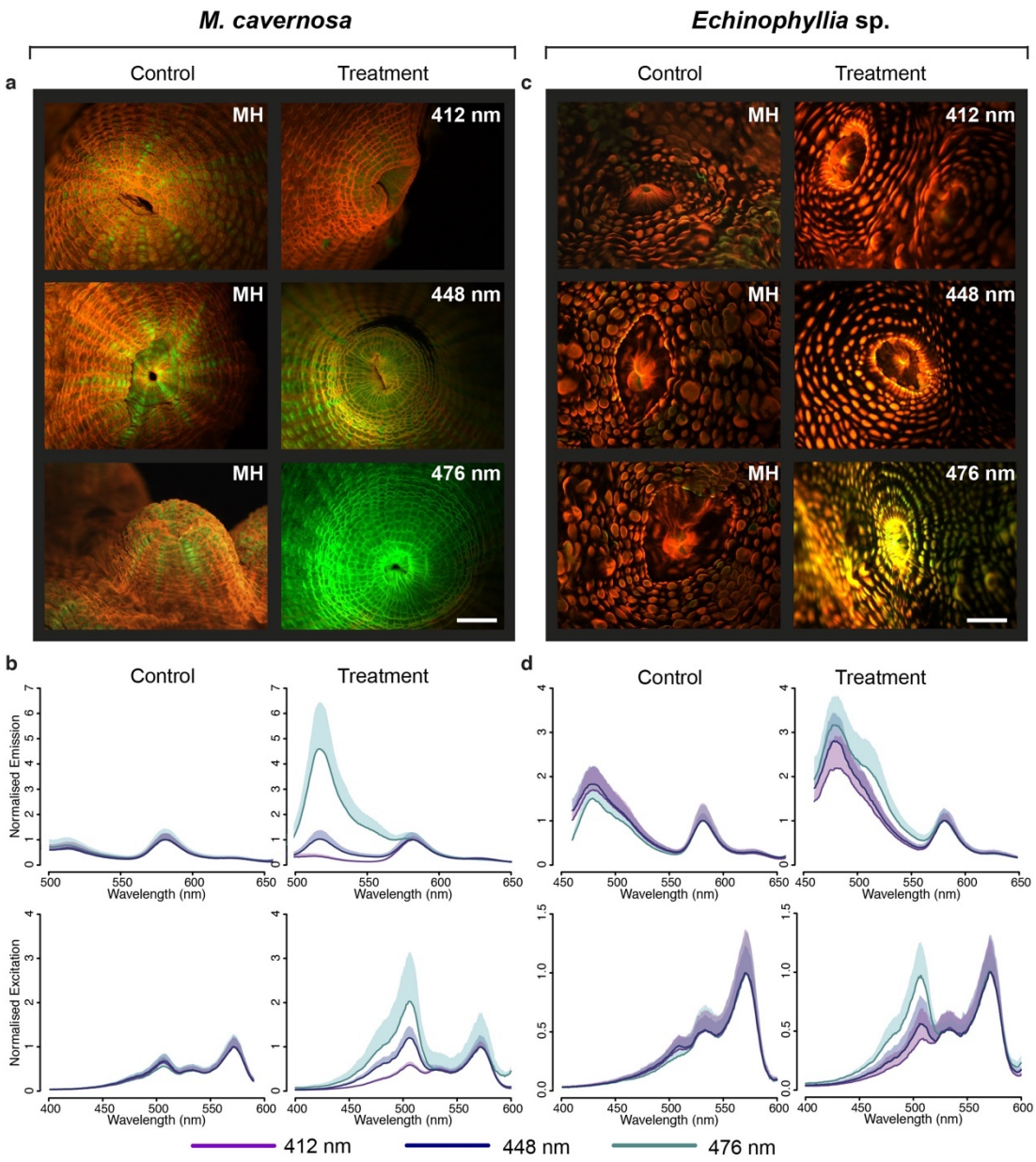

Figure 3.2 Fluorescence of *M. cavernosa* and *Echinophyllia* under metal halide or narrow-waveband light-emitting diode (LED)

(**a**,**c**) Fluorescent micrographs of *M. cavernosa* (**a**), and *Echinophyllia* sp. (**c**) under metal halide (MH; control) or narrow-waveband LED (412 nm, 448 nm, 476 nm; treatment); scale bar = 2 mm; (**b**,**d**) Emission spectra obtained with: 450 nm excitation for *M. cavernosa* (**b**), and 435 nm for *Echinophyllia* sp. (**d**) Excitation spectra obtained for 620 nm emission. Mean + s.d., n = 6. Spectra are normalised to intensity of the 582 nm peak.

3.3.1.3 Purified pcRFPs

To test whether the changes in fluorescence of live coral tissue can be reproduced with purified pcRFPs *in vitro*, we produced the major pigments of *M. cavernosa* (McavRFP), *L. hemprichii* (EosFP) and *Echinophyllia echinata* (EechRFP) in a bacterial expression system. Aliquots of the purified proteins in their green, unconverted state were exposed to light from the same 412 nm, 448 nm and 476 nm LEDs. Photon irradiance was set to 60 μmol photons $m^{-2}s^{-1}$ to match the photon irradiance used in the *in vivo* experiment and the corresponding equivalent depths. Consistently with what observed in live colonies, 476 nm light was ineffective for photoconversion and no changes in red fluorescence emission (581-582 nm, ex = 530 nm) were observed after one hour. Exposure to 412 nm light was most efficient in producing the red fluorescent photoconversion product. In contrast, only a small increase in red emission was observed for pcRFPs under the 448 nm LED (Fig. 3.3).

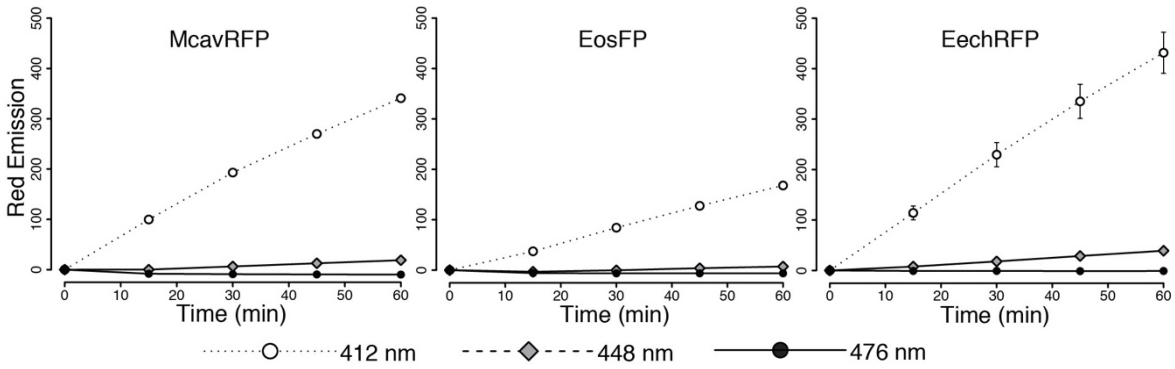

Figure 3.3 *In vitro* photoconversion of purified pcRFPs under 412, 448 and 476 nm light

Photoconversion measured as red (580-581 nm) fluorescence emission (ex = 530) every 15 min for 60 min under 60 μmol photons $m^{-2}s^{-1}$. Mean ± s.d., n = 3.

3.3.2 Photoconversion along a simulated depth-irradiance gradient

To quantify the photoconversion potential of light within the depth range of mesophotic corals, we exposed aliquots of purified, unconverted McavRFP, EosFP, and EechRFP to a series 412 nm light treatments with intensities comparable to those measured along a depth gradient in the Red Sea (Fig. 3.4a). At all intensities, the abundance of the red chromophore measured as fluorescence emission intensity at 580-581 nm (ex = 530 nm) was found to increase linearly with time (Supplementary Table 3.1). For all proteins, photoconversion was fastest at intensities corresponding to the 10 m depth light field and decreased with decreasing intensity. At all intensities, photoconversion was fastest for EechRFP, followed by McavRFP and EosFP.

Since the increase in red emission was essentially linear over the duration of the experiment, the slope of fitted regression lines represents the photoconversion rate for each protein at the specified photon irradiance. When plotted against the simulated depth gradient, the decrease in photoconversion rates can be described by an exponential function (Fig. 3.4b). The model equations and results of statistical analysis are given in Supplementary Table 3.2.

Red fluorescence of the purified protein solutions was compared before and after a 2 h exposure to 0.5 μmol photons $m^{-2}s^{-1}$ in the 412 nm band, a photon irradiance corresponding to a simulated depth of 80 m. The change in red emission over the exposure period was found to be statistically significant (RM-ANOVA, $F_{(5,8)} = 2364.29$, $p < 0.001$), and post-hoc comparison with Tukey's Honest Significant Difference (HSD) test showed that this was the case for all three pcRFPs under study (Fig. 3.4c).

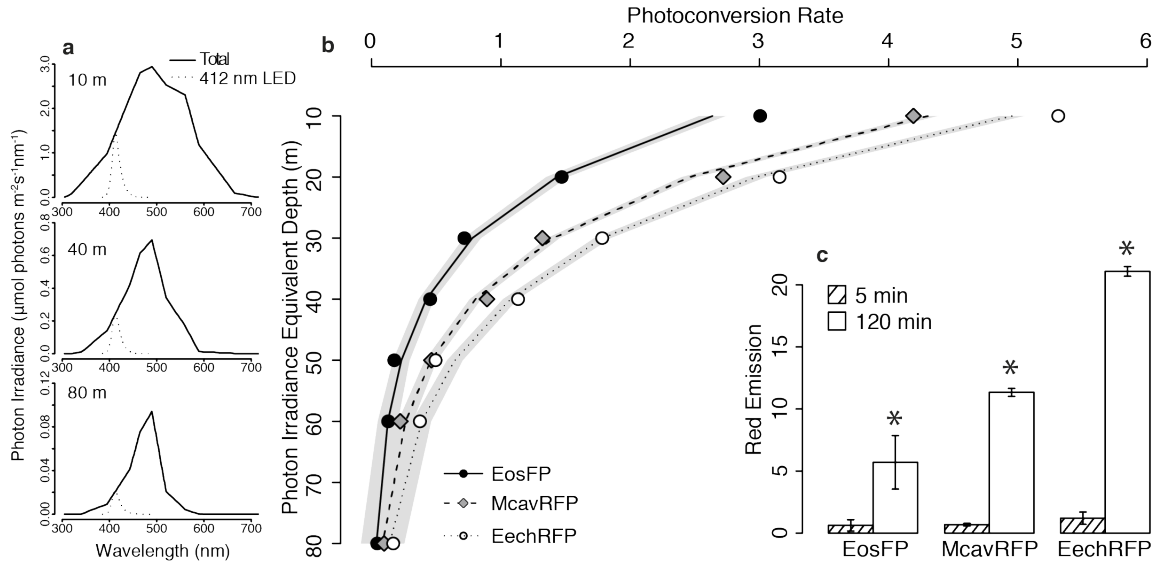

Figure 3.4 Photoconversion of purified McavRFP, EosFP and EechRFP along a simulated depth gradient

(**a**) Scaling of 412 nm LED to photon irradiance measurements at 10, 40 and 80 m in the Red Sea (Eyal *et al.*, 2015); values for total photon irradiance and scaled 412 nm photon irradiance are provided in Supplementary Table 3.1; (**b**) Photoconversion rates of pcRFPs along 412 nm photon irradiance gradient. Points represent the slope of the linear regression equation obtained measuring red fluorescence emission (580-581 nm, ex = 530 nm) during photoconversion every 1 min for 2 h (n = 3 conversions per protein per photon irradiance). Lines represent fitted exponential decay function ±95% c.i. Details and results of statistical analysis are provided in Supplementary Table 3.2. (**c**) Red fluorescence emission (580-581 nm, ex = 530 nm) of purified pcRFPs after 2 h exposure to 0.5 µmol photons $m^{-2}s^{-1}$ from 412 nm LED, comparable to the photon irradiance in the same range at 80 m depth in the Red Sea. Mean ± s.d., n = 3. Stars indicate $p < 0.001$ in post-hoc comparison (Tukey's Honest Significant Difference) following Repeated Measures Analysis of Variance (RM-ANOVA), $F_{(5,8)} = 2364.29$, $p < 0.001$.

3.3.3 Wavelength transfer by Förster Resonance Energy Transfer (FRET)

To investigate whether FRET between the green and the red fluorescent chromophores occurred in live colonies, we placed *M. cavernosa* from the 476 nm light treatment under the 412 nm LED and monitored tissue fluorescence over 10 days. Green (514 nm) emission (ex = 450 nm) decreased within 34 h to 50% of the initial values before reaching a plateau. Red (582 nm) emission (ex = 530 nm) showed the opposite trend, with a value up to five-fold higher being reached after 100 h (Fig. 3.5a). These values were normalised for use as proxy for red and green chromophore concentration, which appeared consistent with the kinetics of a second order reaction with a rate coefficient of 0.03 (non-linear least squares, $p < 0.001$, Fig. 3.5a, Supplementary Table 3.3).

To estimate FRET, we used the FRET-sensitised emission measurement - i.e., emission of the red chromophore (582 nm) upon blue light excitation (450 nm) - to calculate the FRET-derived emission intensity (Fig. 3.5b). This measurement indicated that FRET contribution increased very rapidly during the first hour of the experiment. The rate of increase started to reduce after ~22 h; the maximal FRET contribution values were reached after 100 h (Fig. 3.5b). The same calculation was applied to the data obtained from the long-term 412 nm light treatment, which showed that FRET-derived emission was stable at a low level for the first half of the experiment, and increased in the second half up to maximum values comparable to those reached in the short-term experiment (Fig. 3.5c).

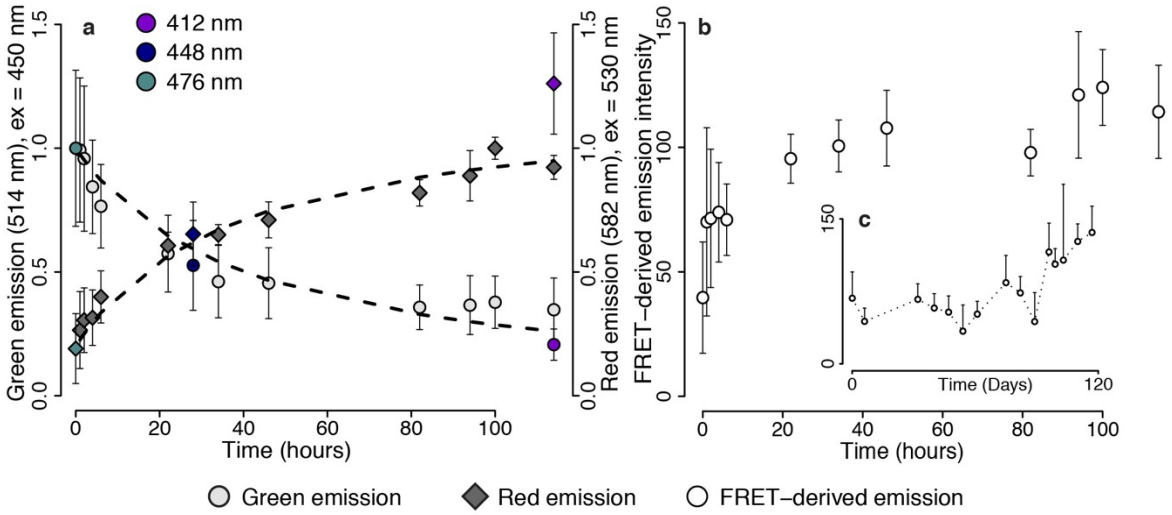

Figure 3.5 ***In vivo*** **photoconversion of green** ***M. cavernosa*** **under 412 nm light**

The colony had been previously kept under 476 nm light for >123 days. (**a**) Green (514 nm) emission measured over 110 h with 450 nm excitation light; red (582 nm) emission measured with 530 nm excitation light. Dashed lines show fitted second order reaction rate models; model equations and results of statistical analysis are provided in Supplementary Table 3.3. Coloured data points show values after long-term exposure to 412, 448 and 476 nm light; (**b**,**c**) FRET-derived emission intensity (582 nm) measured with 450 nm excitation light and corrected according to Eq. 3.2-3.4. Values calculated for short-term exposure to 412 nm LED after acclimation with 476 nm LED, means ± s.d., n = 5 (**b**); and for long-term exposure to 412 nm LED after acclimation with white metal halide, means + s.d., n = 6 (**c**).

3.3.4 Efficiency of FRET-mediated wavelength transfer

To assess the capacity of pcRFPs to convert blue-green light into yellow-red fluorescence *in vitro*, we compared the wavelength transfer efficiency of EosFP at various photoconversion stages with those of the red fluorescent protein eqFP611. Upon excitation at 506 nm, partially converted EosFP samples had considerably higher emission intensity in the 550-700 and 560-610 nm range per µg of functional protein as compared to eqFP611 (Fig. 3.6a–c). Partially photoconverted EosFP with a >3:1 ratio of green to red chromophores (EosFP 2) generated orange-red emission that was ~2.4 times higher than the same protein amount of eqFP611. At a ~1:1 ratio of green and red chromophores of EosFP (EosFP 3), the wavelength conversion of EosFP per µg of protein was ~3.3-fold higher than that of eqFP611 (Fig. 3.6c, Supplementary Table 3.4).

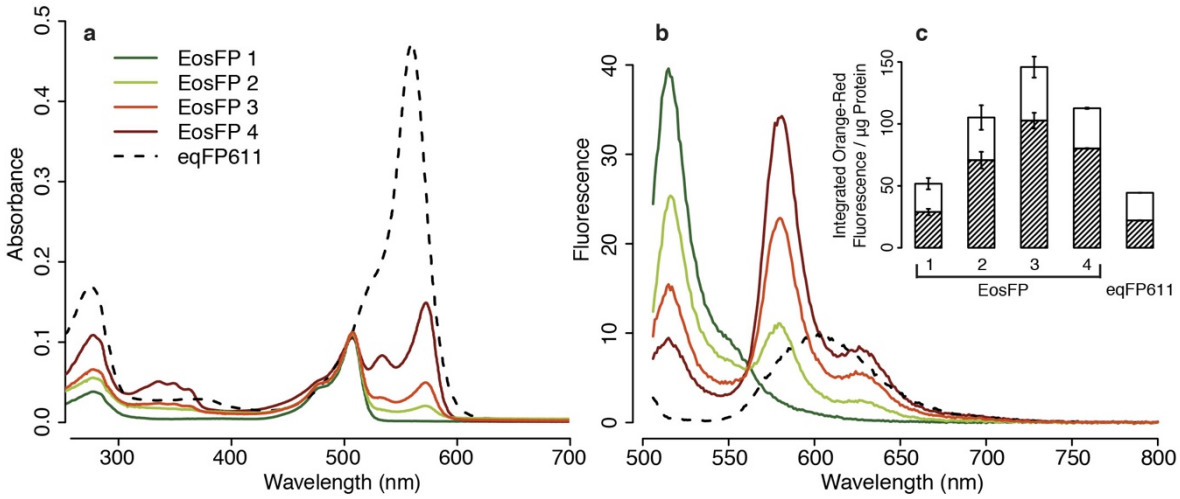

Figure 3.6 Spectra of purified EosFP at various photoconversion stages vs. eqFP611

1 = green EosFP; 2,3,4 = partially converted EosFP. Absorbance (**a**); and fluorescence (**b**) spectra; and integrated fluorescence values (**c**) of protein aliquots diluted in PBS pH 7.4 to 0.1 absorbance at 506 nm. Fluorescence spectra obtained with excitation set to 506 nm. Integrated fluorescence normalised to µg functional protein, concentrations are provided in Supplementary Table 3.4. Integrated orange–red fluorescence values measured between 550 and 700 nm, shaded areas represent 560-610 nm portion. (**a**,**b**) Mean, n = 3; (**c**) mean ± s.d., n = 3.

3.4 Discussion

With growing anthropogenic pressure on shallow water reefs (Hughes *et al.*, 2003), mesophotic ecosystems have been suggested as potential refugia for coral communities (Glynn, 1996; Bongaerts *et al.*, 2010). Since the light environment changes dramatically with depth, the knowledge of how corals and their symbiotic algae can cope with low irradiances and narrow spectra is crucial to understand the capability of various species to survive at greater depths.

pcRFPs have been mostly reported from depth generalist corals (Alieva *et al.*, 2008) and were encountered in individuals collected from mesophotic depths (Eyal *et al.*, 2015). Their expression is not regulated at the transcriptional level by light intensity as compared to counterparts in shallow water corals (Leutenegger *et al.*, 2007a; D'Angelo *et al.*, 2008; Gittins *et al.*, 2015). Together with the finding that their red fluorescence was under positive selection during the evolution of coral FPs (Field *et al.*, 2006), these observations suggest that these pigments could be part of an adaptation strategy to life in low light environments (Schlichter *et al.*, 1986; Salih *et al.*, 2000). The red fluorescent chromophore of pcRFPs, integral to their function, is generated by a post-translational modification of a green fluorescent precursor in a photoconversion process induced by near-UV light. However, while blue-green light penetrates down to the lower limits of the euphotic zone, near-UV wavelengths required for photoconversion and maintenance of red fluorescence in coral colonies are strongly attenuated by the water column, dropping to very low levels at mesophotic depths (Clarke and James, 1939; Jerlov, 1976; Schlichter *et al.*, 1986). Therefore, it is questionable whether a light-driven photoconversion is at all relevant for the adaptation of coral to their natural light environment.

3.4.1 Effects of spectral quality on photoconversion of pcRFPs

Using narrow-waveband LED technology in an experimental study, we were able to address this question and assess the effects of different parts of the light spectrum on the photoconversion of coral pcRFPs, both *in vivo* and *in vitro*. Our >120 days mesocosm experiment showed that the spectral quality has a strong influence on fluorescence of pcRFP-containing corals. Under the narrow-band LED spectrum, only corals exposed to 412 nm light were able to retain ratios of red-to-green fluorescence comparable to those observed under white light; corals exposed to 448 and 476 nm light showed increasing levels of green fluorescence, indicating accumulation of unconverted pcRFPs in the tissue.

The 476 nm light used in our experiment had no spectral overlap with the photoconversion action spectrum (Ando *et al.*, 2002; Wiedenmann *et al.*, 2004a), thus being ineffective in

inducing the post-translational modification both *in vivo* and *in vitro*. The observed increase in green fluorescence reflects the accumulation of unconverted protein in the tissue, caused by failure of newly synthesised protein to photoconvert into the red form. At the same time, red fluorescence decreased due to progressive decay of the converted protein fraction, previously shown to occur in the dark with a half-life of ~20 days (Leutenegger *et al.*, 2007a), as well as photobleaching caused by prolonged excitation of the chromophore with 476 nm light treatment (Salih *et al.*, 2006; Leutenegger *et al.*, 2007a). Exposing purified proteins to the same light conditions yielded comparable results to those obtained for live colonies.

We exposed the purified pcRFPs to a series of different intensities of 412 nm light to simulate the attenuation of downwelling near-UV irradiance in coral reef habitats (Kirk, 1994). While differences in the individual photoconversion rates exist among the pcRFPs under study, all of them showed an exponential decrease, thus appearing to depend entirely on photon irradiance in the near UV range. As our mesocosm experiment results show that photoconversion is near-UV dependent *in vivo*, we assume this exponential trend to also be relevant for live corals in situ. Importantly, even at a photon irradiance as low as 0.5 μmol photons $m^{-2}s^{-1}$, corresponding to values measured at 80 m in the Red Sea (Eyal *et al.*, 2015), we observed successful albeit slow photoconversion of EosFP, McavRFP, and EechRFP after just 2 h of exposure. This suggests that despite stronger attenuation of UV and near-UV compared to blue-green wavelengths by the water column, photoconversion of pcRFPs can indeed happen in the mesophotic zone.

3.4.2 Wavelength transformation via FRET

As demonstrated by our *in vitro* experiments, partially converted pcRFP tetramers represent ideal donor-acceptor FRET pairs due to the close proximity of green and red chromophores in the tetrameric assemblage of the protein (Wiedenmann *et al.*, 2004a; Nienhaus *et al.*, 2005). As a result, green emission of the individual tetramer disappears in presence of even a single photoconverted subunit in EosFP (Wiedenmann *et al.*, 2004a). Consequently, the photoconversion process will alter the emission properties of pcRFPs, starting with a green light emitting pigment that absorbs blue-green light, and then shifting to a mixture of green and red emitting chromophores that still absorb mostly blue-green light but emit predominantly orange-red light. This appears as an intriguing mechanism to transform parts of the blue-green wavelengths that dominate the underwater light field at greater depths into orange-red wavelengths. In this way, the corals may compensate for the depth-dependent attenuation of longer wavelength light and produce an internal light field that more closely resembles the conditions in shallow water.

To assess whether FRET could be a mechanism for wavelength transformation in live *M. cavernosa*, we calculated the FRET-derived emission for a colony pre-treated with 476 nm light undergoing photoconversion. This was achieved by measuring the emission of the red acceptor upon excitation of the green donor (FRET-sensitised emission) and applying a correction to remove spectral contribution by donor emission and by direct acceptor excitation, an approach analogous to the three-filter methodology used in FRET microscopy (Gordon *et al.*, 1998; Hoppe *et al.*, 2002; Müller *et al.*, 2013).

With progressive appearance of red fluorescence during photoconversion we observed a rapid increase in FRET-derived emission, which can be attributed to the increasing acceptor concentration (Wolf *et al.*, 2013). In live colonies, a stabilisation of FRET levels can be expected from the steady-state equilibrium that results from the continuous depletion of red acceptor chromophores by photobleaching and protein turnover (Wiedenmann *et al.*, 2004a; Leutenegger *et al.*, 2007a) and the constitutive expression of pcRFPs, which supplements the pool of green donor chromophores (Leutenegger *et al.*, 2007a). The maximum FRET value for a colony in a given light field will thus depend on: (i) the number of photons available to excite the red and the green chromophores, respectively, causing photobleaching directly and via FRET; (ii) light intensity in the spectral range efficient for photoconversion; and (iii) the protein turnover rate.

After 22 h under a photon irradiance of 60 μmol photons $m^{-2}s^{-1}$ provided by the 412 nm LED, FRET-derived emission began to saturate and it reached its maximum after 100 h. These values were comparable with those obtained under the same light condition in the long-term exposure experiment. While the ratio of green and red fluorescent chromophores in the individuals from the 412 nm treatment is comparable with the ratio determined for the corals cultured under metal halide illumination, both green and red fluorescence emission is lower in the latter corals. This is likely due to the broad spectrum of the metal halide light, which excites both chromophore types very well, resulting in increased levels of photobleaching (Wiedenmann *et al.*, 2004a) and a steady-state equilibrium that contains fewer functional chromophores.

Therefore, when colonies acclimated to the metal halide spectrum were transferred to the LED experiments, the steady-state equilibrium of green and red chromophores characteristic of the 412 nm light condition only became evident after complete turnover of the pool of pigments present at the beginning of the experiment, a slow process that occurs with a half-life of about three weeks (Leutenegger *et al.*, 2007a).

With increasing simulated depth, both photoconversion and photobleaching rates are reduced, producing colonies with a mixture of green and red chromophores. Our *in vitro* experiments with EosFP show that most efficient conversion of blue-green excitation

wavelengths into orange-red fluorescence emission is achieved at roughly equal concentrations of green donor and red acceptor chromophores. Although a 1:3 red:green configuration within a single EosFP tetramer is sufficient to produce efficient FRET (Wiedenmann *et al.*, 2004a), in more complex systems, such as purified proteins in solution or native proteins in animal tissue, a 1:1 ratio maximises the number of partially converted tetramers, thereby achieving the highest potential for FRET-mediated wavelength conversion. Such a ratio resulted from the long-term exposure of *M. cavernosa* to the 448 nm LED. The photoconversion capacity of this light source at a photon irradiance of 60 μmol photons $m^{-2}s^{-1}$ is comparable to that of the Red Sea light field at ~80 m depth. Hence, the results of this experiment provide evidence that FRET-derived production of orange-red light is promoted in the mesophotic depth range, despite the reduced amount of light effective for photoconversion.

In pcRFPs, FRET-mediated fluorescence with excitation/emission maxima of 506/581 nm results in a Stokes shift of 75 nm and, hence, efficient short-to-long wavelength transfer. This Stokes shift is up to three times larger compared to red fluorescent proteins from shallow water corals (Alieva *et al.*, 2008; Gittins *et al.*, 2015), suggesting that FRET-mediated wavelength transformation is an efficient mechanism to supplement the corals and their symbiotic algae with orange-red light that becomes increasingly rare at greater depth. To assess this hypothesis, we compared the potential for blue-green to yellow-red wavelength conversion of partially photoconverted EosFP with that of the non-photoconvertible red protein eqFP611 (Wiedenmann *et al.*, 2002). This protein was selected for its absorption maximum similar to that of red EosFP, the high degree of red fluorophore maturation, the bright fluorescence and the exceptionally large Stokes shift of 52 nm (Wiedenmann *et al.*, 2002). We found that a partially converted EosFP with a ~1:1 ratio of red:green chromophores is over 3x more efficient at converting blue-green light into the 550–700 nm range (>6x in the 560–610 nm range) than the same amount of eqFP611. Considering the metabolic efforts required to reach the high pigment concentrations found in coral tissue (Oswald *et al.*, 2007; Gittins *et al.*, 2015), our results indicate that FRET-mediated wavelength transformation by partially converted pcRFPs is indeed an energetically favourable mechanism to produce orange-red light.

Remarkably, efficient FRET coupling within the tetrameric assemblage has also been found in the red fluorescent protein drFP583 (DsRed) from the disc anemone *Discosoma* sp. (Matz *et al.*, 1999; Baird *et al.*, 2000). In this protein, a mixture of green and red chromophores is generated during the maturation process of the red chromophore, driven by a light-independent oxidation of the chromophore precursor. While the fluorescence properties of both the green and the red chromophores of DsRed and pcRFPs are similar, they have evolved independently from a green fluorescent

common ancestor (Alieva *et al.*, 2008). Notably, *Symbiodinium*-associated disc anemones such as *Discosoma* sp. often dwell in shaded habitats (Kuguru *et al.*, 2008) which suggest that FRET-mediated wavelength transformation has evolved as an adaptation to light-limited habitats at least twice.

It has been suggested that fluorescent pigments in mesophotic corals such as *Leptoseris* sp. act to modify the quality of light available to the symbionts (Schlichter *et al.* 1986; Salih *et al.*, 2000; Field *et al.*, 2006; Eyal *et al.*, 2015). It was hypothesised that granules of host pigments localised within gastrodermal cells below the symbionts could transform short wavelength light into longer, more photosynthetically active wavelengths, which could stimulate symbiont photosynthesis via backscattering (Schlichter *et al.* 1986; Salih *et al.* 2000). Our study demonstrates a remarkable mechanism by which pcRFPs can fine-tune the internal light climate of symbiotic corals along the steep gradient of light quantity and quality that characterises their habitat. Further work should improve our understanding of the significance of orange-red light generated by the FRET-mediated wavelength transfer for the adaptation to low-light environments.

3.5 Materials and methods

3.5.1 Sample culture and aquarium set up

Colonies of *M. cavernosa* (Linnaeus, 1767) and *Echinophyllia* sp. Klunzinger 1879 were cultured and propagated by fragmentation in the Coral Reef Laboratory mesocosm facility (D'Angelo and Wiedenmann, 2012). Prior to the start of the experiment, fragments were kept under a 400 W metal halide lamp (AquaMedic UK, Coalville, UK). To test the influence of the spectral quality of incident light on the photoconversion process, the corals were placed under Aquaray LED strips: (1) Aquaray NUV (emission peak wavelength: 412 nm); (2) Aquaray Fiji Blue (emission peak wavelength: 448 nm); and (3) Aquaray Reef Blue (emission peak wavelength: 476 nm) (TMC, London, UK). LED emission spectra were measured with a USB4000 modular spectrophotometer (Ocean Optics, Dunedin, FL, USA) and are provided in Supplementary Fig. 3.7. PVC pipes were attached under the individual LEDs to restrict the exposure of the replicate corals to stray light from neighbouring LEDs to negligible levels. Photon irradiance was set to ~50-60 μmol photons $m^{-2}s^{-1}$ as measured with a PAR light meter at water surface level (LI-COR, Lincoln, NE, USA). Specimens were acclimatised to the narrow-waveband light regime through progressive increase in daily exposure time over 11 days (1 to 4 h over 3 days, followed by 4 days at 4 h, then 2 h increase daily), after which the photoperiod was set to 12 h light:12 h dark. Colonies were kept under experimental conditions for a total of 123 days including acclimation time.

3.5.2 Live colony fluorescence

In vivo measurements of fluorescence emission/excitation were performed using a fluorescence spectrophotometer (Cary, Varian, Palo Alto, CA, USA) equipped with a fibre optic probe (D'Angelo *et al.*, 2008). Emission spectra were recorded with excitation 450 and 530 nm (for *M. cavernosa*) or 435 and 530 nm (*Echinophyllia* sp.). Excitation spectra were collected using the 620 nm emission band. Six defined areas on each colony were used as replicate measurements. Fluorescence micrographs were obtained with a camera-equipped wide-field fluorescence microscope (MZ10 F, Leica Microsystems, Wetzlar, Germany) using a GFP Plus filter.

3.5.3 Protein expression and purification

Competent *Escherichia coli* cells were transformed with plasmids (pQE30, pGEM-t) containing the coding sequences for the functional expression of the pcRFPs McavRFP, EosFP, and EechRFP, and grown on LB-ampicillin agar plates. The 5 most fluorescent colonies of each protein type were used to inoculate 300 mL 2xYT liquid cultures; the cultures were incubated overnight at 30 °C, then transferred to 4 °C and shaken at 135 rpm in the dark for 11 to 17 days until they exhibited strong green fluorescence (Wiedenmann *et al.*, 2002). Harvested cells were disrupted by sonication and centrifuged at 7000 rpm at 4 °C for 10 min. Proteins were purified from the supernatant by Immobilised Metal Ion Affinity Chromatography (IMAC) using TALON® Metal Affinity resin (Clontech, Mountain View, CA, USA); the eluate was desalted in Amicon centrifugal filters (Merck Millipore, Darmstadt, Germany) and re-buffered in TRIS (50 mM, 300 mM NaCl), pH 8.2 to recreate the internal pH of live coral colonies (Kühl *et al.*, 1995; Al-Horani *et al.*, 2003). The solutions were diluted in the same buffer until optical density values at 505 nm reached 0.12 to minimise inner filter effects from self-shading of the chromophores in the solution.

3.5.4 Photoconversion and spectroscopy of purified proteins

Field measurements of spectral irradiance in the Red Sea were obtained as courtesy of Eyal et al. (2015). Irradiance values at each measurement wavelength were converted into photon irradiance following Eq. 3.1:

$$\Phi_P = \frac{E_e}{E_P \times N_A} \qquad \text{Equation 3.1}$$

where Φ_P is the photon irradiance in μmol $m^{-2}s^{-1}$, E_e is the irradiance at measurement wavelength in Wm^{-2}, E_P is the energy of a photon at measurement wavelength (calculated following Planck-Einstein relation) in J, and N_A is Avogadro's number. For each depth level in the dataset, the spectrum of the 412 nm LED was scaled to match the natural values at peak wavelength to determine the LED photon irradiance required to simulate the light environment at the respective depth. LED total photon irradiance was then inferred by integrating this curve.

Aliquots (375 µL) of the purified protein solution were placed in a 500 µL quartz cuvette in a fluorescence spectrophotometer (Cary Eclipse, Varian, Palo Alto, CA, USA). The 412 nm LED strip was placed directly above the cuvette holder and photon irradiance was adjusted with a controller (TMC, London, UK) to match the corresponding value in the natural depth profile. The aliquots were then irradiated for 120 min and red fluorescence emission spectra were recorded at 1 min intervals using 530 nm light provided by the spectrometer for excitation. The conversion experiments were repeated 3 times per protein for each simulated depth level. Maximal fluorescence emission values at 580 nm (EosFP) or 581 nm (McavRFP and EechRFP) were plotted against time. The increase in fluorescence over time could be best-fitted with linear models and the resulting slopes were used to infer photoconversion rates and to fit a linear regression after natural logarithm transformation.

For comparison of photoconversion efficiency of the 412, 448 and 476 nm spectral bands, the respective LED strip was in turn placed above the cuvette and intensity was set to 60 μmol photons $m^{-2}s^{-1}$; for the 412 nm LED, this value corresponded to the amount of light in the same spectral band that would be received by corals at ~7 m depth. Three replicate conversion experiments per protein type and spectral band were performed. Red emission spectra (excitation 530 nm) were recorded every 15 min for 1 h. During measurements, the LEDs were switched off to avoid additional excitation by the 448 and 476 nm light sources.

3.5.5 Photoconversion potential of light sources

For each depth in the Red Sea field photon irradiance dataset, the published action spectrum of photoconversion for EosFP (Wiedenmann *et al.*, 2004a) was used to calculate the relative probability that a photon in the light field would trigger a photoconversion event. These probabilities were fitted with a log-linear model to obtain an equation relating photoconversion potential with depth. The same probability calculation was applied to the spectra of the 412, 448, and 476 nm LEDs (Supplementary Fig. 3.7a, 60 μmol photons $m^{-2}s^{-1}$) and to the spectrum of a metal halide (Supplementary Fig. 3.7b,

200 μmol photons $m^{-2}s^{-1}$); these probabilities were then used with the previously obtained equation to calculate an equivalent depth of photoconversion potential for each of our experimental light sources.

3.5.6 Estimation of FRET in live colonies

Following the exposure to 476 nm light for 123 days, *M. cavernosa* was placed under a 412 nm LED strip with photon irradiance set to 60 μmol photons $m^{-2}s^{-1}$ (12 h:12 h, light:dark) and photoconversion was monitored over 10 days. Emission spectra were collected with excitation wavelength set to 450 and 530 nm. Normalised 514 nm emission (ex = 450 nm) and 582 nm emission (ex = 530 nm) were used as proxy for green and red chromophore concentrations, and fitted with integrated second order rate reaction models using non-linear least squares for parameterisation.

In order to quantify FRET at different stages of photoconversion, we calculated the FRET-derived emission intensity for each set of measurements following the approach of Müller et al. (2013), Eq. 3.2:

$$FRET = I_F - \alpha I_A - \beta I_D \qquad \text{Equation 3.2}$$

where I_F is the FRET-sensitised donor emission, αI_A is the acceptor spectral bleed through caused by direct excitation of the acceptor by donor excitation wavelength, and βI_D is the donor spectral bleed through caused by direct emission of the donor at the acceptor emission wavelength. For each measurement in the dataset we used 582 nm emission (ex = 450 nm) as I_F, 582 nm emission (ex = 530 nm) as I_A, and 514 nm emission (ex = 450 nm) as I_D (n = 5).

In order to estimate donor and acceptor spectral bleed through, we measured I_F, I_A, and I_D for fully unconverted and fully converted samples of purified pcRFPs. These values were then used to calculate the parameters α and β according to Eq. 3.3 and 3.4 (Hoppe *et al.*, 2002; Müller *et al.*, 2013):

$$\alpha = \frac{I_F}{I_A} \qquad \text{Equation 3.3}$$

where I_F and I_A are measured for fully converted protein;

$$\beta = \frac{I_F}{I_D} \qquad \text{Equation 3.4}$$

where I_F and I_D are measured for fully unconverted protein. The same approach was applied to calculate the FRET-derived emission for *M. cavernosa* exposed to 412 nm LED during the 123 days time series.

3.5.7 Evaluation of wavelength conversion *in vitro*

In order to compare the potential for wavelength conversion of pcRFPs with that of other cnidarian RFPs, we performed spectroscopic measurements on aliquots of purified EosFP (Stage 1: unconverted; Stages 2-4: partially converted) and eqFP611 (Wiedenmann *et al.*, 2002). Partial photoconversion was achieved by placing aliquots under 412 nm LED and monitoring absorbance every 5 min, until the desired red:green ratios were achieved. Both proteins were diluted in PBS pH 7.4 until absorbance at 506 nm reached a value of 0.1; absorbance spectra of 100 µL aliquots were measured with a spectrophotometer (Cary 50 Scan, Varian, Palo Alto, CA, USA) in a 10 mm quartz cuvette (3 replicate measurements) and blank-corrected. Fluorescence spectra of the same aliquots were measured in a fluorescence spectrophotometer (Cary Eclipse, Varian, Palo Alto, CA, USA) with excitation wavelength set to 506 nm (3 replicate measurements) and blank-corrected. Two integrated fluorescence values were calculated, one in the yellow to red range ($\int_{550}^{700} f(\lambda)d\lambda$) and one in the yellow-amber range ($\int_{560}^{610} f(\lambda)d\lambda$). Integrated fluorescence values were normalised to µg functional protein, calculated from the measured absorbance after spectral decomposition and the published extinction coefficients of each chromophore (Wiedenmann *et al.*, 2002, 2004a).

3.6 Supplementary Figures

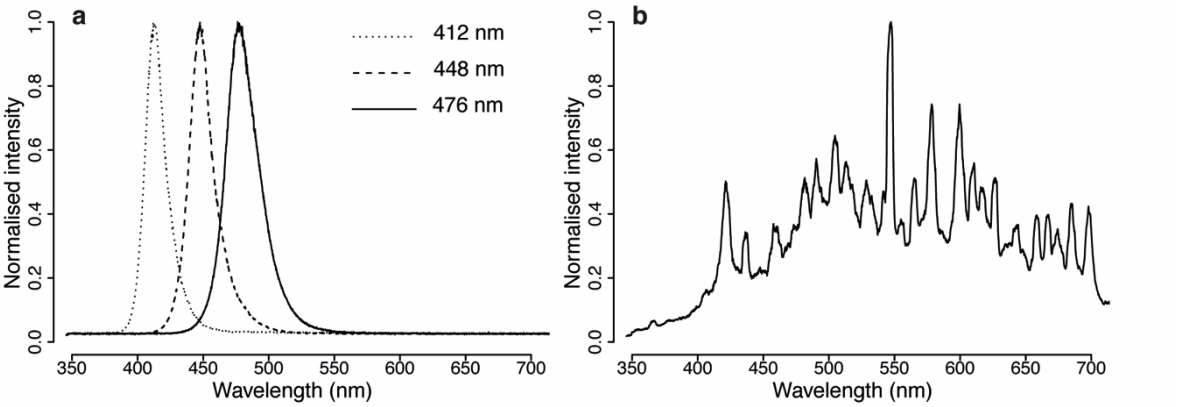

Figure 3.7 Spectra of light sources

(**a**) Spectra of 412 nm (Aquaray NUV), 448 nm (Aquaray Fiji Blue) and 476 nm (Aquaray Reef Blue). (**b**) Spectrum of 400 W metal halide lamp.

3.7 Supplementary Tables

Table 3.1 Linear regression results for photoconversion of purified proteins

Measured field photon irradiance, calculated 412 nm photon irradiance and linear regression results for each depth. Tot. ph. f. = total photon irradiance (μmol photons $m^{-2}s^{-1}$). 412 nm ph. f. = 412 nm photon irradiance (μmol photons $m^{-2}s^{-1}$)

			McavRFP			**EosFP**			**EechRFP**		
Depth (m)	Tot. ph.f.	412 nm ph.f.	Slope	R^2 adj	p	Slope	R^2 adj	p	Slope	R^2 adj	p
10	525	30.70	4.19	0.99	<0.001	3.01	1.00	<0.001	5.31	0.99	<0.001
20	219	14.60	2.72	0.99	<0.001	1.47	1.00	<0.001	3.16	1.00	<0.001
30	108	7.30	1.32	1.00	<0.001	0.72	0.99	<0.001	1.78	0.99	<0.001
40	74.4	5.29	0.89	1.00	<0.001	0.45	0.98	<0.001	1.13	0.99	<0.001
50	39.5	2.65	0.46	0.99	<0.001	0.17	0.99	<0.001	0.49	1.00	<0.001
60	20.4	1.30	0.22	0.96	<0.001	0.13	0.99	<0.001	0.37	1.00	<0.001
80	7.15	0.44	0.10	0.94	<0.001	0.04	0.81	<0.001	0.17	0.99	<0.001

Table 3.2 Details of regression analysis for slopes as a function of depth

	Model	R^2 adj	p
McavRFP	$e^{2.02 - 0.06 \times depth}$	0.99	<0.001
EosFP	$e^{1.59 - 0.06 \times depth}$	0.99	<0.001
EechRFP	$e^{2.11 - 0.05 \times depth}$	0.99	<0.001

Table 3.3 Model equations and statistical test results for non-linear least squares analysis of normalised green and red fluorescence of *M. cavernosa* during photoconversion.

	Model	**k Estimate**	**SE**	**t-value**	**p**
Green Emission	1/(k*x+1)	0.025	0.003	9.163	<0.001
Red Emission	y0+1-(1/k*x+1)	0.026	0.002	13.06	<0.001

Table 3.4 Absorbance maxima after spectral decomposition of purified FPs, and calculated concentration values.

Abs = Absorbance, Conc = concentration

	Green chromophore		**Red Chromophore**		
Protein	Abs	Conc µgµL^{-1}	Abs	Conc µgµL^{-1}	**Total conc µgµL^{-1}**
EosFP Stage1	0.108	0.039	-	-	0.039
EosFP Stage2	0.11	0.039	0.021	0.013	0.052
EosFP Stage3	0.1	0.036	0.05	0.031	0.067
EosFP Stage4	0.067	0.024	0.149	0.094	0.118
EqFP611	-	-	0.472	0.158	0.158

Chapter 4 Bleaching corals express bright colours to facilitate recovery

4.1 Abstract

Coral bleaching, caused by the loss of brownish-coloured photosymbionts from the tissue of reef-building corals, is a major threat to reef survival. Occasionally, bleached corals become extremely colourful rather than white. These colours derive from photoprotective green fluorescent protein (GFP)-like pigments produced by the coral host. There is currently no consensus regarding what causes colourful bleaching events, and whether the perceived increase in colours is an ecophysiologically significant upregulation of the photoprotective pigments or an optical artefact associated with the declining symbiont density. Here we show that the increase of light fluxes in symbiont-depleted tissue induces strong host pigment expression. We demonstrate that corals increase the production of photoprotective pigments to mitigate light stress in symbiont-free tissue to facilitate recolonization by symbionts. Our data show that extreme colouration can help predict the recovery potential from distinct bleaching events, and identify local environmental drivers that can exacerbate the impact of elevated temperatures on corals.

4.2 Main text

In 2015-2017, the world's coral reefs experienced the most extensive and devastating mass coral bleaching ever recorded (Hughes *et al.*, 2017). The increasing frequency and extent of these events has been linked to anthropogenic climate change and poses a major threat to coral reef functioning, productivity and biodiversity (Hughes *et al.*, 2017). Rising sea water temperatures are the main driver of this phenomenon (Williams and Bunkley-Williams, 1990), although a number of environmental factors, including nutrient stress, are known to induce bleaching and/or increase the susceptibility of corals to thermal stress (Gleason and Wellington, 1993; Anthony *et al.*, 2008; Wiedenmann *et al.*, 2013). Bleaching is the breakdown of the symbiosis between reef-building corals and *Symbiodinium* dinoflagellates (zooxanthellae) harboured in the host gastrodermal cells, which supply part of the host's metabolic requirement via photosynthate translocation (Muscatine, 1990). The term bleaching refers to the whitening of the animal tissue caused by the loss of symbionts and their photosynthetic pigments, such as chlorophyll and peridinin (Jeffrey and Haxo, 1968), which are responsible for the brownish colouration of healthy corals (Hochberg *et al.*, 2004; Oswald *et al.*, 2007).

In some instances, bleaching renders corals vibrantly green, orange or purple-blue rather than white. These colours derive from green fluorescent protein (GFP)-like pigments found in high concentrations in the host tissue of many reef-building corals (Salih *et al.*, 2000; Dove *et al.*, 2001; Oswald *et al.*, 2007). This group of homologous pigments includes fluorescent proteins (FPs) containing a light-absorbing chromophore which emits red-shifted wavelengths (Shimomura, 1979), and chromoproteins (CPs) that strongly absorb light in the visible range but emit few or no photons (Alieva *et al.*, 2008). Many FPs and CPs found in shallow water corals are localised in the ectoderm of the host coral tissue and are transcriptionally regulated by blue light intensity (D'Angelo *et al.*, 2008), providing photoprotection for the gastrodermal symbionts by screening of excess light (Salih *et al.*, 2000; Smith *et al.*, 2013; Gittins *et al.*, 2015; Quick *et al.*, 2018).

Despite the incidence of brightly coloured corals during mass coral bleaching, the mechanisms involved and the ecological significance of these changes in colouration remain unknown. In 2010, colourful bleaching events were reported from Taytay Bay, Philippines (Fig. 4.1a) and from Lizard Island, Great Barrier Reef (GBR) (Fig. 4.1b, Supplementary Fig. 4.6). In Taytay Bay, corals exhibited extreme colouration after being exposed to temperatures that marginally exceeded the local bleaching threshold, ahead of a major heat stress episode (Supplementary Fig. 4.7a). On Lizard Island, colourful bleaching followed a heat stress episode that was short and mild compared to other years (Supplementary Fig. 4.7b) during which widespread coral bleaching and mortality was reported from the GBR (Hughes *et al.*, 2018); no mortality was observed in the aftermath. In both cases, extreme colours were observed ~3 weeks after the bleaching threshold was first exceeded (Supplementary Fig. 4.7).

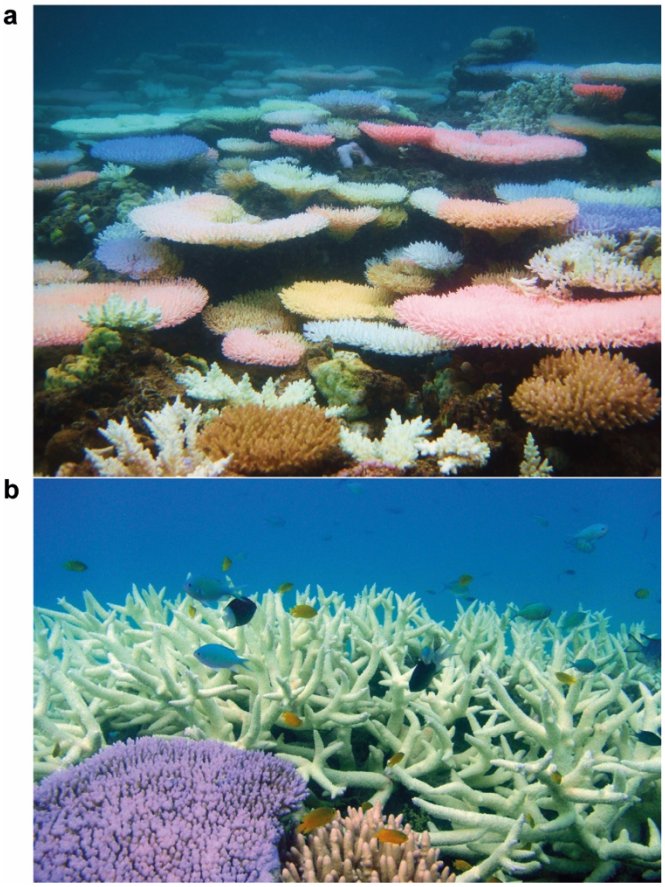

Figure 4.1 Colourful corals during bleaching events in 2010

Coral bleaching in Taytay, Palawan, Philippines (**a)** (credit: Ryan Goehrung) and Lizard Island, Great Barrier Reef, Australia (**b) (**credit: Morgan Pratchett). The bright colours are due to photoprotective green fluorescent protein (GFP)-like pigments expressed in the host tissue.

Previous experimental studies have shown that heat stress causes a downregulation of coral pigments, and suggested that increase in the fluorescence of bleached corals is due to enhanced excitation and emission light fluxes in the absence of "shading" by the symbionts (Smith-Keune and Dove, 2008; Roth and Deheyn, 2013). In this case, the change in colouration would have no functional significance for the corals. Conversely, the enhanced light fluxes in bleached coral tissue (Enríquez *et al.*, 2005; Wangpraseurt *et al.*, 2017) may cause upregulation of photoprotective FPs and CPs as shown for the symbiont-free growth zones of healthy corals where these pigments are thought to facilitate colonisation by symbionts (D'Angelo *et al.*, 2012; Smith *et al.*, 2013). Under this scenario, the enhanced coral pigmentation would be of eco-physiological importance as the associated increase in photoprotection could promote recovery from bleaching. To test this hypothesis, we applied a biomarker approach in three representative model coral species, using light-regulated FPs and CPs as indicators for altered photon fluxes in coral tissue (D'Angelo *et al.*, 2008).

Cyan FPs (CFPs) are usually expressed at low light intensity and their concentration in coral tissue becomes saturated or reduces at high light intensities (D'Angelo *et al.*, 2008). In contrast, CPs and green FPs (GFPs) in shallow water species are commonly expressed under higher photon fluxes and their tissue concentrations increase with the intensity of incident blue light (D'Angelo *et al.*, 2008). Our model coral *Porites lichen* expresses a CFP with a 489 nm emission peak and low light induction threshold, and a 519 nm emitting GFP with high induction threshold (Fig. 4.2a,b), a combination of pigments representative of many species from shallow reefs (Alieva *et al.*, 2008; D'Angelo *et al.*, 2008) and ideally suited as biomarkers for light exposure. As predicted, during high-light acclimation of healthy corals, the 519 nm to 489 nm ratio of fluorescence emission increases over time, following a saturating exponential function, reflecting the changes in the tissue concentration of both proteins (Fig. 4.2c,d). Following bleaching by focussed red light stress (Wijgerde *et al.*, 2014), an identical in change in 519 nm to 489 nm fluorescence ratio was observed in colonies of *P. lichen* that were exposed to blue light, but not in those that were exposed to green light (Fig. 4.2e,f). The latter experiment unambiguously demonstrates that differential changes in host pigment expression are not an intrinsic response to bleaching stress, but an independent bioindicator for changes in the quantity and spectral quality of the light experienced by corals. In the present study, we used this unique reporter system for non-invasive monitoring of changes in the internal light climate in bleaching corals.

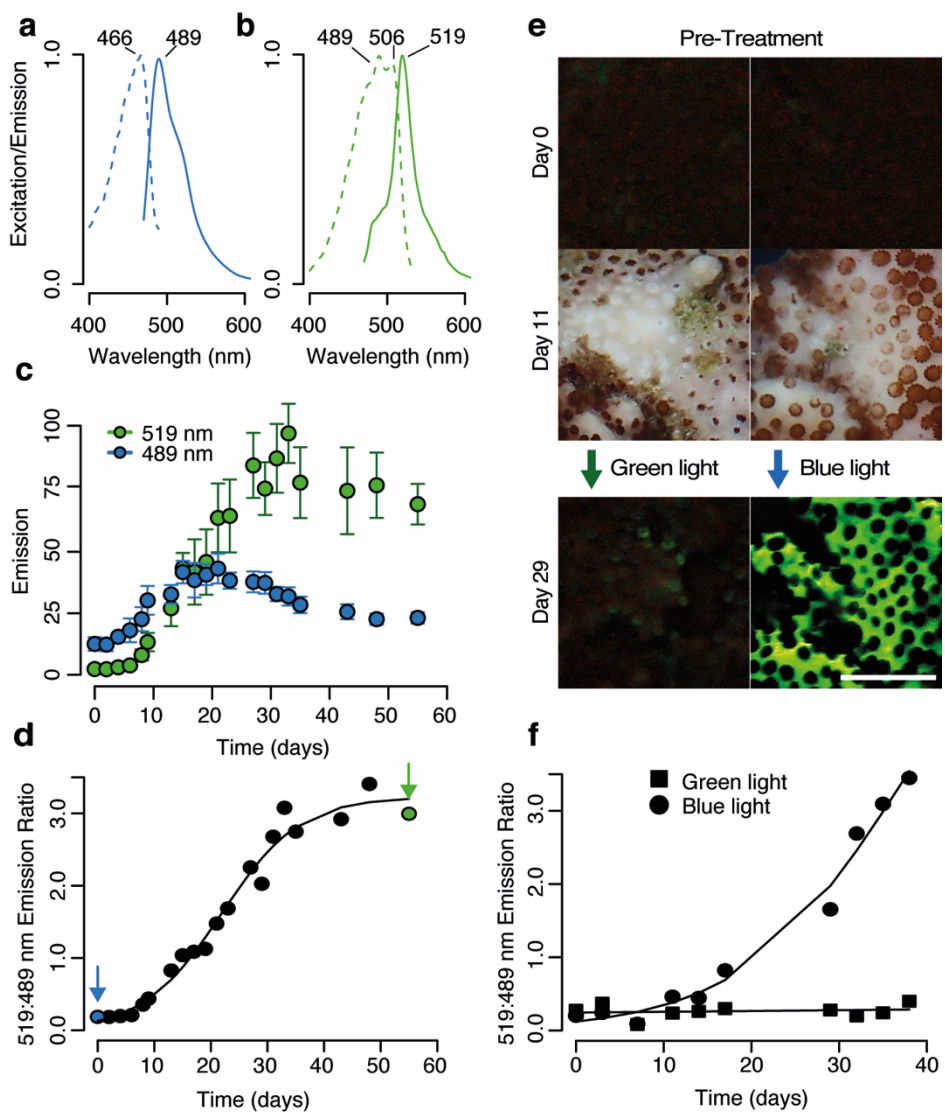

Figure 4.2 Photoacclimation of *Porites lichen* indicated by changes in host pigment levels

(**a**, **b**) *In vivo* spectral characterisation of *P. lichen* under low (**a**) and high (**b**) light. Dashed lines: excitation (emission = 550 nm). Solid lines: emission (excitation = 450 nm). (**c**) Time course of green (519 nm) and cyan (489 nm) emission during acclimation of unbleached colonies to ~290 µmol photons m^{-2} s^{-1}. Mean ± s.d., n = 6. (**d**). Time course of green:cyan emission ratio during high light acclimation of unbleached colonies. Arrows indicate time points for collection of spectra in (**a**) (cyan) and (**b**) (green). (**e**) Photographs of *P. lichen* before bleaching (Day 0, fluorescence image), after bleaching with focussed red light (Day 11, white light image), and after exposure to green or blue light (Day 29, fluorescence image). Scale 10 mm. (**f**) Time course of green:cyan emission ratio for bleached colonies exposed to green or blue light.

To assess whether thermal bleaching can induce a light-driven upregulation of FPs, and cause the extreme colours observed in the field, we exposed colonies of *P. lichen* to gradually increasing temperatures up to 31-32°C. We used 680 nm fluorescence as indicator of changes in the amount of photosynthetic symbiont pigment in the coral tissue since this fluorescence band is specifically caused by photosystem II (PSII) emission and a function of PSII concentration (Falkowski and Kiefer, 1985). Fluorescence spectra collected from heat-stressed colonies of *P. lichen* showed a rapid drop in 680 nm emission (ex=450 nm) at temperatures ≥31°C (Fig. 4.3a). While the variability of PSII fluorescence quantum yield under environmental stress puts some limitations to the use as truly quantitative marker for photosynthetic pigment concentration (Falkowski and Kiefer, 1985), our symbiont cell counts confirmed that the drop in chlorophyll fluorescence was due to a loss of symbionts and corresponded to the onset of bleaching (Fig. 4.3b). Bleaching resulted in strongly increased light fluxes at the colony surface measured as spectral reflectivity (Wangpraseurt *et al.*, 2012) (Supplementary Fig. 4.8a). In particular, the absence of photosynthetic pigments of the symbionts resulted in increased blue light fluxes in the spectral range that is responsible for the upregulation of FPs and CPs in shallow water species (D'Angelo *et al.*, 2008). Fluorescence emission of the high-threshold GFP increased following bleaching, and exceeded 100x pre-treatment values after the acute heat stress treatment was terminated (Fig. 4.3a,c). The fluorescence intensity ratio of GFP (high induction threshold) and CFP (low induction threshold) increased following a saturating exponential function (Fig. 4.3d), as recorded for healthy corals during high light acclimation (Fig. 4.2d) and for bleached corals exposed to blue light (Fig. 4.2f). Furthermore, host protein extracts exhibited significantly higher GFP fluorescence when normalised to total protein or the corresponding coral surface area (Fig. 4.3e). Importantly, all meaningful increases in tissue fluorescence occurred after the symbionts were lost from the tissue; the timescale of this response is consistent with the interval between the onset of heat stress and observations of colourful bleaching in the Philippines and on Lizard Island in 2010 (Fig. 4.1, Supplementary Fig. 4.6, 4.7). Together, these data provide evidence that extreme colouration of bleached corals is due to increased pigment concentrations in the host tissue and not caused by an optical artefact resulting from the absence of symbionts. This also explains upregulation of a CP-coding gene previously detected in corals during natural bleaching (Seneca *et al.*, 2010).

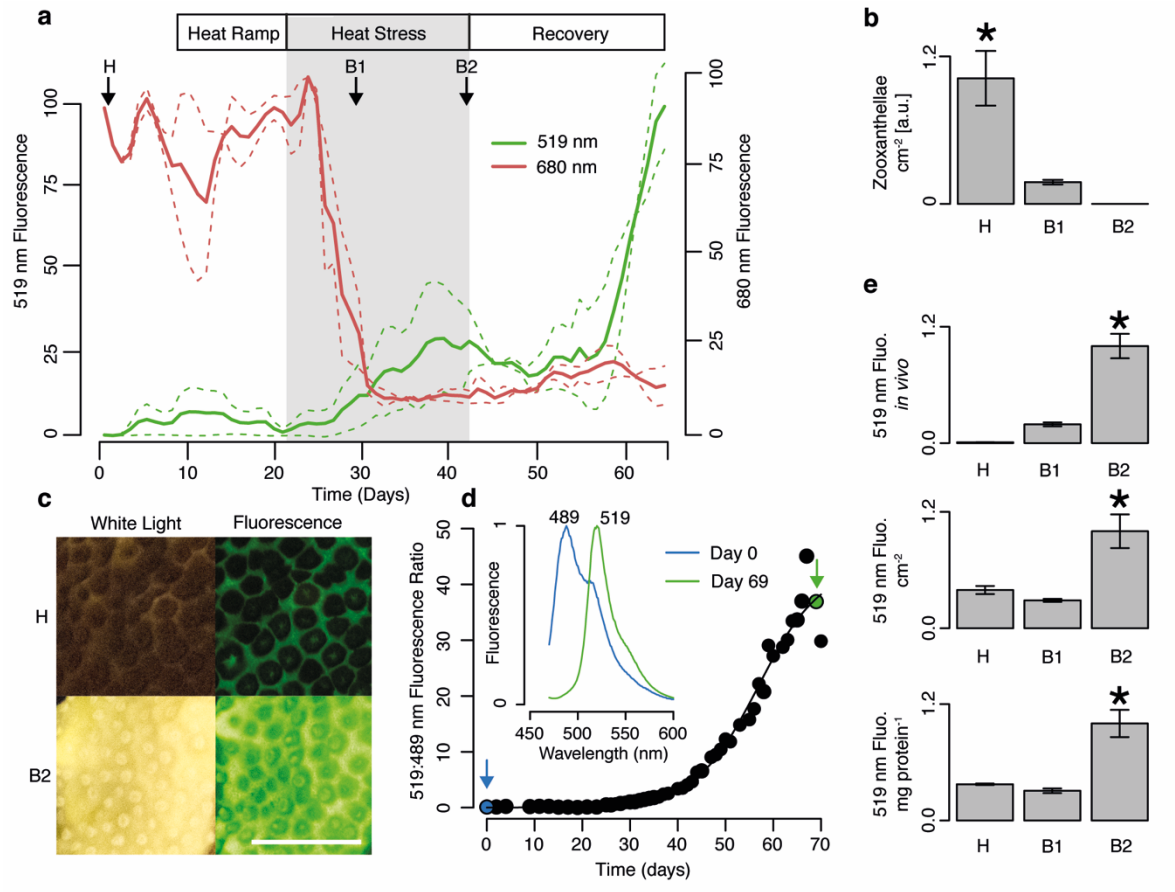

Figure 4.3 Fluorescence of Porites lichen undergoing thermal bleaching

(**a**) Time series of *in vivo* host GFP (519 nm) and chlorophyll (680 nm) fluorescence emission during treatment. Dashed lines show means of fully independent experiments (n = 6); solid lines show midpoint. H: healthy; B1: partially bleached; B2: bleached. (**b**) Zooxanthellae cell counts. (**c**) Photographs of H and B2 (white light or 450 nm excitation). Scale 10 mm. (**d**) Ratio of GFP (519 nm) to CFP (489 nm) fluorescence emission during treatment, with *in vivo* spectra taken at time points indicated. (**e**) Host GFP (519 nm) fluorescence measured *in vivo* (top), as emission of host tissue homogenate normalised to colony surface area (middle) and to total host protein (bottom). In (**b**) and (**e**), bars show mean ± s.d., n = 3; asterisks show $p<0.05$.

To test whether colourful bleaching may indicate also other forms of environmental stress, we applied nutrient stress as a heat-independent stressor to induce bleaching. Phosphate starvation caused by elevated levels of dissolved inorganic nitrogen (DIN) has been shown to cause chemically imbalanced growth of the photosymbionts, resulting in alteration of the membrane lipid complement, impairment of photochemistry and eventually bleaching (Wiedenmann *et al.*, 2013; Rosset *et al.*, 2017). Accordingly, colonies of *P. lichen* kept under high nitrate/low phosphate (HN/LP) conditions (Wiedenmann *et al.*, 2013) bleached gradually as signified by the loss of symbionts from the tissue and the corresponding decrease of chlorophyll fluorescence (Supplementary Fig. 4.9a,b). As expected, the light fluxes increased as indicated by the higher surface reflectivity (Supplementary Fig. 4.8b). GFP emission and concentration increased accordingly during bleaching (Supplementary Fig. 4.9a,c,e) and the fluorescence intensity ratio of high to low induction threshold pigments increased exponentially (Supplementary Fig. 4.9d). We also assessed the host pigment response to bleaching in *Pocillopora damicornis*, a species capable of expressing high levels of a pink CP (Dove *et al.*, 1995) that belongs to the group of highlight-induced, photoprotective pigments of shallow water corals (D'Angelo *et al.*, 2008; Smith *et al.*, 2013). As observed for green FPs in *P. lichen*, the pink CP of *P. damicornis* increases exponentially after bleaching only in the presence of blue light (Supplementary Fig. 4.10a,b). When exposed to nutrient stress, *P. damicornis* exhibited a colourful bleaching response (Supplementary Fig. 4.10c). Again, the visually striking change in colouration was the result of significantly higher host pigment concentrations in tissue extracts (Supplementary Fig. 4.10d) that can be attributed to an upregulation of pigment expression in response to the ~4x higher blue light fluxes detected at the surface of bleached colonies (Supplementary Fig. 4.10e).

Taken together, these data confirm that the enhanced coloration of bleached corals is caused by increased light fluxes in symbiont-free tissue, regardless of the stress that caused loss of symbionts.

Next, we tested whether the increase in host pigmentation promotes the recolonization by symbionts following bleaching. We used *Montipora foliosa* in this experiment as it can serve as a representative model for corals that show a strong expression of photoprotective CPs in symbiont-free growth zones such as colony margins (Fig. 4.4a,b), tips or areas of wound regeneration and interactions with epibionts (D'Angelo *et al.*, 2012). In these areas, the CPs reduce the internal light fluxes to facilitate the colonisation of newly formed tissue with symbionts (D'Angelo *et al.*, 2012; Smith *et al.*, 2013). After the corals were bleached by phosphate starvation (Fig 4.4a), the colour of the bleached areas changed to purple. The CP concentration in these parts of the colony matched those in the growth margins of healthy individuals (Fig 4.4c). When nutrient replete conditions were

restored, the corals recovered and their colour reverted to show the initial state where the CP expression is limited to the growth margins (Fig 4.4a). These observations provide further evidence that the colour changes observed during bleaching are part of a light-mediated feedback loop in which the expression of host pigments is influenced by the presence of the symbiont and vice versa (Fig. 4.5). Importantly, our experiment demonstrates that increased pigmentation in bleached corals can reach physiologically significant concentrations that could promote the recolonization with symbionts and aid in recovery of bleached corals. To provide experimental evidence for such a protective function, we locally bleached *P. damicornis* colonies by focussed light stress, then promoted or prevented CP production by exposure to blue or green light, respectively (Fig. 4.4d). Afterwards, the corals were exposed to white light illumination to monitor the recovery of the symbiont population in the presence or absence of enhanced levels of light-screening host pigments. The absorption properties of the corals indicated that tissue areas expressing high initial levels of pink CP (Fig. 4.4e) show a significant increase in amount of symbiont pigments after 25 days (Fig. 4.4f). Measurements conducted at this timepoint revealed that the changes in tissue absorption properties in the areas of increased levels of CP-mediated photoprotection held higher symbiont cell densities, indicative of a faster recovery of the symbiont population (Fig. 4.4g). In line with previous light-stress experiments (Smith *et al.*, 2013), the efficiency of symbiont photosynthesis indicated by photosystem II (PSII) maximum quantum efficiency (Fv/Fm) was significantly higher in areas that had a higher CP content (Fig. 4.4g). A decrease in Fv/Fm has been widely correlated with photoinhibition and photoprotective downregulation of PSII photochemistry in corals, and can be measured on a diel basis corresponding to the mid-day irradiance peak (Hoegh-Guldberg and Jones, 1999; Warner *et al.*, 2011). Lower Fv/Fm and an associated decline in the PSII D1 protein have also been identified as key features of symbiont damage in corals exposed to heat stress and during bleaching (Warner *et al.* 1999; Warner *et al.* 2011).

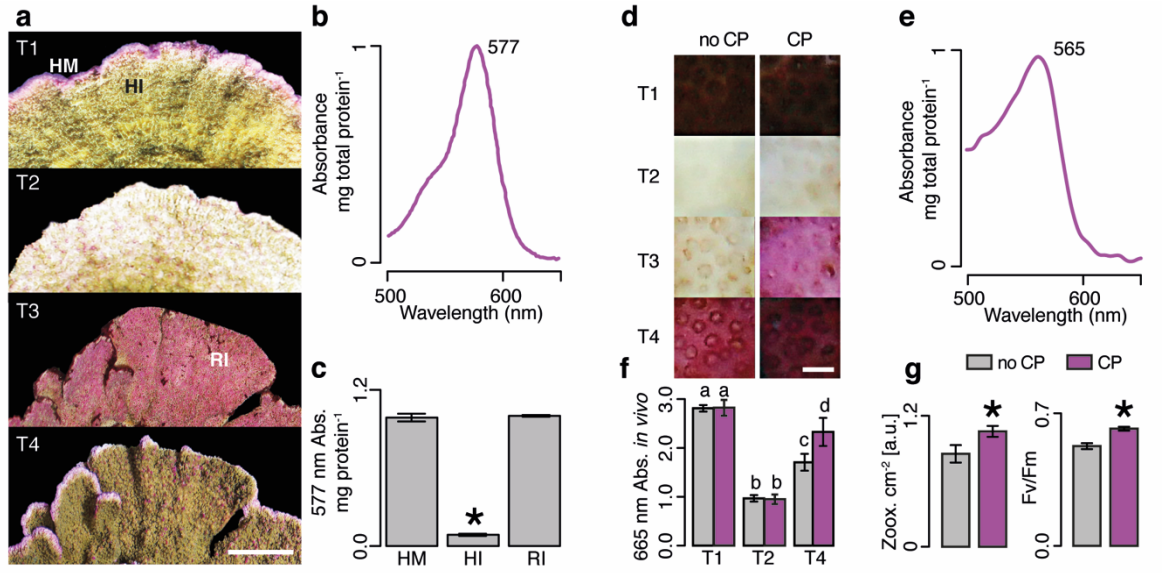

Figure 4.4 Chromoproteins and coral recovery from bleaching

(**a**) *M. foliosa* during nutrient-induced bleaching and recovery. T1. Pre-treatment (HM = healthy margin; HI = healthy inner region). T2. Bleached. T3. After 28 days recovery (RI = recovering inner region); T4. Fully recoverd coral, after 56 days. Scale 10 mm. (**b**) Absorbance spectrum of *M. foliosa* CP. (**c**) Absorbance of sampled host tissue. (**d**) Representative photographs of the time series of bleaching and recovery of *P. damicornis* with and without CP expression. T1: Pre-treatment. T2: Bleached. T3: After CP induction. T4: After 26 days recovery. Scale 3 mm. (**e**) Absorbance spectrum of *P. damicornis* CP. (**f**) Contribution of symbiont pigments to *in vivo* absorbance. (**g**) Zooxanthellae cell counts and photosynthetic quantum yield (Fv/Fm) for corals sampled at T4. In (**c**), (**f**), and (**g**), bars show mean ± s.d., n = 3; asterisks show $p<0.05$; letters show $p<0.05$ in post-hoc pairwise comparison.

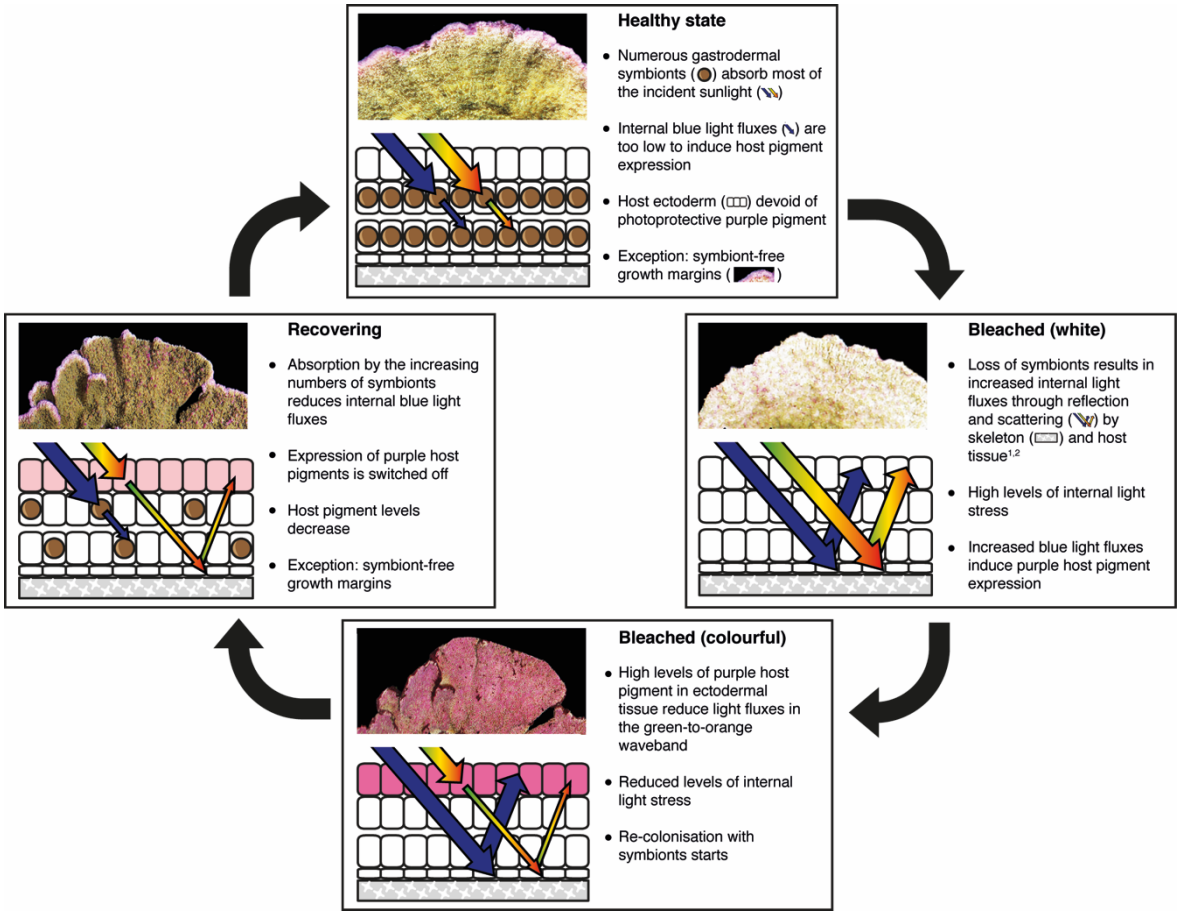

Figure 4.5 The host-symbiont feedback loop of light-mediated pigment expression in reef corals

Photographs show changes in colouration of *Montipora foliosa* during bleaching and recovery. Schematic drawings conceptualise the changes in light fluxes and gene expression in dependence of the concentration of symbiont cells and the photoprotective purple host pigment in the coral tissue.

References:

1. S. Enríquez, E.R. Méndez, R. Iglesias-Prieto, Multiple scattering on coral skeletons enhances light absorption by symbiotic algae. *Limnol. Oceanogr.* **50**, 1025–1032 (2005).

2. D. Wangpraseurt, A. W. D. Larkum, P. J. Ralph, M. Kühl, Light gradients and optical microniches in coral tissues. *Front. Microbiol.* **3**, 316 (2012).

This study shows that increased expression of photoprotective pigments, rendering some corals brightly coloured during mass bleaching episodes, is a mechanism that enables the host to minimise light fluxes and promote recovery. Why then, do corals exhibit extreme coral colouration only under certain circumstances? Since previous experimental work showed a downregulation of FPs expression in response to acute heat stress (Smith-Keune and Dove, 2008), we suspected that the intensity of the stress may play a critical role. Indeed, we consistently observed that replicate colonies of our *P. damicornis* model

exposed to acute heat stress bleached white and died, while colonies that were bleached by nutrient stress at ambient temperatures showed enhanced pigmentation and recovered (Supplementary Fig. 4.11). This is consistent with the 2010 climatology data showing that corals on Lizard Island and in Taytay Bay were exposed to temperatures that only marginally exceeding the local bleaching thresholds (Supplementary Fig. 4.7) before extreme colourations were observed (Fig. 4.1, Supplementary Fig. 4.6). Notably, in two other years, 2004 and 2013, heat stress exposure of corals on Lizard Island was higher than in 2010 (Supplementary Fig. 4.7b), yet no bleaching was reported (Hughes *et al.*, 2018). Either these bleaching episodes went unnoticed or other environmental parameters such as nutrient stress may have increased the bleaching susceptibility and resulted in extreme colouration of corals in 2010. In this scenario, colourful bleaching events could provide a useful visual warning that reefs are impacted by local stressors.

The question arises why only some corals produce high levels of photoprotective pigments when being bleached. This can be explained by the energetic costs of strongly expressing multiple copies (>8) of the relevant genes to achieve physiologically relevant tissue concentrations and the resulting balancing selection for genetically determined colour polymorphisms (Gittins *et al.*, 2015; Quick *et al.*, 2018). Depending on the genetic background of the colour morphs, their maximal capacity to produce pigments in response to light stress can differ significantly between individuals (Gittins *et al.*, 2015; Quick *et al.*, 2018).

We conclude that colourful bleaching is an emergency response that can facilitate the recovery of corals from mild stress events. In cases of rapid heating or strong heat stress, the host pigment production is not upregulated either because the transcription machinery is failing, or energy reserves are allocated to other stress responses such as the expression of heat shock proteins (Rosic *et al.*, 2014). As a consequence, the corals bleach mostly white under the latter conditions. The stress-level dependent variation in regulation patterns can also explain why the largest increase in fluorescence in our experiments was observed after the corals were relieved from acute heat stress (Fig. 4.3a).

In summary, our study highlights the ecophysiological significance of colourful bleaching and identifies an important role of the host in recovery of the symbiont population. We have also shown the potential of colourful bleaching to identify events during which the temperature tolerance of corals may be compromised by interacting stressors such as nutrient stress. In contrast to climate change related warming of seawater that needs to be addressed at a global level, the latter stressor can be managed at the regional scale, supporting efforts to mitigate the coral reef crisis in a two-pronged approach (D'Angelo

and Wiedenmann, 2014). Hence, future work should define the temperature thresholds for colourful bleaching and how the contribution of nutrient stress can be discriminated.

4.3 Materials and Methods

4.3.1 Field images collection

Coral colonies displaying enhanced host pigmentation were photographed on reefs in Taytay Bay, off the coast of Taytay, Palawan, Philippines (10°50'N, 119°32'E) on 10/06/2010 at a depth of ~6 m, and on Lizard Island, Northern Great Barrier Reef, Australia (14°40'S, 145°07'E) on 25/03/2010 at a depth of ~4 m.

4.3.2 Coral propagation and aquarium set up

Colonies of *Porites lichen* (Dana 1846), *Pocillopora damicornis* (Linnaeus 1758), and *Montipora foliosa* (Pallas 1766), were initially obtained from the UK ornamental trade and propagated in the Coral Reef Laboratory mesocosm facility for >10 years (D'Angelo and Wiedenmann, 2012). Fragments for experimental treatment were mounted flat on ceramic tiles to ensure an even distribution of incident light. The fragments were left to recover and grow for at least a month before the start of experimental treatments; for all corals, such acclimation phase was completed under replete nutrient conditions (Wiedenmann *et al.*, 2013), 24-26°C water temperature, and 12h:12h light:dark cycle.

4.3.3 Experimental treatments

4.3.3.1 High light treatment

Colonies of *P. lichen* were acclimated to 80 μmol photons $m^{-2}s^{-1}$ for 35 days, then exposed to 290 μmol photons $m^{-2}s^{-1}$ for 55 days.

4.3.3.2 Light-induced bleaching

Colonies of *P. lichen* and *P. damicornis* were bleached by exposure to 400 μmol photons $m^{-2}s^{-1}$ of red light (Wijgerde *et al.*, 2014) (Lumileds, peak wavelength λ=660 nm, full width at half maximum FWHM=40 nm) over 7 days. Colonies were then either placed under 100 μmol photons $m^{-2}s^{-1}$ of blue light (Lumileds, λ=450 nm, FWHM=40 nm) for 21 days to stimulate CP upregulation (D'Angelo *et al.*, 2008), or placed under an equal photon irradiance of green light (Lumileds, λ=530 nm, FWHM=60 nm) to prevent CP expression (D'Angelo *et al.*, 2008). To monitor recovery of *P. damicornis*, colonies previously treated

with blue or green light were placed to recover under 200 μmol photons $m^{-2}s^{-1}$ of white light from a metal halide lamp (Aquamedic) for 26 days.

4.3.3.3 Heat-induced bleaching

To monitor changes in coral colour during bleaching over time, two separate experiments were performed using *P. lichen*. Per experiment, six replicate measurements were performed. At the beginning of the experiments, corals were acclimated to the light fluxes in the treatment tanks (200-240 μmol photons $m^{-2}s^{-1}$) for at least 20 days. Afterwards, temperatures were ramped up to 31-32°C over ~2 weeks (Δ~0.5°C/d) and kept stable at the maximal temperature for ~3 weeks. Finally, temperatures were ramped down to 25-28°C and kept stable for the remainder of the experiment. Average values were calculated from the two experiments.

Bleached corals were sampled after 10 (B1) or 18 (B2) days of heat stress; control corals (H) were sampled from another, identical compartment of the experimental system where the corals were kept in parallel at 26°C under the same light intensity (120 μmol photons $m^{-2}s^{-1}$).

To monitor the recovery of *P. damicornis* from acute heat stress, temperature was increased from 26°C to 31°C over 8 days, kept stable for 9 days, and ramped down to 26°C over 6 days. The colony was then imaged periodically over 77 days.

4.3.3.4 Nutrient stress-induced bleaching

For the time series data, colonies of *P. lichen* were kept at 26°C under 180 μmol photons $m^{-2}s^{-1}$ in either replete (high nitrate / high phosphate; HN/HP) or imbalanced (high nitrate / low phosphate; HN/LP) nutrient conditions (D'Angelo and Wiedenmann, 2012; Wiedenmann *et al.*, 2013) for 100 days. For endpoint sampling, colonies of *P. lichen* and *P. damicornis* were kept in HN/HP or HN/LP conditions at 26°C under 190 μmol photons $m^{-2}s^{-1}$ for 107 days. An intact colony of *P. damicornis* was left to recover in HN/HP conditions and periodically imaged over 77 days. *M. foliosa* colonies were kept in HN/LP conditions under 200 μmol photons $m^{-2}s^{-1}$ for 56 days, then left to recover in HN/HP conditions for a further 56 days. Margins (HM) and inner regions (HI) of healthy colonies were sampled before HN/LP treatment, while recovering inner regions (RI) were sampled after 28 days HN/HP recovery.

4.3.4 Quantification of *in vivo* fluorescence and reflectance

All i*n vivo* fluorescence emission measurements were performed with a fluorescence spectrophotometer (Varian) equipped with a fibre optic probe (D'Angelo *et al.*, 2008),

using 450 nm excitation light. For *P. lichen*, spectra were unmixed using the least-squares method (Hedley *et al.*, 2004) into 3 endmembers: CFP (489 nm), GFP (519 nm) and zooxanthellae pigments (680 nm). Endmember contributions to measured spectra were used to plot time series.

Fluorescence images were taken with a 450 nm LED (Aquaray Fiji Blue, TMC) for excitation through a 500 nm long-pass emission filter (Nightsea). Photographs were obtained by imaging colonies side by side with a digital compact camera (Olympus).

Reflectance spectra were collected with a USB4000 modular spectrometer and a tungsten halogen light source connected to a dip probe (Ocean Optics), using a Spectralon 99% reflectance standard (Labsphere) as reference. Absorbance of *P. damicornis* was calculated from reflectance spectra as log(1/R) (Enríquez *et al.*, 2005); spectra were unmixed into two endmembers, pink CP (565 nm) and intact zooxanthellae (665 nm). The Photosystem II maximum quantum efficiency (Fv/Fm) of *P. damicornis* was recorded after 12h dark acclimation with a DIVING-PAM (Walz) under exposure to dim light (<5 μmol photons $m^{-2}s^{-1}$) prior to and during measurement to minimise the impacts of chlororespiration (Warner *et al.*, 2010).

4.3.5 Quantification of zooxanthellae numbers and host pigment content in tissue extracts

Tissue was harvested by airbrushing corals with artificial seawater. Surface area sampled was measured from skeleton photographs using image analysis software Fiji (Schindelin *et al.*, 2012). 50 μL of each sample were separated for zooxanthellae cell counts, performed in 10 μL aliquots with a haemocytometer (Marenfeld) under a fluorescence microscope (Leica). Host lysate was separated from intact symbiont cells by centrifugation at 4°C (2000 rcf, 2 min followed by 3000 rcf, 5 min, followed by 20,000 rcf, 45 min). Total protein concentration was measured via BCA colorimetric assay (Pierce) against BSA standard. For *P. lichen*, fluorescence was measured by loading 0.25 $\mu g \mu L^{-1}$ protein diluted in artificial seawater (total volume 200 μL) in a fluorescence spectrophotometer (Varian) equipped with 96-well plate reader; emission spectra (ex = 450 nm) were unmixed as described for *in vivo* data. For *P. damicornis*, absorbance of tissue lysate diluted in artificial seawater (1.5 $\mu g \mu L^{-1}$, total volume 100 μL) was measured in a 10 mm quartz cuvette using a UV-Vis spectrophotometer (Varian). Spectra were background corrected and unmixed as described for *in vivo* data, to remove contribution of symbiont protein to measured absorbance. For *M. foliosa*, the purple CP was further purified from the cleared extracts by size-exclusion chromatography (D'Angelo *et al.*, 2012) and normalised to the total protein content of the sample.

4.3.6 Statistical analysis

The 519:489 nm ratio time series data were fitted with logistic functions parameterised using non-linear least squares, with the exception of the HN/LP *P. lichen* dataset which was cropped at 80 days and fitted with an exponential function; this was due to the 489 nm contribution reaching zero at this point, and driving the ratio to infinity. Endpoint measurements were tested for significant difference in means using ANOVA, with α=0.05; where more than two samples were compared, Tukey's HSD was used for post-hoc testing (α=0.05) upon detection of a significant difference. Results of statistical analysis and model equations are presented in Supplementary Tables 4.1-4.3.

4.3.7 Satellite heat stress data

Sea surface temperature data for Lizard Island and El Nido virtual stations and local bleaching thresholds were obtained from NOAA Coral Reef Watch (2000, updated twice-weekly. *NOAA Coral Reef Watch 50-km Satellite Virtual Station Time Series Data for Lizard Island and El Nido*, Jan. 1, 2002-Dec. 31, 2016. Silver Spring, Maryland, USA: NOAA Coral Reef Watch. Data set accessed 2017-10-31 at http://coralreefwatch.noaa.gov/satellite/vs/index.php). Bleaching years in each region were identified based on data for the closest location in Hughes *et al.* (2018) (Australia, GBR Northern, for Lizard Island and Philippines, Central/Southern for El Nido).

4.4 Supplementary Figures

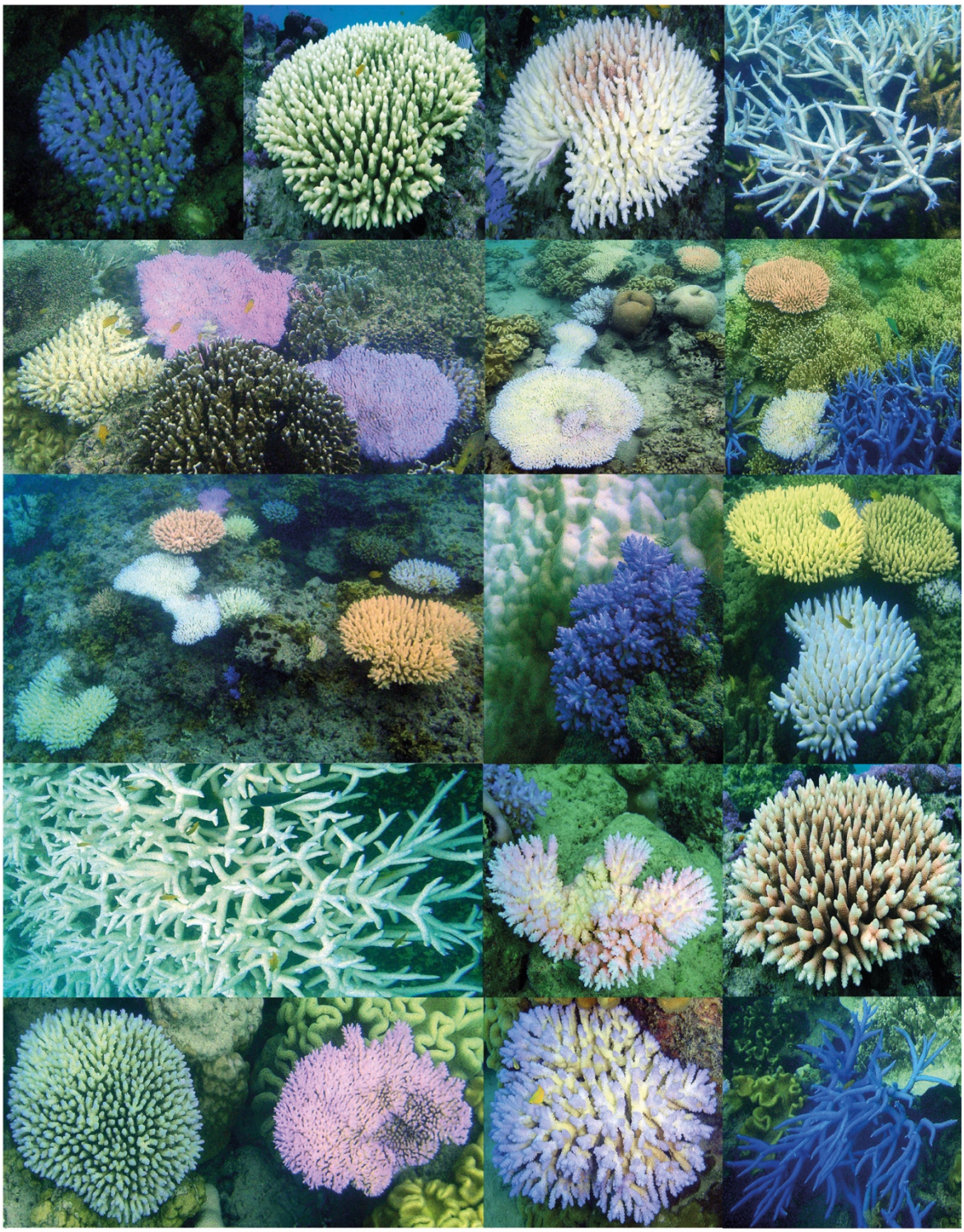

Figure 4.6 Individual differences in host pigment levels in response to bleaching

Images taken on Lizard Island reefs, Great Barrier Reef, Australia, in March 2010 at a depth of ~4 m. Credit: Morgan Pratchett.

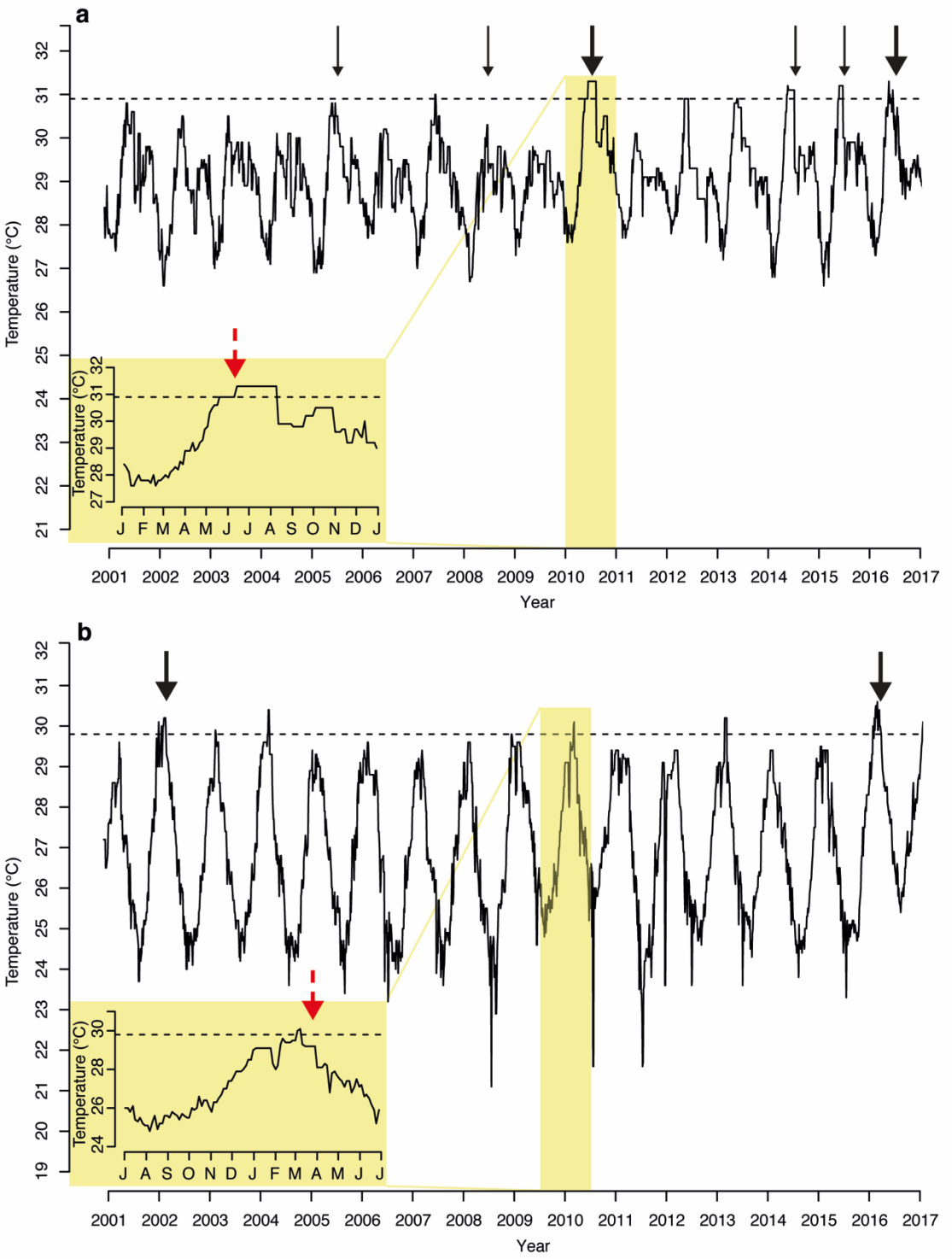

Figure 4.7 Heat stress and colourful bleaching events

Time series of satellite 50 km sea surface temperature for El Nido, Palawan, Philippines (**a**) and Lizard Island, Great Barrier Reef, Australia (**b**). Black arrows show years of severe (thick arrows) and moderate (thin arrow) bleaching reported in Hughes *et al.* (2018); dashed red arrows show timing of colourful bleaching photographed in Fig. 4.1 and Supplementary Fig. 4.5. Dashed line shows bleaching threshold temperature (maximum monthly mean temperature + 1°C).

Data: NOAA Coral Reef Watch. 2000, updated twice-weekly. NOAA Coral Reef Watch Operational 50-km Satellite Coral Bleaching Degree Heating Weeks Product, Jan. 1, 2001-Dec. 31, 2016. Silver Spring, Maryland, USA: NOAA Coral Reef Watch. Data set accessed 2017-10-31 at http://coralreefwatch.noaa.gov/satellite/hdf/index.php

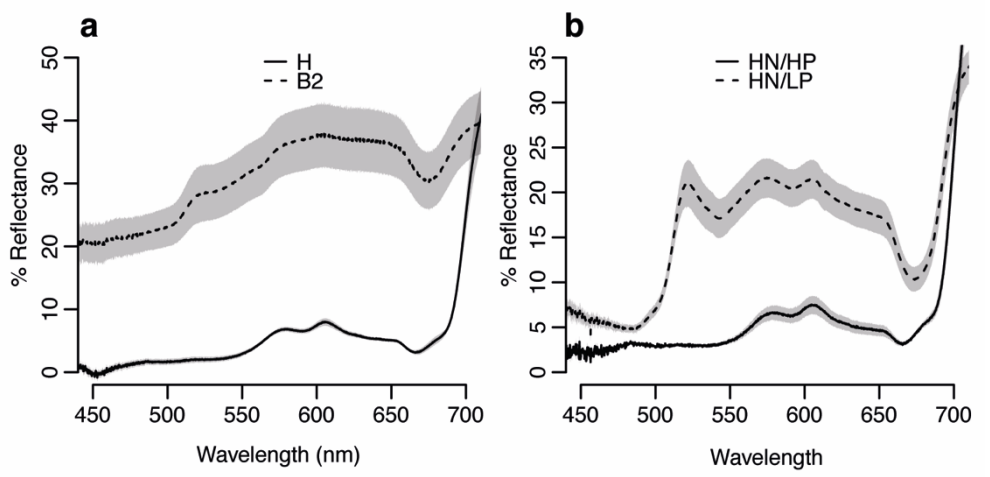

Figure 4.8 Spectral reflectance of healthy and bleached *P. lichen*

(**a**) Before (H) and after (B2) 17 days heat stress treatment. (**b**). After 98 days in replete (HN/HP) or imbalanced (HN/LP) nutrient conditions. Mean ± s.d., n = 5.

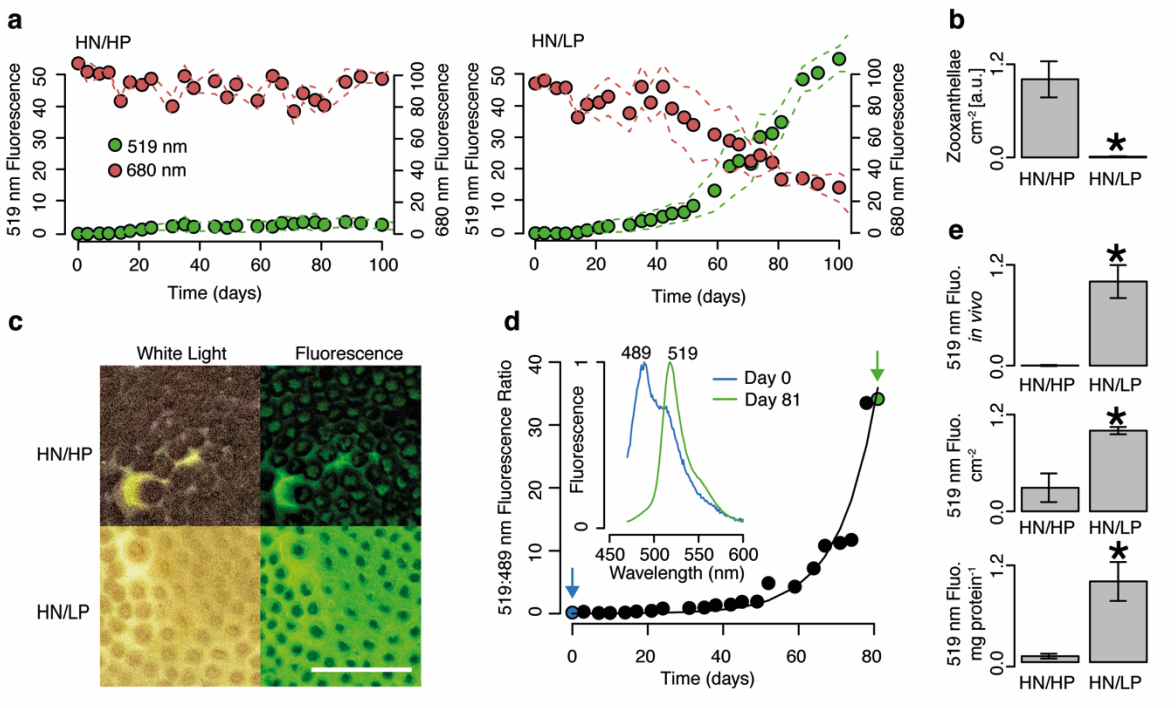

Figure 4.9 Fluorescence of *P. lichen* during nutrient-induced bleaching

(**a**) Time series of *in vivo* host GFP (519 nm) and chlorophyll (680 nm) fluorescence emission for colonies kept in replete nutrient conditions (high nitrate/high phosphate, HN/HP), or transferred to imbalanced nutrient conditions (high nitrate/low phosphate, HN/LP). Means (spheres) ± s.d. (dashed lines), n = 3. (**b**) Post-treatment zooxanthellae cell counts. (**c**) Post-treatment photographs (white light or 450 nm excitation). Scale 10 mm. (**d**) Ratio of GFP (519 nm) to CFP (489 nm) fluorescence emission for HN/LP coral, with *in vivo* spectra taken at time points indicated. (**e**) Host GFP (519 nm) fluorescence measured *in vivo* (top), as emission of host tissue homogenate normalised to colony surface area (middle) and to total host protein (bottom). In (**b**) and (**e**), bars show mean ± s.d., n = 3; asterisks show $p<0.05$.

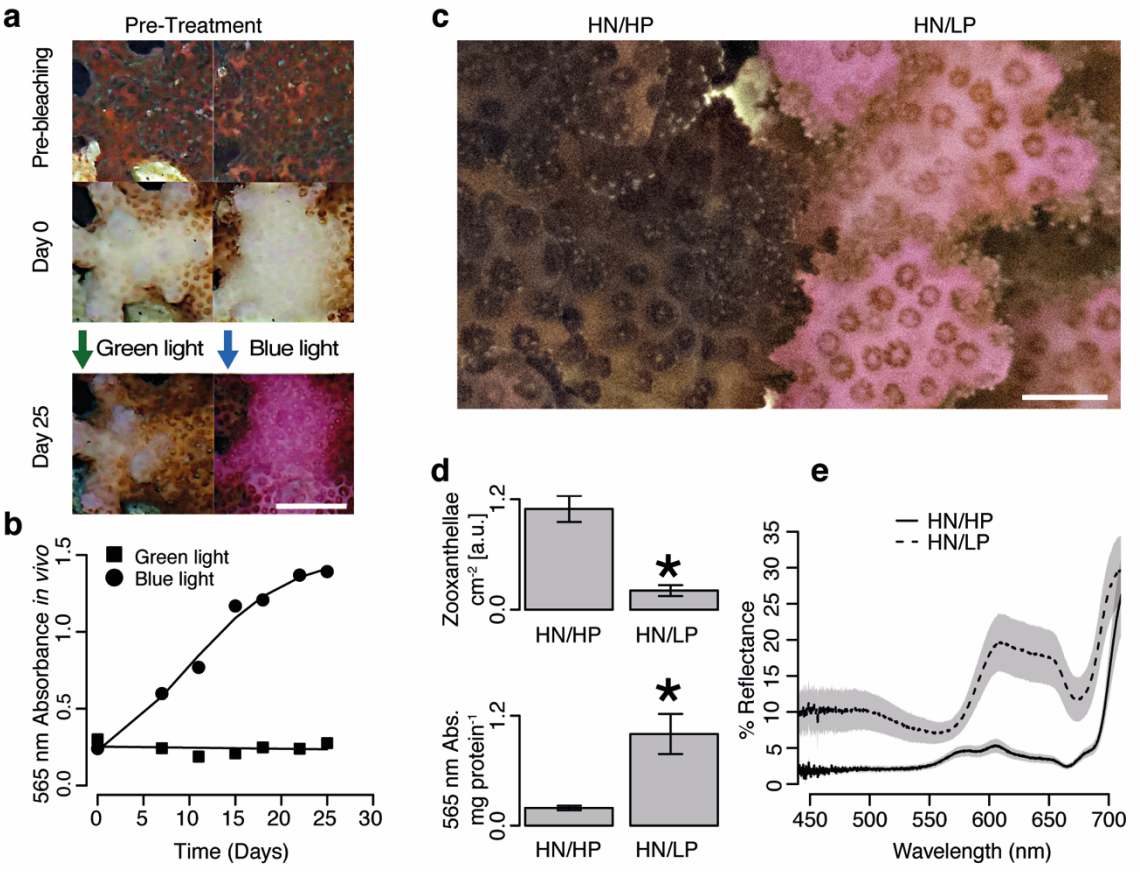

Figure 4.10 Enhanced expression of the pink photoprotective chromoprotein of *P. damicornis* under nutrient stress

(**a**) Photographs of *P. damicornis* before treatment (Pre-bleaching), after bleaching with focused red light (Day 0), and after exposure to green or blue light for 25 days. Scale 10 mm. (**b**) Contribution of pink CP to absorbance spectrum, calculated from *in vivo* reflectance, for bleached *P. damicornis* exposed to green or blue light. (**c**) Photographs of *P. damicornis* kept under replete (HN/HP) and imbalanced (HN/LP) nutrient conditions for 109 days. Scale 2 mm. (**d**) Zooxanthellae cell counts in sampled tissue and contribution of the pink CP to measured absorbance spectrum for HN/HP and HN/LP colonies. Mean ± s.d., n = 3. Asterisks show $p<0.05$. (**e**) Reflectance spectra of HN/HP and HN/LP *P. damicornis*.

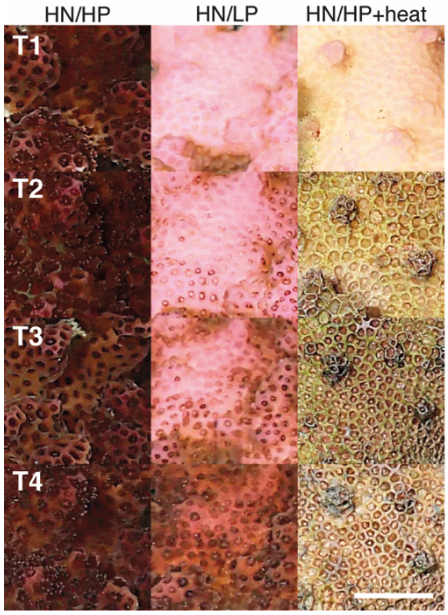

Figure 4.11 Recovery of *P. damicornis* following heat or nutrient stress-induced bleaching

P. damicornis kept under control (HN/HP, 26°C) conditions, imbalanced nutrients (HN/LP, 26°C) conditions, or heat stress (HN/HP, 31°C for 9 days) conditions. Photographed during recovery in HN/HP conditions after 0 (T1), 34 (T2), 53 (T3) and 77 (T4) days. Scale 10 mm.

4.5 Supplementary Tables

Table 4.1 Analysis of variance (ANOVA) results

(a) *P. lichen*, heat-induced bleaching (Fig. 4.3b,e)

Variable	F	p	Tukey's HSD	
Zooxanthellae cm^{-2}	$F_{2,6}$=53.84	<0.001	H, B1	p<0.001
			H, B2	p<0.001
			B1, B2	p=0.287
519 nm fluorescence *in vivo*	$F_{2,6}$=26.18	0.001	H, B1	p=0.403
			H, B2	p=0.001
			B1, B2	p=0.004
519 nm fluorescence cm^{-2}	$F_{2,6}$=10.08	0.012	H, B1	p=0.890
			H, B2	p=0.025
			B1, B2	p=0.015
519 nm fluorescence mg^{-1}	$F_{2,6}$=14.26	0.005	H, B1	p=0.952
			H, B2	p=0.010
			B1, B2	p=0.007

(b) *M. foliosa*, nutrient-induced bleaching and recovery (Fig. 4.4c)

Variable	F	p	Tukey's HSD	
577 nm absorbance mg^{-1}	$F_{2,6}$=3153	<0.001	HM, RI	p=0.988
			HM, HI	p<0.001
			HI, RI	p<0.001

(c) *P. damicornis*, 665 nm absorbance *in vivo* during light-induced bleaching and recovery (Fig. 4.4f)

	F	p
Treatment	$F_{1,4}$=7.3021	0.054
Time	$F_{2,8}$=200.2141	<0.001
Treatment*Time	$F_{2,8}$=7.4626	0.0148

Tukey's HSD

T1 no CP, T2 no CP	p<0.001

T1 no CP, T3 no CP	p<0.001
T1 no CP, T1 CP	p=1.000
T1 no CP, T2 CP	p<0.001
T1 no CP, T3 CP	p=0.003
T2 no CP, T3 no CP	p<0.001
T2 no CP, T1 CP	p<0.001
T2 no CP, T2 CP	p=1.000
T2 no CP, T3 CP	p<0.001
T3 no CP, T1 CP	p<0.001
T3 no CP, T2 CP	p<0.001
T3 no CP, T3 CP	p<0.001
T1 CP, T2 CP	p<0.001
T1 CP, T3 CP	p=0.002
T2 CP, T3 CP	p<0.001

(d) *P. damicornis*, recovery under white light after light-induced bleaching (Fig. 4.4g)

Variable	F	p
Zooxanthellae cm^{-2}	$F_{1,4}$=14.28	0.019
Fv/Fm	$F_{1,4}$=73.25	0.001

(e) *P. lichen*, nutrient-induced bleaching (Supplementary Fig. 4.9b,e)

Variable	F	p
Zooxanthellae cm^{-2}	$F_{1,4}$=55.42	0.002
519 nm fluorescence *in vivo*	$F_{1,4}$=168.6	<0.001
519 nm fluorescence cm^{-2}	$F_{1,4}$=44.78	0.003
519 nm fluorescence mg^{-1}	$F_{1,4}$=43.34	0.003

(f) *P. damicornis*, nutrient-induced bleaching (Supplementary Fig. 4.10d)

Variable	F	p
Zooxanthellae cm^{-2}	$F_{1,4}$=100.3	<0.001

565 nm absorbance mg^{-1}	$F_{1,4}$=40.35	0.003

Table 4.2 Model parameterisation and statistical analysis for 519:489 nm fluorescence emission time series data

Treatment	Model	Parameters	SE	t-value	p
High light acclimation (Fig. 4.2d)	$y = \frac{a}{1 + e^{-\frac{x-b}{c}}}$	a=3.229	0.114	28.30	<0.001
		b=21.883	0.814	26.87	<0.001
		c=6.912	0.618	11.18	<0.001
Green light exposure following bleaching (Fig. 4.2f)	$y = a + bx$	a=0.244	0.051	4.842	0.001
		b=0.001	0.002	0.489	0.638
Blue light exposure following bleaching (Fig. 4.2f)	$y = \frac{a}{1 + e^{-\frac{x-b}{c}}}$	a=6.945	3.175	2.187	0.064
		b=37.632	8.075	4.660	0.002
		c=9.351	1.815	5.153	0.001
Heat Stress (Fig. 4.3d)	$y = \frac{a}{1 + e^{-\frac{x-b}{c}}}$	a=43.321	2.862	15.14	<0.001
		b=56.828	1.166	48.75	<0.001
		c=6.558	0.600	10.93	<0.001
Nutrient Stress (Suppl. Fig. 4.9d)	$y = e^{a+bx}$	a=-4.362	0.747	-5.843	<0.001
		b=0.098	0.010	10.221	<0.001

Table 4.3 Model parameterisation and statistical analysis for *P. damicornis* pink CP absorbance time series data

Treatment	Model	Parameters	SE	t-value	p
Green light exposure following bleaching (Suppl. Fig. 4.10b)	$y = a + bx$	a=0.254	0.031	8.195	<0.001
		b=0	0.002	-0.366	0.729
Blue light exposure following bleaching (Suppl. Fig. 4.10b)	$y = \frac{a}{1 + e^{-\frac{x-b}{c}}}$	a=1.498	0.086	17.466	<0.001
		b=9.559	0.949	10.069	<0.001
		c=5.543	0.835	6.642	0.003

Chapter 5 A multi-excitation fluorescence imaging method to improve detection of coralline algae in benthic surveys

5.1 Abstract

Automatic annotation of imaging data is increasingly applied in coral reefs surveys. However, identification of some of benthic groups from reflectance images can present a challenge even for local experts. This includes crustose coralline algae (CCA), a group of calcifying red algae which fulfil key ecological roles such as reef accretion and providing settlement cues for coral larvae. Here, we develop the concept for an imaging method based on off-the-shelf components to improve automatic classification of CCA and other biotic substrates. We used RGB cameras to image fluorescence emission of coral and algal pigments stimulated by narrow-waveband blue and green light, and combined the information into 3-channel pseudocolour images. Using a set of *a priori* rules defined by the relative pixel intensity produced in different channels, the method achieved successful classification of organisms into three groups based on the dominant fluorescent pigment expressed. The rationale, advantages and limitations of the method are discussed. This work builds on previous findings that fluorescence imaging facilitates automatic annotation, and aims to provide a conceptual foundation to future technological developments that will improve cost, accuracy and rapidity of coral reef surveys.

5.2 Introduction

In the last 50 years, advances in underwater imaging technology have allowed us to characterise benthic marine ecosystems through the collection of increasingly detailed datasets (Jaffe, 2015). Even in shallow water environments easily accessible by divers such as coral reefs, imaging-based techniques have found wide application; these methods allow larger areas to be surveyed using less in-water time and fewer operators compared to manual recording, and they provide a permanent visual record of the survey site, which can be re-analysed when required (Jokiel *et al.*, 2015). Analysis of benthic imaging datasets requires that the organisms and substrates encountered are identified, and the images annotated; however, a number of issues are associated with annotation of coral reef imaging data. First, imaging datasets can be very large, to the point that years of analysis would be required if relying on manual annotation alone (González-Rivero *et al.*, 2014). To overcome this bottleneck, computer vision and machine learning methods

have been applied to coral reef benthic datasets in an effort to automate the image annotation process (Mehta *et al.*, 2007; Pizarro *et al.*, 2008; Stokes and Deane, 2009; Beijbom *et al.*, 2012, 2015; Shihavuddin *et al.*, 2013).

A second issue is that for some groups of benthic organisms, identification from photographs is problematic even when performed by experts (Ninio *et al.*, 2003; Beijbom *et al.*, 2015). The lowest classification accuracy is often found within algal groups, particularly between turf and crustose coralline algae (CCA) (Beijbom *et al.*, 2012, 2015; Mahmood *et al.*, 2016); this has led some studies to treat algae as a single group for the purposes of classification, or to group CCA with abiotic substrates (Soriano *et al.*, 2001; Stokes and Deane, 2009; Beijbom *et al.*, 2016). However, from a functional perspective these organisms are widely distinct. For example, CCA contribute to reef accretion (Goreau, 1963; Bak, 1976), produce settlement cues for coral larvae (Morse *et al.*, 1988; Heyward and Negri, 1999), and are often the main substrate-forming species in high-energy environments such as intertidal reef crests (Tracey *et al.*, 1948); CCA are also sensitive to a number of anthropogenic stressors, including sedimentation, ocean warming and acidification (Fabricius and De'ath, 2001; Anthony *et al.*, 2008; Jokiel *et al.*, 2008; Kuffner *et al.*, 2008). In contrast, other benthic algae can respond positively to eutrophication, can inhibit coral recruitment, and are associated with reduced coral cover and calcification (Kuffner *et al.*, 2006; Loya, 2004; Fabricius, 2005). The ability to accurately classify algal groups in imaging surveys is thus of relevance for monitoring and management of reef ecosystems.

A number of imaging techniques have been developed to improve the identification and automatic classification of functional benthic groups, many of which rely on knowledge of the optical properties of reef organisms and abiotic substrates (Strand *et al.*, 1997; Gleason *et al.*, 2007; Treibitz *et al.*, 2015; Chennu *et al.*, 2017). One example is multispectral or hyperspectral imaging, where reflectance images acquired in specific wavebands are used to facilitate classification (Gleason *et al.*, 2007; Chennu *et al.*, 2017) (Table 5.1). This approach can also be implemented from airborne remote sensing platforms (Andréfouët *et al.*, 2004; Kutser *et al.*, 2006; Garcia *et al.*, 2018); however, specialised and often expensive imaging equipment is required. An alternative approach, and the focus of this study, is to use fluorescence to complement (or replace) reflectance imaging data (Strand *et al.*, 1997; Mazel *et al.*, 2003a; Treibitz *et al.*, 2015; Beijbom *et al.*, 2016).

Fluorescence occurs when light absorbed by a molecule is re-emitted in a red-shifted waveband on a very short timescale; many shallow water benthic organisms contain one or more pigments that are capable of emitting a fluorescence signal strong enough to be detected with imaging techniques (Mazel, 1995; Treibitz *et al.*, 2015). Hard corals and

other Cnidaria produce fluorescent pigments homologous to the green fluorescent protein (GFP) from the jellyfish *Aequorea victoria* (Shimomura *et al.*, 1962; Matz *et al.*, 1999; Dove *et al.*, 2001), known as GFP-like proteins or FPs, which can accumulate in high concentrations in the animal tissue (Oswald *et al.*, 2007). Photosynthetic organisms also produce a fluorescence signal, commonly emitted by chlorophyll a but also by accessory pigments such as phycoerythrin (PE) (French and Young, 1952; Falkowski and Kiefer, 1985). While the relationship might not always appear straightforward, fluorescence of reef organisms is in many cases intimately linked to their photobiology (Falkowski and Kiefer, 1985; Salih *et al.*, 2000; Gittins *et al.*, 2015; Smith *et al.*, 2017); as such, it is a promising feature for a functional approach to classification (Zawada and Mazel, 2014). Field studies have shown that fluorescence can indeed enable or even improve automatic classification compared to reflectance imaging alone (Mazel *et al.*, 2003a; Beijbom *et al.*, 2016).

So far, efforts to include fluorescence data in benthic imaging surveys have used monochromatic or narrow waveband blue light to excite fluorescence in multiple emission bands, separated either by interference filters on a multispectral imager (Strand *et al.*, 1997; Mazel *et al.*, 2003a) or by the intrinsic colour sensitivity of an RGB camera (Treibitz *et al.*, 2015; Beijbom *et al.*, 2016) (Table 5.1). With the former method, Mazel *et al.* (2003a) were able to separate CCA from other photosynthetic organisms using the orange emission band of PE; however, their imaging system was a highly specialised laser line scanner (Strand *et al.*, 1997). The latter method used off-the-shelf professional photography equipment but only allowed discrimination between coral GFP and chlorophyll fluorescence (Treibitz *et al.*, 2015; Beijbom *et al.*, 2016). Here, we propose that adding a second excitation waveband to an off-the-shelf camera-based imaging system can improve discrimination of benthic categories, particularly between functional groups of algae. Our imaging concept is based on knowledge that deep-red chlorophyll fluorescence of algae is excited more or less efficiently by light in different spectral bands depending on the accessory pigment complement of the organism. Specifically, we hypothesised that comparing fluorescence images obtained under blue excitation with images obtained under green excitation would facilitate identification of CCA; we therefore explored the possibility of a multi-excitation fluorescence imaging system built with off-the-shelf components, and evaluated the concept in a laboratory setting.

Table 5.1 *In situ* spectral imaging systems currently used in automatic image annotation

System name	Imager	Illumination band	Detection channels	Detection range	Reference
FILLS	Laser line scanner	Narrow (488 nm, fluorescence)	3 fluorescence	520 nm (10 nm FWHM); 580 nm (10 nm FWHM); 685 nm (20 nm FWHM)	Strand *et al.*, 1997
MSCAM	CCD camera	Wide (reflectance)	6 reflectance	Set 1: 520 nm, 543 nm, 566 nm, 585 nm, 602 nm, 622 nm (8 nm FW) Set 2: 480 nm, 508 nm, 525 nm, 543 nm, 565 nm, 585 nm (8 nm FW)	Gleason *et al.*, 2007
FluorIS	Modified CMOS camera	Narrow (466 nm, fluorescence) + Wide (reflectance)	2 fluorescence + 3 reflectance	~590-744 nm	Treibitz *et al.*, 2016
HyperDiver	Push broom hyperspectral imager	Wide (reflectance)	480 reflectance	400-900 nm	Chennu *et al.*, 2017

5.3 Results

5.3.1 The multi-excitation imaging and image processing concept

The multi-excitation imaging system is designed to acquire two separate fluorescence images for each subject, one under blue and one under green illumination. The excitation light source is in both cases a high-power colour LED with a narrow full width at half maximum (FWHM) of 40 nm for the 450 nm LED, and 60 nm for the 530 nm LED (Fig. 5.1). The 450 nm images are acquired through a yellow long-pass emission filter with a cut-on wavelength of ~510 nm, and the 530 nm images through a red long-pass filter with a cut-on wavelength of ~610 nm (Fig. 5.1a); the filters are designed to minimise contribution of excitation light, including scattered light, to the fluorescence images. For this proof-of-concept study, we coupled the excitation lights into the illumination system of a fluorescence microscope and used the microscope CCD camera for imaging (Fig. 5.2). Due to the spectral sensitivity of the RGB camera sensor (Fig. 5.1b), the 510 nm filter excludes the majority of wavelengths that would produce signal in the B channel, as does the 610 nm filter for both B and G channels (Fig. 5.1a,b). All meaningful fluorescence signal from both images can thus be stored as a single 3-channel image; therefore, we processed the image pairs acquired with 450 nm and 530 nm excitation as pseudocolour RGB images and defined the new colour space as R'G'B', where:

R' = 450 nm excitation, R channel

G' = 450 nm excitation, G channel

B' = 530 nm excitation, R channel

We included a channel-specific background correction step to account for differences in the bleed-through of each light/filter combination.

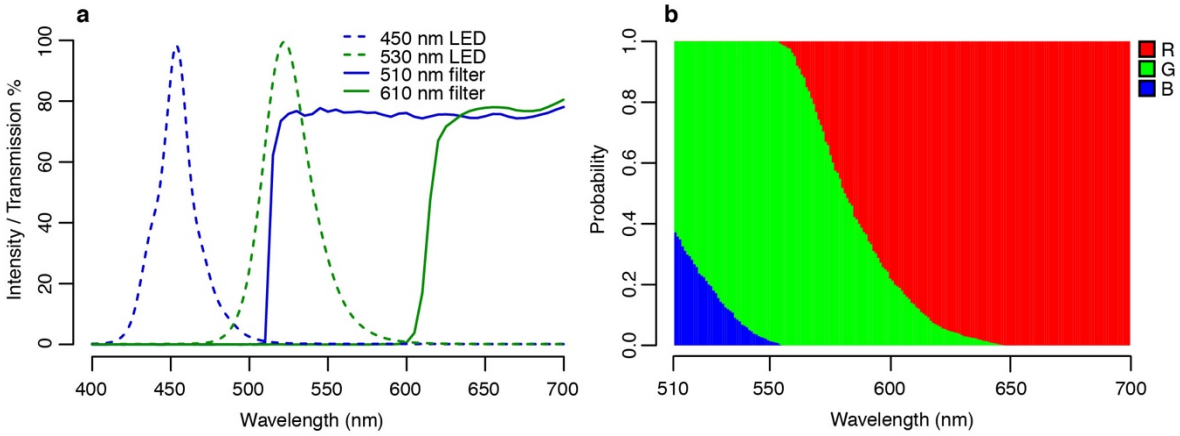

Figure 5.1 Spectral properties of the multi-excitation imaging system

(a) Relative spectral intensity of excitation light sources (dashed lines) and transmission spectra of emission filters (solid lines) used for microscope image collection. (**b**) Relative probability of spectral light being detected in the R, G, or B channel of the microscope camera CCD sensor.

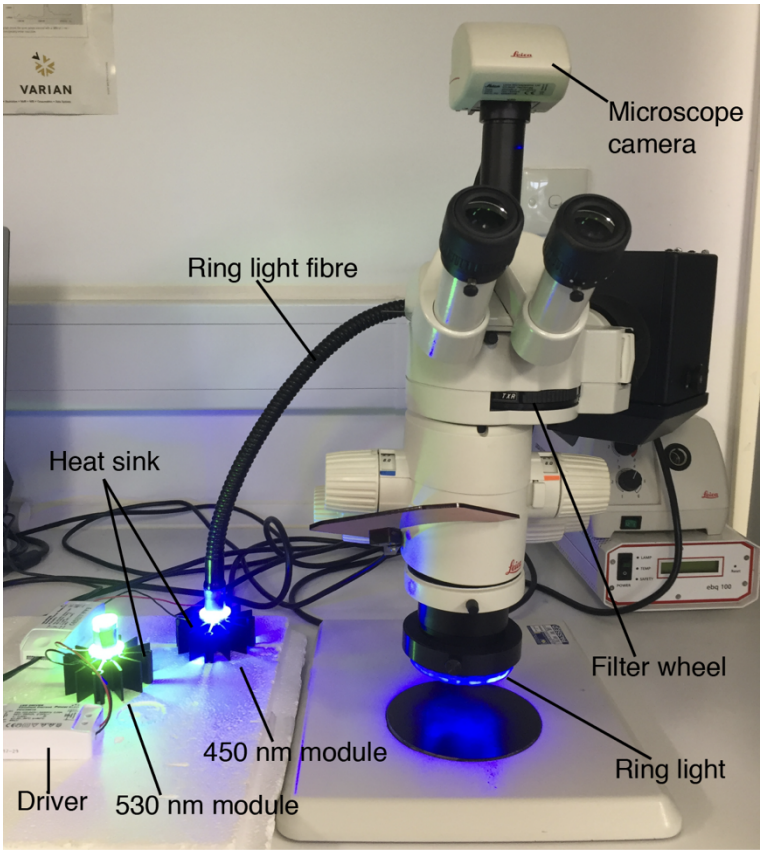

Figure 5.2 The microscope CCD camera multi-excitation imaging system

5.3.2 Fluorescence of purified marine pigments

To assess how well the multiexcitation system can detect fluorescence spectra that are relevant for reef surveys, we isolated and characterised marine fluorescent pigments representative of different benthic categories. We used lipid-soluble pigments from *Codium* sp. as an example of chlorophylls from green algae, water-soluble pigments from *Solieria chordalis* as red algae phycoerythrin (PE), amilFP497 as cyan/green cnidarian fluorescent protein (CFP/GFP), amilFP597 as red cnidarian fluorescent protein (RFP), and eechRFP as cnidarian photoconvertible red fluorescent protein (pcRFP) (Fig. 5.3).

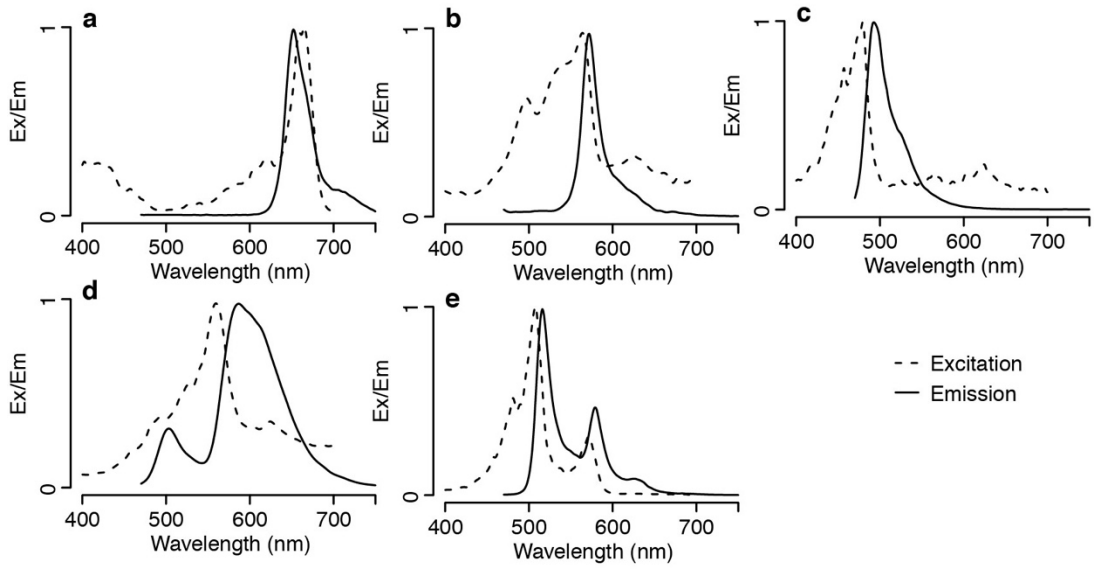

Figure 5.3 Fluorescence spectra of isolated marine pigment

Excitation (Ex, emission = zero order) and emission (Em, Excitation = 450 nm) spectra of chlorophyll (**a**) and PE (**b**) extracted from macroalgae, and of recombinantly produced coral FPs amilfP497 (**c**), amilFP597 (**d**), and eechRFP (**e**).

Extracted chlorophyll presented a single emission peak at 652 nm, with excitation maxima at 659 and 665 nm and lowest excitation values between 500 and 550 nm (Fig. 5.2a). These values are indicative of the presence of both chlorophyll a and b, with the latter being more efficiently excited by the 450 nm measuring light thus causing an apparent hypsochromic shift in the emission spectrum compared to the excitation spectrum. Red algae water-soluble pigment spectra presented a single emission peak at 572 nm and excitation maxima at 497 and 564 nm, confirming that the extract contained mostly PE (Fig. 5.3b). Spectra of recombinantly produced *Acropora millepora* FPs presented excitation (emission) maxima at 479 nm (493 nm) for amilFP497 (Fig. 5.3c) and 559 nm (587 nm) for amilFP597 (Fig. 5.3d); eechRFP spectra showed contribution from a green

and a red species, with peaks at 507 nm (516 nm) and 571 nm (579 nm) respectively (Fig. 5.3e).

This spectral data was used to calculate predicted pixel intensities in the R', G' and B' channels, taking into account the spectral properties of the excitation lights (Fig. 5.1a), of the emission filters (Fig. 5.1a) and of the camera sensor (Fig. 5.1b). Chlorophylls had the highest predicted intensity in the R' channel and amilFP497 in the G' channel; PE and amilFP597 had comparable predicted signal in all 3 channels; eechRFP was predicted to have the strongest signal it the G' channel but to also present signal in R' and B' (Fig. 5.4a).

We then used the multiexcitation system to image aliquots of the same purified pigments under 450 nm and 530 nm excitation, and processed the images acquired into R'G'B' format (Fig. 5.4b). As predicted, imaging of chlorophyll and amilFP497 produced signal almost exclusively in the R' and G' channels, respectively; PE, amilFP597, and eechRFP produced signal in all three channels, with variable intensity (Fig. 5.4b). The pixel intensity measured from R'G'B' images showed a strong significant correlation with the calculated predictions (Pearson's product-moment, $r_{13}=0.92$, $p<0.001$) (Fig. 5.4c).

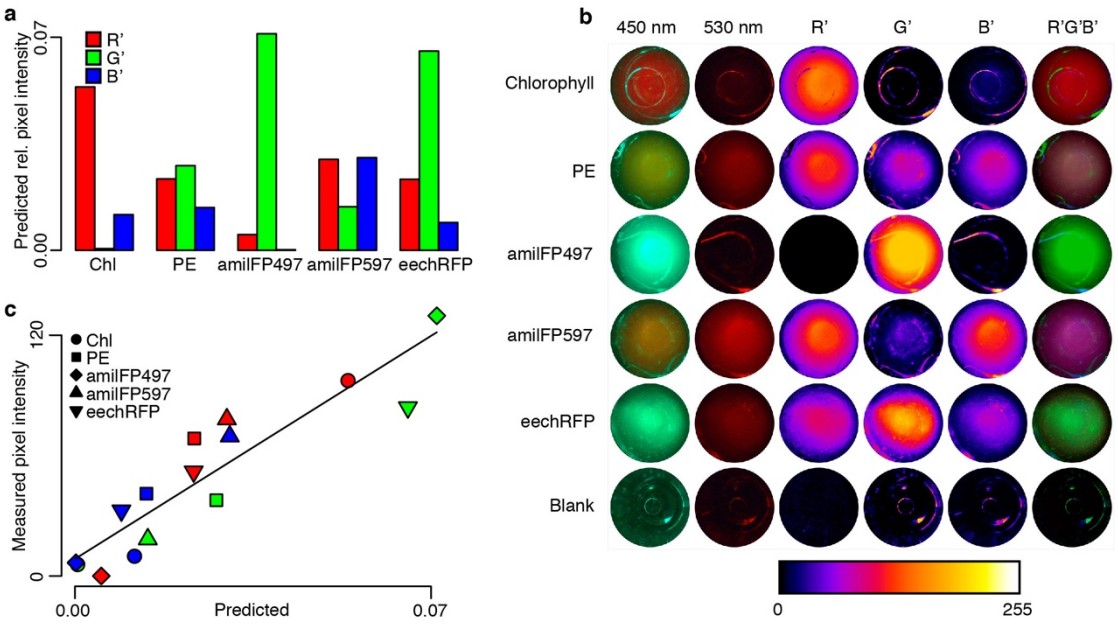

Figure 5.4 Pixel intensity of isolated pigments

(a) Predicted pixel intensity in the R', G', and B' channels calculated from spectral properties of the imaging system (Fig. 5.1) and of purified pigments (Fig. 5.3). (**b**) Pigments imaged with the CCD camera under 450 nm (510 nm emission filter) and 530 nm excitation (610 nm emission filter), pixel intensity in the R', G', and B' channels on a false colour scale, and the resulting combined R'G'B' images. (**c**) Relationship between pixel intensity predicted in (**a**) and measured in (**b**).

5.3.3 Definition of classification rules

After establishing the relationship between spectral data and R'G'B' multispectral images, we explored the possibility of using this image format to automatically classify benthic organisms into categories based on the dominant fluorescent pigment present. As it was not practical to obtain a dataset large enough to train and test a computer vision model with our prototype imaging system, we adopted the approach of defining set of *a priori* classification rules using the R'G'B' intensity measured for purified pigments (Fig. 5.4b).

To define the set of rules, we first described each pigment by its R'G'B' pixel intensity ratios R'/G', R'/B', and G'/B' (Fig. 5.5). In this colour space, chlorophyll was strongly separated from the other pigments by its much higher R'/B' and R'/G' values; amilFP497 was characterised by G'/B' >> 1, and R'/G' << 1; PE, amilFP597, and eechRFP clustered together due to similar R'/B' values between 1 and 2, but with some separation in the R'/G' and G'/B' dimensions (Fig. 5.5). Based on these values, we defined regions in the

R'G'B' ratio colour space for broad classification into 3 categories: *Chl*, *CFP/GFP*, and *RFP/PE* (Table 5.2, Fig. 5.5).

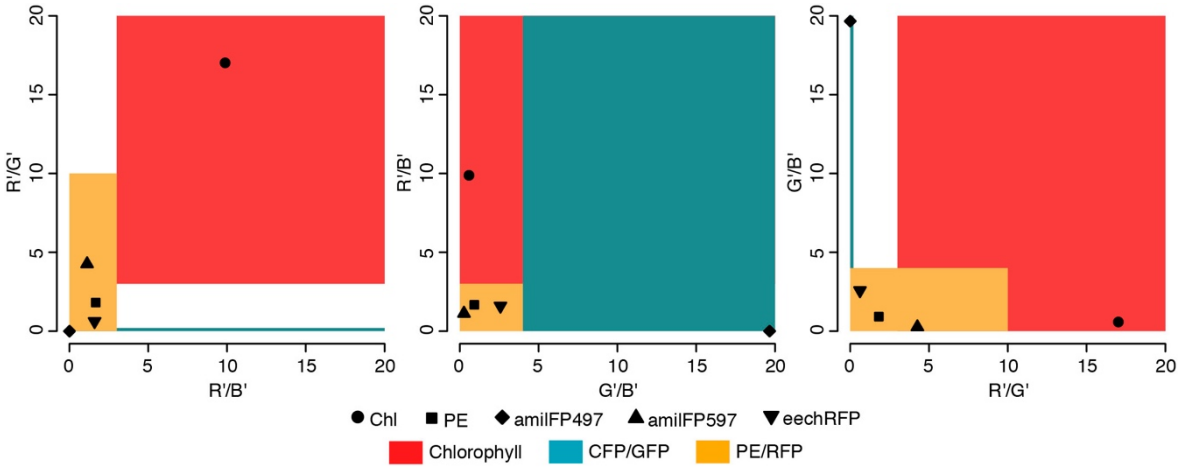

Figure 5.5 R'G'B' ratios of purified pigments and of categories defined

Data points represent values measured for purified pigments (Fig. 5.4b), polygons represent boundaries of categories.

The G'/B' ratio was ignored in the definition of the *Chl* category, as was the R'/B' ratio for *CFP/GFP*, since the respective purified pigments had only background signal in these channels (Fig. 5.4b). Although R'G'B' images were background corrected during initial processing, we also set a minimum intensity threshold in the relevant channels for each category in order to exclude low intensity pixels produced by bleed-through of reflected excitation light (Table 5.2). Finally, we defined an *Other* category to classify pixels with above-threshold intensity in any channel, but with channel ratios that did not match any of the three explicit categories.

Table 5.2 Rules for classification of R'G'B' images.

thr = threshold

R'/G'	R'/B'	G'/B'	Intensity	Category
>3	>3	ignore	R'>thr	*Chl*
<10	<3	<4	R' and B' >thr	*PE/RFPs*
<0.2	ignore	>4	G'>thr	*CFP/GFP*

5.3.4 Classification of live organisms

We then collected spectral data and multi-excitation images for a range tropical benthic organisms, including green and red algae, CCA, and a number of coral species, we converted the 450 nm / 530 nm image pairs into R'G'B' images, and applied the classification algorithm (Fig. 5.6, 5.7). Green algae had chlorophyll-like emission spectra and excitation maxima <500 nm, and correspondingly showed stronger red fluorescence under 450 nm light. Red algae, which present the excitation/emission signature of PE as well as the emission signature of chlorophyll, appeared brighter under 530 nm light. CCA spectra had a stronger PE emission contribution and were strongly fluorescent in both images (Fig. 5.6). Coral spectra reflected the excitation/emission signature of the dominant FP and showed the emission contribution of chlorophyll to a variable degree; red *Montipora foliosa* and *Oxypora* had strong signal in both 450 nm and 530 nm images, while *A. millepora*, brown *M. foliosa*, *Porites lichen* and *Seriatopora hystrix* appeared only brightly green under 450 nm light (Fig. 5.7). The algorithm classified green algae as *Chl*, cyan and green corals as *CFP/GFP*, and CCA and red corals as *RFP/PE* (Fig. 5.6, 5.7). A few small areas near coral polyps or margins were also classified as chlorophyll, and some pixels on a brown *M. foliosa* colony were classified as *RFP/PE* or *Other* (Fig. 5.7). Non-coralline red algae and some regions of rocks covered in algal films were classified as *Other*, with the exception of a few heteropigmented regions on red algae fronds which were classified as *RFP/PE* (Fig. 5.6).

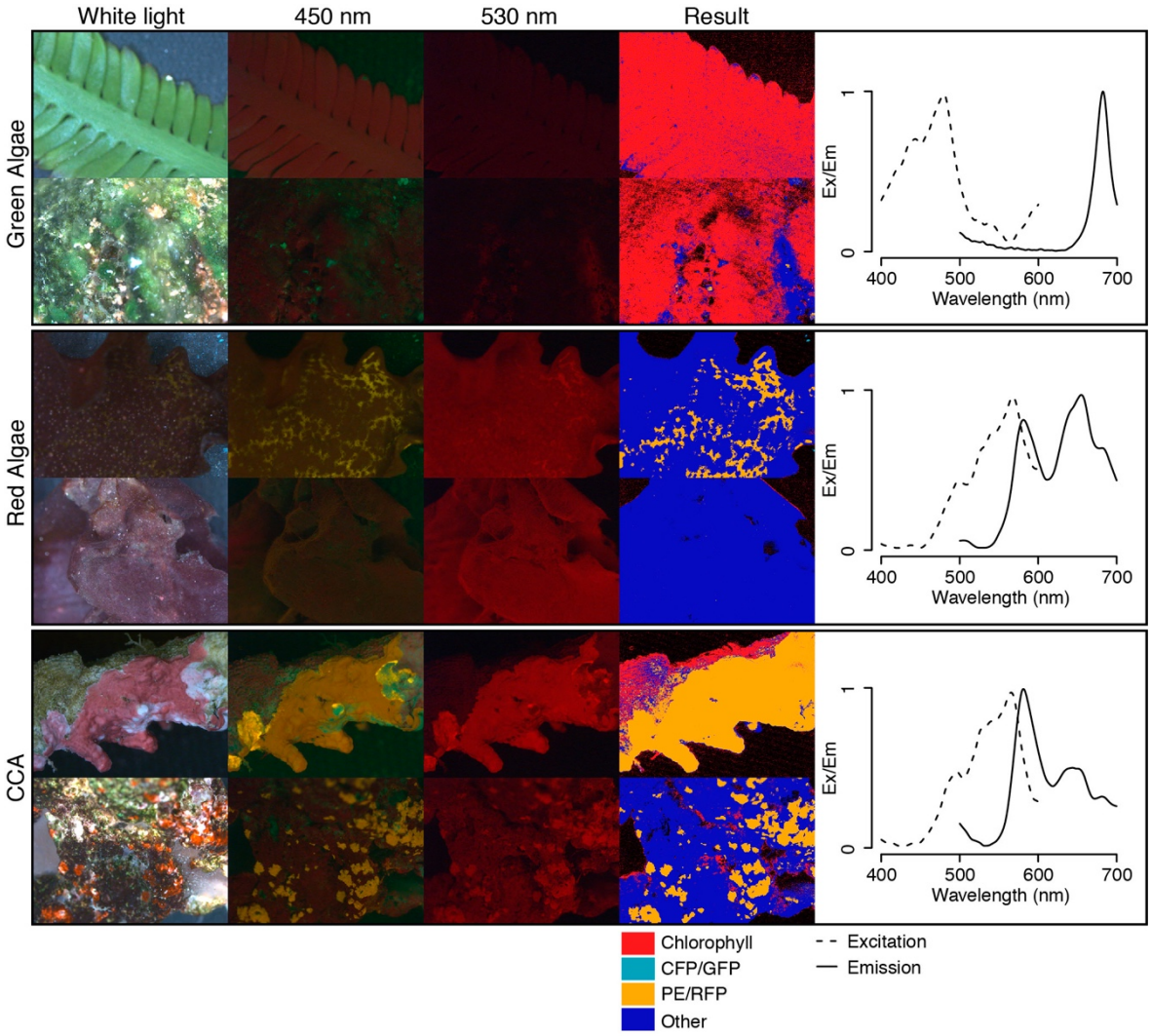

Figure 5.6 Classification of multi-excitation fluorescence images of algae groups

Algae imaged with the CCD microscope camera under white light, 450 nm excitation (510 nm emission filter) and 530 nm excitation (610 nm emission filter), results of image classification, representative excitation (Ex) and emission (Em) spectra. Green algae: *Caulerpa* sp. (top and spectra), unidentified turf species growing on coral skeleton (bottom). Red algae: unidentified fleshy macroalgae (top and spectra), unidentified turf species (bottom). CCA: unidentified species growing on coral skeleton (top and spectra), unidentified species growing on live rock (bottom).

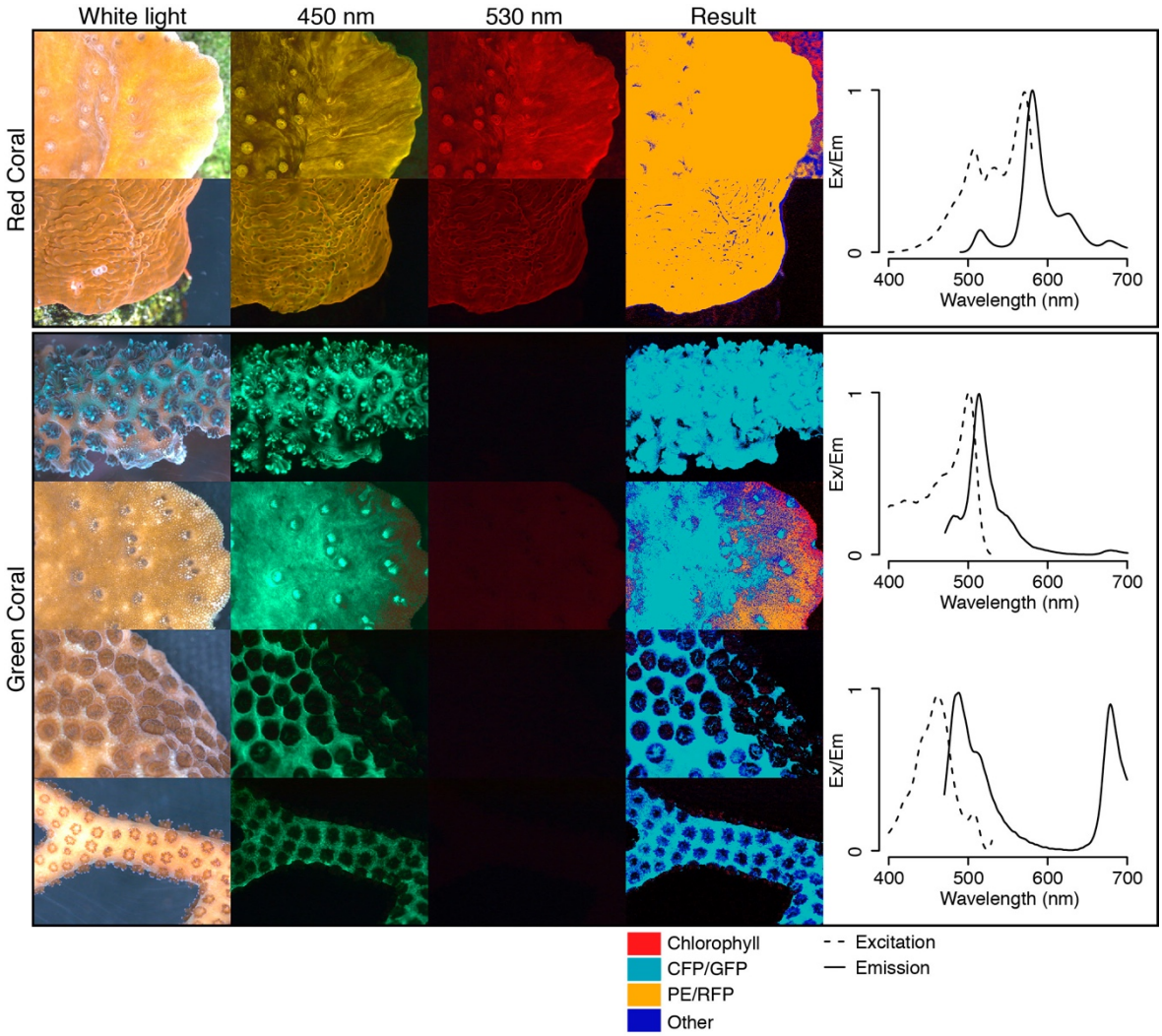

Figure 5.7 Classification of multi-excitation fluorescence images of hard corals

Corals imaged with the CCD microscope camera under white light, 450 nm excitation (510 nm emission filter) and 530 nm excitation (610 nm emission filter), results of image classification, representative excitation (Ex) and emission (Em) spectra. Red coral: red morph of *Monitpora foliosa* (top), *Oxypora* sp. (bottom and spectra). Green coral: (top to bottom) *Acropora millepora* (top spectra), brown morph of *M. foliosa*, *Porites lichen* (bottom spectra) and *Seriatopora hystrix*.

5.3.5 Compact camera

Finally, we wished to assess whether a compact underwater camera could be used effectively in place of the microscope CCD camera to generate R'G'B' multispectral images. Therefore, we adapted the same illumination system to image aliquots of isolated pigments with a digital compact camera (Fig. 5.8), using emission filters of similar optical properties to the ones mounted on the microscope filter wheel (Fig. 5.1a, Supplementary Fig. 5.10); the results were markedly different from those obtained with the microscope camera (Fig. 5.4c, 5.8). Most notably, PE and amilFP597 had only background-level signal in the G' channel, making these pigments indistinguishable from chlorophyll from the 450 nm image alone; the difference could however be easily resolved in the 530 nm image (Fig. 5.8). The strongest signal for amilFP497 was in the G' channel, consistently with the CCD camera results, but eechRFP had stronger signal in R' (Fig. 5.4c, 5.8). All pigments produced a strong enough fluorescence signal to appear clearly above background.

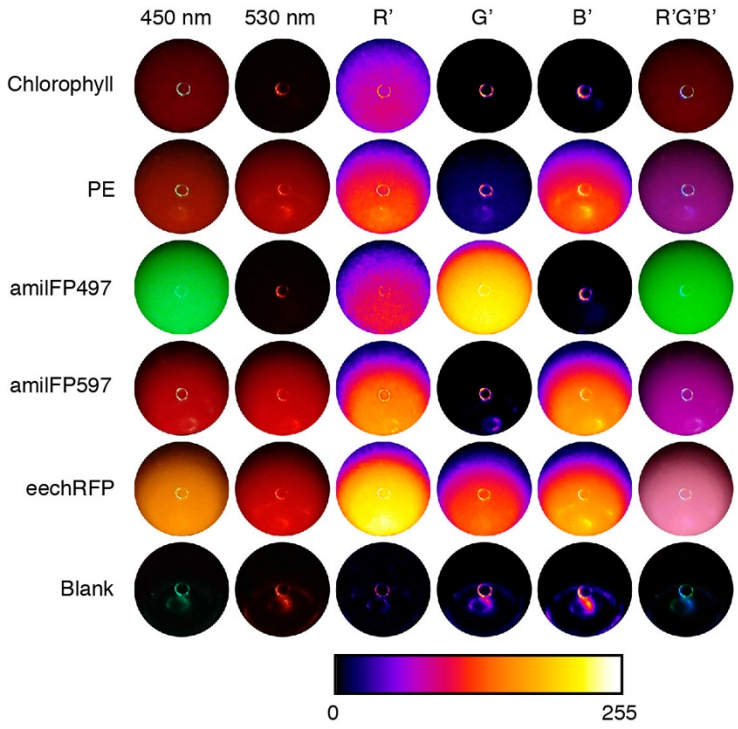

Figure 5.8 Multi-excitation imaging of isolated pigments with a compact camera

Pigments imaged under 450 nm excitation (510 nm emission filter) and 530 nm excitation (610 nm emission filter), pixel intensity in the R', G', and B' channels on a false colour scale, and the resulting combined R'G'B' image.

We then used the same compact camera set-up at a wider angle to image an assemblage of organisms from our tropical mesocosm (Fig. 5.9). In this image, red and green corals produced a strong fluorescence signal in the R', G', and B' channels; lower intensity signal was also detected in the R' and B' channel for red algae and CCA (Fig. 5.9). However, the same green macroalgae that produced clear signal in the R' channel when imaged with the CCD camera did not produce above-background fluorescence in any channel when imaged with a compact camera (Fig. 5.6, 5.9).

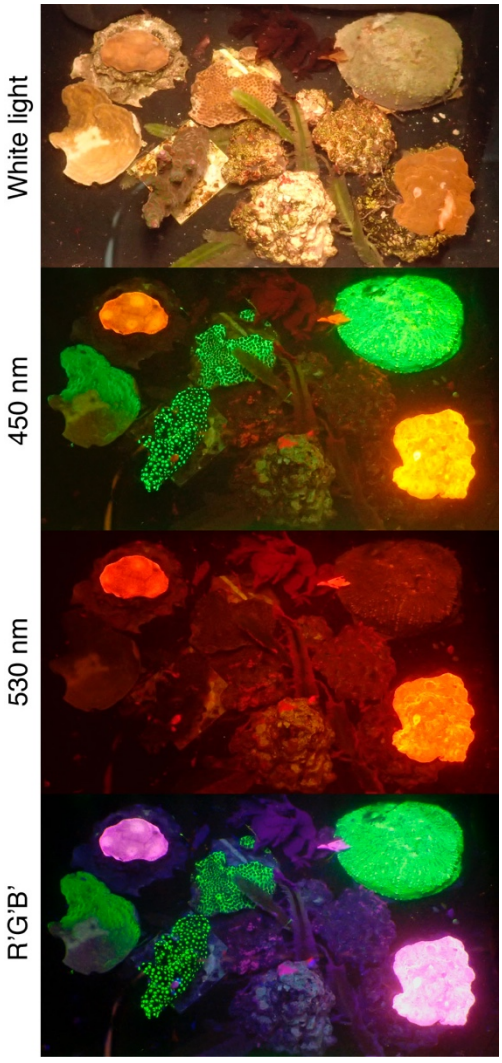

Figure 5.9 Multi-excitation imaging of coral reef organisms with a compact camera

Scene imaged under white light, 450 nm excitation (510 nm emission filter), 530 nm excitation (610 nm emission filter), and the resulting combined R'G'B' image.

5.4 Discussion

5.4.1 Design of a multi-excitation fluorescence imaging system

We have developed the concept for an imaging system designed to collect information on the fluorescence excitation and emission spectra of marine benthos. The system relies on high-power colour LEDs to excite fluorescence in two spectral bands, centred at 450 nm and 530 nm, and on a camera equipped with long-pass filters to detect fluorescence emission in the spectral bands corresponding to the R and G channels of the camera sensor. Narrow-waveband illumination and red-shifted detection are a pre-requisite of fluorescence imaging, and can provide the additional advantage of reducing scattering artefacts produced by particles in the water column, common in reflectance images (Treibitz *et al.*, 2012; Murez *et al.*, 2015). In both recreational and scientific underwater fluorescence photography, narrow-waveband illumination is commonly achieved using off-the-shelf professional strobes equipped with band-pass or short-pass filters (Mazel, 2005; Treibitz *et al.*, 2015); as a result, only a fraction of light emitted by the instrument is used to excite fluorescence. However, high intensity illumination is required to image fluorescence in the marine environment due to the attenuation of signal by water (Mazel *et al.*, 2003a), the low quantum yield of certain pigments *in vivo* (Falkowski and Kiefer, 1985), and the requirement to maintain fast shutter speeds to compensate for water movement or ambient light (Mazel, 2005); thus, multiple strobes are often employed (Treibitz *et al.*, 2015). High-power, narrow waveband LEDs offer a potential solution to this issue. From a single diode, the LEDs used in this study can provide up to 100 lumens concentrated within a ~50 nm spectral width; this makes them an ideal component to build a multi-excitation illumination system that can produce high intensities while keeping size, cost and battery requirements within practical limits.

One disadvantage of this approach to illumination is the absence of a sharp cut-off in the LED emission spectra, which resulted in some background reflectance signal caused by bleed-through of excitation light into the camera sensor channels. To remove this contribution from the fluorescence images, we included a channel-specific background subtraction step in the image processing workflow. While this method produced good results, we note that imaging substrates with a wider range of optical properties such as highly reflective coral or sand (Hochberg *et al.*, 2003; Enríquez *et al.*, 2005) might accentuate the issue. Combining narrow-waveband LEDs with a short-pass excitation filter might thus be a more suitable approach for field applications.

Following background correction, we processed multi-excitation fluorescence data as pseudocolor RGB images. A commonplace approach in fluorescence microscopy,

pseudocolor RGB has also been employed to present and classify multispectral fluorescence images in coral benthic surveys (Mazel *et al.*, 2003a). This approach provides a means to summarise all spectral information into a single frame, and results in good visual separation of the pigments in the colour space. The aim is not only to facilitate image interpretation by the user, but also to enable the application of colour or texture-based automatic classification methods developed for reflectance images (Mehta *et al.*, 2007; Stokes and Deane, 2009; Beijbom *et al.*, 2012; Mahmood *et al.*, 2016). However, combining data acquired as two separate frames into a single multichannel image makes later classification steps sensitive to registration errors (Beijbom *et al.*, 2016). While our prototype imaging system was designed to eliminate or greatly reduce this issue, the need to obtain registered image pairs poses a challenge to the application of this technique in the field. Previous studies have successfully used a custom-built framer and a post-processing transformation to register reflectance/fluorescence image pairs obtained with two separate cameras (Beijbom *et al.*, 2016; Zweifler *et al.*, 2017); however, convolutional neural network annotation done on the combined image was less accurate than the same method applied in a two-stage approach on the image pairs (Beijbom *et al.*, 2016). A similar approach to classification could be explored for multi-excitation imaging. Future developments of this imaging system for *in situ* application should be designed to minimise movement between frames.

5.4.2 Signal interpretation of multi-excitation images

To assess the ability of multi-excitation fluorescence imaging to generate spectral data that are meaningful for the discrimination of functional benthic groups, we tested the concept on representative marine pigments in isolation. With knowledge of the spectral properties of the illumination system and of the camera sensor, we were able to accurately predict R'G'B' pixel intensity from the purified pigment spectra. This confirmed that data collected with our imaging technique are a function of both the excitation and the emission spectra of the subject imaged, and can be directly related to measurements obtained with laboratory-based spectroscopic methods.

In R'G'B' images acquired with either a CCD microscope camera or a compact CMOS camera, chlorophylls purified from green algae appear almost exclusively red, coral GFP appears green, while coral RFPs and red algae PE appear as shades of pink and purple. The 450 nm light source has a strong overlap with the Soret absorption band of chlorophyll a and b, therefore efficiently exciting deep-red fluorescence emission (Mackinney, 1941; Falkowski and Kiefer, 1985); the green gap in the chlorophyll absorption spectrum, on the other hand, results in negligible excitation by the 530 nm light. These spectral properties cause chlorophyll to be clearly defined in the R'G'B' colour

space by the strong R' signal and negligible signal in the other channels. Coral GFPs and CFPs are also strongly excited by 450 nm light (Alieva *et al.*, 2008); while the blue part of their spectrum is blocked by the emission filter, the rest falls almost entirely within the sensitivity of the G channel of camera sensors, resulting in clear separation of this pigment group as strong G' signal (Treibitz *et al.*, 2015; Beijbom *et al.*, 2016). PE and coral RFPs have similar spectral properties; both are strongly excited by 530 nm light, which produces the signal in the B' channel that clearly separates them from the other pigments. Orange-red fluorescence of RFPs and PE is also excited to a lesser extent by 450 nm light; however, emission is blue-shifted from chlorophyll fluorescence by about 100 nm, and as such it is expected to generate signal in either just R, or both R and G channels in variable proportions depending on the spectral sensitivity of the camera sensor and on the exact emission peak of the pigment considered. Of the two cameras tested here, emission alone was sufficient to separate PE and RFPs from other pigments in the 450 nm image when using the CCD microscope camera, but not when using the CMOS compact camera; in fact, with the latter system chlorophyll, PE and RFPs appear almost identical under 450 nm excitation. In this case, the information provided by the 530 nm image and conveyed by the B' channel is thus the sole discriminant between these pigments, demonstrating the potential of multi-excitation imaging for improvement of fluorescence-based classification.

Proteins belonging to the pcRFP group emit green fluorescence upon synthesis, but they are converted into a red-emitting form upon irradiation with light in the near-UV range (Ando *et al.*, 2002; Wiedenmann *et al.*, 2004a). The purified pcRFP used in this study had a high proportion of unconverted, green-emitting chromophores, which conferred it a different spectral signature from PE or other RFPs and produced G' signal when imaged with either camera. However, in shallow water environments coral pcRFPs have a higher proportion of red chromophores and emit mostly orange-red fluorescence (Bollati *et al.*, 2017); these pigments will thus group more closely to other orange-red pigments under multi-excitation imaging in the field.

5.4.3 Classification of multi-excitation images

Mazel *et al.* (2003a) showed that a set of *a priori* rules based on relative signal in different channels can be used to classify multispectral fluorescence images of coral reefs. We adopted a similar approach for multi-excitation images, defining a set of rules based on the R'G'B' ratios of purified pigments and applying it to images of live organisms. While we anticipate that machine learning techniques could yield better results for field surveys (Beijbom *et al.*, 2016), the *a priori* method was effective in establishing a conceptual basis for classification of multi-excitation fluorescence data using a limited number of images.

The algorithm was able to assign areas of images that corresponded to green algae, green or cyan corals, and red corals or CCA to three separate groups based on their pixel intensity in the R'G'B' channels. For other red macroalgae, pixel intensity values fell outside the three explicit categories resulting in classification as a separate group. While separation of coral from algal and abiotic substrates had been previously demonstrated with a fluorescence camera (Treibitz *et al.*, 2015; Beijbom *et al.*, 2016), resolution of different groups of algae had only been achieved with a multispectral imager by exploiting spectral separation between the emission peaks of chlorophyll and PE (Mazel *et al.*, 2003a). However, studies performed on micro and macroalgae have shown that functional groups can be discriminated by comparing chlorophyll emission upon blue and green excitation (Yentsch and Phinney, 1985; Topinka *et al.*, 1990). Due to the high efficiency of coupling between photosynthetic pigments, fluorescence emission of algae occurs predominantly from de-excitation of PSII chlorophyll a (Falkowski and Kiefer, 1985); however, in green algae much of the PSII excitation energy is transferred from chlorophyll a and b molecules found in light harvesting complexes (Thornber, 1975), while in red algae it is transferred from phycobiliproteins found in the phycobilisomes (French and Young, 1952). Thus, spectral fluorescence excitation rather than emission is particularly suited to provide information about the accessory pigment composition of photosynthetic organisms, and consequently on their taxonomic and functional grouping.

A particular case is that of PE, which can emit detectable fluorescence even when coupled to other pigments *in vivo* (French and Young, 1952). In this study, the relative intensities of chlorophyll and PE emission differed between CCA and non-calcifying red macroalge, a difference reflected in the results of automatic classification. The concentrations of the two pigments are known to vary interspecifically (Kim *et al.*, 2007); while our set of rules was not designed to account for pigment combinations, we anticipate that these differences might be useful to improve classification within the red algae. Relative proportions of chlorophyll and PE are also known to vary intraspecifically with photoacclimation in CCA (Payri *et al.*, 2001), as are some groups of FPs in corals (D'Angelo *et al.*, 2008). Multi-excitation imaging could thus contribute to the development of fluorescence as a biomarker of organism-level physiological processes (Hardy *et al.*, 1992; Zawada and Jaffe, 2003; D'Angelo *et al.*, 2008, 2012).

One limitation of our method is that, due to considerable spectral overlap between PE, RFPs and pcRFPs (Oswald *et al.*, 2007), these pigments do not separate enough in the R'G'B' ratio space to enable classification of CCA and red corals as two different categories. While this poses a constraint to the use of R'G'B' ratios alone as the basis for automatic classification, confusion of CCA with hard coral is not commonly an issue when classification is done with reflectance images (Beijbom *et al.*, 2012, 2015). Integrating

R'G'B' colour with other image properties currently used by computer vision models, such as texture (Mehta *et al.*, 2007; Stokes and Deane, 2009; Beijbom *et al.*, 2012), or combining fluorescence images with reflectance ones (Beijbom *et al.*, 2016) might facilitate discrimination between these groups.

Finally, while we were able to image fluorescence of all purified pigments using either a microscope CCD camera or a compact CMOS camera, with the latter we could not detect a clear chlorophyll emission signal when imaging live organisms. This can be attributed to the lower quantum yield of chlorophyll fluorescence *in vivo* due to photochemical quenching of the excitation energy (Falkowski and Kiefer, 1985). In addition, off-the-shelf camera sensors are normally equipped with an infrared (IR) filter, which reduces sensitivity of deep-red wavelengths including the chlorophyll emission band (Treibitz *et al.*, 2015). With an unmodified camera, classification of CCA from multi-excitation fluorescence images would thus need to be primarily based on the PE emission signal; however, Treibitz and co-workers (2015) showed that wide-angle imaging of chlorophyll fluorescence can be achieved by removing the IR filter from an off-the-shelf professional camera. Using a modified camera for multi-excitation imaging would improve detection of green algae in the R' channel, and increase signal in the B' channel for groups of red algae that have higher chlorophyll emission relative to PE. Further studies should assess the efficacy of a modified and unmodified camera approach for the classification of benthic algae.

5.4.4 Potential commercial application

Developing an *in situ* instrument based on the multi-excitation fluorescence imaging concept would introduce a novel approach to underwater spectral imaging on the market. The use of two different illumination bands to excite fluorescence separates this technique from other *in situ* fluorescence imaging methods (Table 5.1), which employ a single narrow excitation band (Strand *et al.* 1997, Treibitz *et al.* 2016). Multi and hyperspectral reflectance imaging systems (Gleason *et al.*, 2007; Chennu *et al.*, 2017) utilise broad band illumination (Table 5.1), and are therefore also unable to provide information on the excitation spectra of the pigments surveyed, particularly in the case of efficient coupling between multiple pigments. In addition, multi or hyperspectral reflectance imaging requires the use of specialised cameras, in contrast with multi-excitation fluorescence imaging which can be implemented using an off-the-shelf professional camera, a modified professional camera, or even a compact camera.

As well as having commercial potential as an instrument to facilitate benthic survey annotation, a multi-excitation fluorescence imager could be deployed in the context of *in situ* experiments. For example, spectral monitoring of coral-algae interfaces (Barott *et al.*,

2009) is of relevance to studies assessing the effects of algal-associated microbiomes on coral health (Smith *et al.*, 2006), or investigating recovery of reefs following disturbance (Diaz-Pulido *et al.*, 2009). Changes in coral pigmentation in colonies affected by disease could also be monitored with this technology (Sussman *et al.*, 2006), as could changes in pigmentation associated with bleaching or stress response (Chapter 4 of this thesis). In all these cases, long-term or permanent quadrats containing target organism assemblages could be imaged at regular time intervals with multi-excitation fluorescence. This approach would allow greater monitoring frequency compared to destructive sampling, while facilitating a quantitative interpretation of the image compared to a reflectance photoquadrat.

Finally, customised systems could be produced by modifying the original design to include different excitation wavelengths and filter combinations; this would enable the use of the multi-excitation fluorescence imager to fulfil an even wider range of survey requirements.

5.5 Methods and materials

5.5.1 Design and characterisation of multi-excitation illumination system

Two high power LEDs (Lumiled Luxeon Rebel in Royal Blue, 450 nm, and Green, 530 nm) were soldered onto single-diode star printed circuit boards (Bergquist), mounted onto a 2.5 cm anodised aluminium heat sink (Ohmite), and ran at 350 mA using a constant current driver (PowerLED). The LED modules were fitted with plastic connectors to enable alternate coupling of each LEDs into an optical fibre connected to a 66 mm microscope ringlight (Leica), which was mounted onto the objective of a fluorescence microscope (Leica MZ10 F) (Fig. 5.2). For reflectance images, a photonic cold light source (Leica) was used with the same fibre and ringlight. The LED light sources produced a photon irradiance of 49 μmol photons m^{-2} s^{-1} (450 nm LED) and 28 μmol photons m^{-2} s^{-1} (530 nm) when the microscope was focused on the surface of a 180° quantum sensor attached to a PAR light meter (Li-Cor). Relative irradiance spectra of the LEDs were measured with a USB 4000 modular spectrometer (Ocean Optics).

5.5.2 Sample origin

Fronds of *Codium* sp. Stackhouse 1797 and *Solieria chordalis* (C. Agardh) J. Agardh 1842 were collected from the intertidal shore in Portland, UK, frozen and maintained at -20°C before processing. Live corals and algae used for imaging were obtained from the UK ornamental trade and cultured long term in the Coral Reef Laboratory tropical mesocosm at the National Oceanography Centre, Southampton, UK (D'Angelo and Wiedenmann, 2012).

5.5.3 Algal pigment extraction

Frozen fronds were homogenised with a pestle and mortar in 0.1 M sodium phosphate buffer (pH 7.4). For extraction of *Codium* lipid-soluble pigments, 0.5 mL saturated $MgCO_3$ solution was added to the mortar to prevent pheophytinisation. Pigments were extracted in 90% acetone at -20°C for 1 hour, and debris was removed by centrifugation (3 min, 2000 rcf, 4°C, twice). For water-soluble pigment extraction from *S. chordalis*, homogenisation was followed by 5 min sonication on ice in 30 second bursts; the extract was then clarified by centrifugation (3 min, 2000 rcf, 4°C, twice, followed by 45 min, 20000 rcf, 4°C). All samples were frozen at -20°C before further analysis.

5.5.4 Coral GFP-like protein expression and purification

Fluorescent proteins amilFP497 and amilFP597 from *Acropora millepora* (Ehrenberg 1834) and EechRFP from *Echinophyllia echinata* (Saville-Kent 1871) were produced in a bacterial expression system as described by Wiedenmann *et al.* (2002). For amilFP497 and amilFP597, the clarified supernatant was used for imaging. EechRFP was purified from the clarified supernatant and desalted as described by Bollati *et al.* (2017); partial photoconversion was induced by placing the purified protein under a 412 nm LED (Aquaray NUV, TMC) for 10 min.

5.5.5 Fluorescence spectroscopy

Excitation/emission spectra of purified pigments were measured with a fluorescence spectrophotometer (Cary Eclipse, Agilent) in a 10 mm quartz cuvette. For pigment characterisation, all emission spectra were collected using 450 nm excitation, and excitation spectra were measured for emission 400-700 nm (zero order).

Excitation/emission spectra of live corals and algae were measured by coupling the spectrophotometer with a fibre optic probe (D'Angelo *et al.*, 2008). Emission/excitation wavelength used for measurement were selected based on the pigment composition of each organism, and are presented in Table 5.2.

Table 5.3 Spectrophotometer settings used to collect fluorescence spectra of live organisms

Organism	Excitation λ (nm)	Emission λ (nm)
Green algae	476	680
Red algae	476	680
CCA	476	680
Oxypora sp.	470	590
A. millepora	435	550
P. lichen	450	550

5.5.6 Pixel intensity prediction

Information on the spectral sensitivity of an equivalent fluorescence CCD camera was obtained from the manufacturer and used to produce a set of wavelength-specific RGB probabilities (Fig. 5.1b). Purified pigment excitation and emission spectra, and LED relative irradiance spectra, were background corrected and normalised to the integrated intensity; normalised LED spectra were scaled to the respective measured photon irradiance. For each pigment, the relative excitation by 450 nm (Ex_{450}) and 530 nm (Ex_{530}) light sources was then calculated as follows:

$$Ex_{450} = \int_{400}^{700} Ex(\lambda)\, Int_{450}(\lambda)\, d\lambda$$

$$Ex_{530} = \int_{400}^{700} Ex(\lambda)\, Int_{530}(\lambda)\, d\lambda$$

Where Ex is the normalised excitation, Int_{450} and Int_{530} are the scaled relative intensities of the two light sources, and λ is wavelength.

For each pigment, the predicted pixel intensity in the R'G'B' channels was then calculated as follows:

$$R'_{predicted} = Ex_{450} \int_{510}^{700} p_R(\lambda)\, Em(\lambda)\, d\lambda$$

$$G'_{predicted} = Ex_{450} \int_{510}^{700} p_G(\lambda)\, Em(\lambda)\, d\lambda$$

$$B'_{predicted} = Ex_{530} \int_{610}^{700} p_R(\lambda)\, Em(\lambda)\, d\lambda$$

Where p_R and p_G are the R and G probabilities (Fig. 5.1b), and Em is the normalised emission.

5.5.7 Microscopic imaging

Images of purified pigments in a micro well plate and of live organisms were taken with a CCD camera (Leica DFC 420 C) through the fluorescence microscope. The wheel-mounted emission filters used were a long-pass UV filter for reflectance images (cut-on 420 nm), a GFPplus filter for 450 nm images, and a Texas Red filter for 530 nm images (Fig. 5.1a); filter transmission spectra were measured with a UV-Vis spectrophotometer (Cary 50, Agilent).

Purified pigments were imaged with an exposure time of 6 s, as were all live algae and the brown morph of *M. foliosa*; all other corals were imaged with an exposure time of 980 ms. Images for background correction were collected using the same exposure times; an empty well was imaged as background for purified pigments, while a black non-reflective material was used for live organisms.

5.5.8 Macroscopic imaging

Macroscopic images were taken with a compact camera (Olympus TG4) in aperture priority mode, mounted on a tripod; illumination was from the same ringlight system, fixed ~20 cm above the scene to image. Emission filters were held in front of the camera lens; plastic long-pass filters (Nightsea) were used to image purified pigments in a 96-well plate. The wider-angle image of an assemblage of tropical benthic organism was obtained using gel emission filters (Rosco #10 Medium Yellow and #19 Fire) to avoid distortion produced by the convex plastic filters. Filter transmission spectra were measured as above and are presented in Supplementary Fig. 5.10. A well containing water was used for background correction of the purified pigment image, and an area of the tank free from organisms was used for background correction of the reef assemblage image.

5.5.9 Image processing

To convert 450 nm and 530 nm image pairs into R'G'B' images, each 8-bit RGB image was first split into the 3 colour channels. The R and G channels of the 450 nm image and the R channel of the 530 nm image were background corrected by subtracting the mean pixel intensity of the corresponding background images from every pixel, then merged into a new 8-bit RGB image.

Pixel intensity of purified pigment images in each channel was measured using software Fiji (Schindelin *et al.*, 2012) and compared to predicted values using a Pearson's product-moment correlation test.

Classification rules were manually defined after plotting the R'/G', R'/B' and G'/B' ratios of purified pigments in a 3D space. The rules were selected to be exclusive, so it would not be possible for a pixel to be classified as more than one category. The background value was set to 20 for all channels and all categories. The classification algorithm was implemented in Matlab.

Images obtained with the compact camera were registered using the ImageJ plugin StackReg (Thévenaz *et al.*, 1998) to compensate for the convex emission filter and for any small movements of the camera.

5.6 Supplementary Figures

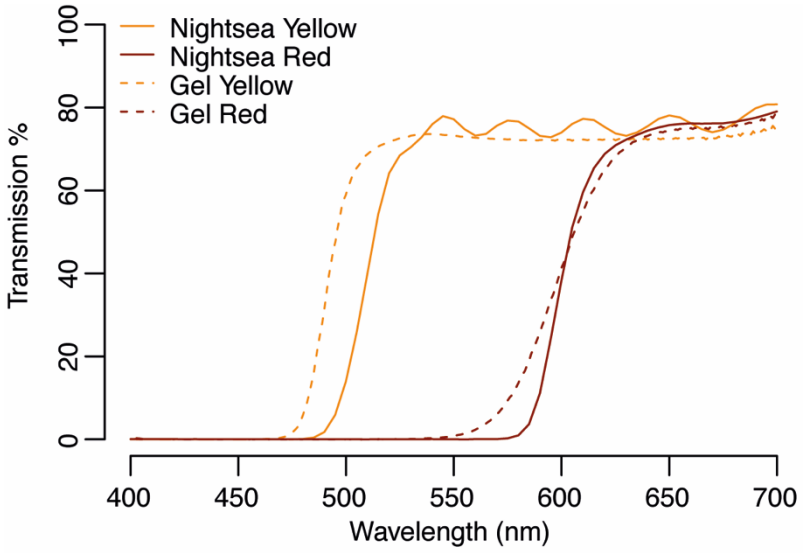

Figure 5.10 Transmission spectra of filters used for compact camera imaging

Chapter 6 Conclusions

6.1 Key findings

The following sections summarise the main findings presented in chapters 3-5 in the context of the research questions outlined in section 1.2.1.

6.1.1 Q1. How do corals maintain red fluorescence in the mesophotic light environment?

This research question stemmed from the incompatibility of *in vitro* studies, showing that ~400 nm light is the sole driver of red chromophore maturation in pcRFPs (Ando *et al.*, 2002; Wiedenmann *et al.*, 2004a), with field observations of red pcRFPs in environments where this waveband is reduced, such as mesophotic reefs (Eyal *et al.*, 2015). During the 4-month mesocosm experiment presented in chapter 3, only colonies kept under spectral light regimes that contained ~400 nm wavelenghts were able to maintain a pool of converted pcRFPs. This confirmed that red fluorescence of pcRFP-containing corals is dependent on the presence of this waveband in their environment. However, colonies were able to maintain a degree of red fluorescence even when acclimated to very low ~400 nm photon irradiance, comparable to what measured on mesophotic reefs. *In vitro* measurements of photoconversion rates performed on different recombinant pcRFPs confirmed that slow but significant photoconversion can be achieved at this photon irradiance. Red fluorescence of mesophotic corals (Eyal *et al.*, 2015) is therefore the result of photoconversion of pcRFPs driven by the rare ~400 nm photons present in the mesophotic light field. The slow turnover of pcRFPs *in vivo* (Leutenegger *et al.*, 2007a) allows accumulation of a population of converted chromophores before the protein is degraded. Under a constant low ~400 nm photon irradiance, the protein pool is thus maintained in a partially converted steady state. Red emission, directly or via FRET, is the dominant de-excitation mechanism in partially converted pcRFP tetramers (Wiedenmann *et al.*, 2004a). A partially converted pcRFP pool is thus the source of red fluorescence in mesophotic corals.

6.1.2 Q2. Is intratetrameric FRET part of the function of GFP-like proteins in mesophotic coral?

It had been previously hypothesised that a FRET-based mechanism for long-range wavelength conversion by groups of GFP-like proteins arranged in close proximity could be part of the function of these proteins (Gilmore *et al.*, 2003; Cox *et al.*, 2007). Green and

red subunits of partially converted pcRFP tetramers are an ideal system to investigate the existence of a similar mechanism, because of the obligate small distance and dipole orientation between donor and acceptor. However, intratetrameric FRET in pcRFPs had not been previously investigated *in vivo*. When a colony with a predominantly unconverted pcRFP pool was exposed to ~400 nm light, the FRET-derived red emission increased more rapidly than the direct emission of the red chromophore, confirming the existence of FRET in live corals. The FRET-derived red emission saturated at a level of photoconversion equivalent to that achieved in the mesocosm experiment by corals exposed to a simulated mesophotic light field. When compared to proteins with fully green or fully red tetramers, partially converted pcRFPs were the most efficient fluorophore for transforming blue-green wavelengths into orange-red ones; more specifically, pcRFPs with a 1:1 green:red ratio, similar to what expected at mesophotic depths, had the greatest wavelength conversion potential. Work published in parallel with this study showed that orange-red light can achieve greater penetration through coral tissue compared to other wavelengths, reaching deeper symbiont layers and enhancing photosynthesis (Smith *et al.*, 2017). Taken together, these studies suggest that FRET-mediated wavelengths conversion in pcRFPs plays a role in adaptation of mesophotic corals to their light environment. Intratetrameric FRET is thus likely part of the function of pcRFPs in mesophotic corals.

6.1.3 Q3. How does bleaching affect the regulation of GFP-like proteins?

Previous studies had shown that GFP-like proteins are downregulated in response to heat stress (Smith-Keune and Dove, 2008; Hume *et al.*, 2013). However, the relationship between protein concentration and *in vivo* fluorescence measurements was suggested to uncouple upon the onset of bleaching (Roth and Deheyn, 2013), hindering the application of these proteins as biomarkers. In the series of mesocosm experiments presented in chapter 4, corals that had undergone bleaching induced by light stress, heat stress or nutrient stress showed an increase in the content of GFP-like proteins, measured both *in vivo* and in harvested tissue. This response was observed when bleached corals were exposed to blue light, but not when exposed to an equivalent photon irradiance of green light, confirming that the increase in GFP-like protein expression was caused by a transcriptional response to enhanced blue light fluxes in the tissue (D'Angelo *et al.*, 2008). The study therefore shows that, by enhancing internal light fluxes (Wangpraseurt *et al.*, 2017), bleaching induces the expression of GFP-like proteins. However, this study also suggested that the response might be dampened or absent under acute heat stress.

6.1.4 Q4. Are GFP-like proteins involved in coral recovery after bleaching?

In the growing margins of coral colonies, high concentrations of GFP-like proteins have been proposed to promote colonisation with symbionts as part of a mechanism for colony expansion (D'Angelo *et al.*, 2012). Chapter 4 assessed the possibility that a similar process could be part of the function of the described GFP-like protein regulation mechanism in bleached corals. Measurements of GFP-like proteins showed that the concentrations found in bleached tissue are equivalent to those measured in the growing margins of healthy colonies, indicating a potential similarity in function between the two. Furthermore, after being allowed to recover under high light, tissue areas expressing high concentrations of GFP-like proteins harboured a higher number of symbionts. The PSII quantum yield measured *in vivo* was also higher for symbionts in high GFP-like protein areas. This study therefore proposed that GFP-like proteins are involved in coral recovery via an optical feedback mechanism, which can be summarised as: i) enhancement of light fluxes following bleaching induces GFP-like protein expression, ii) photoprotection by GFP-like proteins reduces light fluxes promoting symbiont recolonisation, iii) symbiont absorption further reduce light fluxes preventing GFP-like protein expression.

6.1.5 Q5. Is multi-excitation fluorescence imaging a suitable approach to automatic classification of coral reef communities?

Chapter 5 presented the conceptual development of an underwater fluorescence imaging system based on excitation in two separate wavebands, green and blue. Previous approaches to underwater fluorescence imaging for automatic classification either involved the use of specialised multispectral equipment (Mazel *et al.*, 2003a), or were limited to two detection channels (Beijbom *et al.*, 2016). This study showed that by adding a second excitation waveband, it is possible to design a 3-channel system using off-the-shelf components. A set of *a priori* classification rules defined using the spectral properties of purified pigments was able to classify the organisms imaged into broad groups, showing that multi-excitation imaging is indeed a suitable approach to automatic classification. The study highlighted that multi-excitation is particularly useful for classifying groups of algae, previously reported to pose a challenge to automatic and manual annotation (Beijbom *et al.*, 2015), and for use with CMOS cameras, which cannot separate chlorophyll and phycoerythrin emission upon blue excitation alone.

6.2 Implications

This study has provided novel insights into the function and regulation of coral GFP-like proteins, has demonstrated some practical applications of fluorescence as an *in vivo* biomarker, and has provided the basis for further technological development. Taken together, these findings contribute to the development of fluorescence as a tool to monitor coral reef organisms and communities. The following sections consider the results presented in this thesis in the wider context of coral reef science, and propose future research directions.

6.2.1 Understanding the function of GFP-like proteins in corals

The hypothesis that host pigments act to modify the internal light environment of coral colonies in order to benefit the symbiosis was proposed before these pigments were identified as GFP-like proteins (Kawaguti, 1969; Schlichter *et al.*, 1986). To an extent, this hypothesis was challenged by studies showing that chlorophyll excitation was unaffected by some GFP-like proteins (Gilmore *et al.*, 2003; Mazel *et al.*, 2003b). A number of studies have proposed alternative roles of these proteins in oxidative stress response (Bou-Abdallah *et al.*, 2006; Roth and Deheyn, 2013; Shikina *et al.*, 2016) or visual ecology (Matz *et al.*, 2006; Gruber *et al.*, 2008). Different mechanisms through which GFP-like proteins can fine-tune the internal light environment of coral colonies have now been described, showing that these pigments are able to both enhance and reduce light fluxes (Smith *et al.*, 2013, 2017; Lyndby *et al.*, 2016, chapters 3-4). Although the presence of these proteins in azooxanthellate, non-bioluminescent Anthozoa (Vogt *et al.*, 2008) indicates that alternative functions are likely to exist within the group, it is clear that light modification is a key function of GFP-like proteins in corals. However, the great incidence of colour polymorphism in conspecific colonies from similar light environments (Wiedenmann *et al.*, 1999; Eyal *et al.*, 2015) suggests that light modification by GFP-like proteins is beneficial, but not essential to the symbiosis. The metabolic investment required for high-level expression of these pigments, despite slow turnover, can reduce fitness in other aspects of physiology such as growth (Leutenegger *et al.*, 2007a; Gittins *et al.*, 2015; Quick *et al.*, 2018). GFP-like proteins are thus likely to constitute one of a number of adaptations that have resulted from balancing selection and that have allowed corals to persist in a highly variable environment (Gittins *et al.*, 2015; Quick *et al.*, 2018). In chapter 4, high concentrations of CPs were shown to promote recolonisation with symbionts after a bleaching event; however, this does not exclude that conspecifics exhibiting low-level expression under high light (Gittins *et al.*, 2015) might be more resistant to bleaching in the first place. For example, GFP-like proteins might cause high-expression corals to heat more rapidly compared to their low-expression conspecifics

(Lyndby *et al.*, 2016). A parallel could be drawn with the spread of adaptive strategies observed in the optical properties of coral skeleton and tissue (Marcelino *et al.*, 2013; Wangpraseurt *et al.*, 2016; Enríquez *et al.*, 2017): corals with structures that redistribute light more efficiently were shown to be more susceptible to bleaching, and to the bleaching-induced optical feedback loop (Marcelino *et al.*, 2013; Swain *et al.*, 2016; Enríquez *et al.*, 2017; Wangpraseurt *et al.*, 2017). The diversification of strategies to regulate light fluxes is likely a key aspect of the evolution of coral reef ecosystems.

6.2.2 Developing fluorescence as a biomarker

The studies presented in this thesis have shown that optical measurements of fluorescence can be a powerful tool to investigate physiological processes in corals. In chapter 3, repeated *in vivo* measurements of red and green fluorescence provided information on the long-term acclimation to different spectral regimes, and enabled estimates of FRET during photoconversion. In chapter 4, GFP-like proteins with different induction thresholds were used to detect a host-specific high light acclimation response. In both cases, optical monitoring of fluorescence allowed a degree of temporal resolution that would have not been possible with an invasive approach. These studies exemplify that, with knowledge of how GFP-like proteins are regulated, it is possible to create fluorescence-based biomarkers for monitoring coral response to environmental conditions. However, as extensively discussed, regulation of GFP-like proteins in corals is fundamentally heterogeneous (Leutenegger *et al.*, 2007a; D'Angelo *et al.*, 2008). Therefore, biomarkers must be specific to the GFP-like protein complement expressed by a particular species, colour morph, or even genotype. GFP-like protein regulation should always be characterised in the study organism under consideration before new biomarkers can be applied. Eventually, this might lead to the identification of a number of model species that are particularly suitable for use in fluorescence biomarker studies.

The biomarkers used in chapters 3 and 4 were based on simultaneous monitoring of fluorescence in two different spectral bands. Other studies have previously suggested that *in vivo* stress biomarkers could be created by correlating changes in the relative proportions of GFP-like proteins with other physiological parameters (Zawada and Jaffe, 2003). The work presented here suggests that a mechanistic approach, rather than correlation, can provide a stronger basis for biomarker development. Using two proteins with different regulation and different spectral properties in a single biomarker can help differentiate a true physiological response from measurement artefacts, caused for example by changes in the optical properties of the tissue during bleaching. As well as acting as organisms-level biomarkers of photoacclimation, the relative proportions of fluorescent pigments can be used for community-level classification of organisms into

functional groups (chapter 5). This suggests that the ratio approach is robust, is applicable on multiple levels of biological complexity, and might be applicable to *in situ* studies.

In chapter 4, it was proposed that extreme colours derived from GFP-like proteins could be a sign that local stressors are in action, and that corals are bleaching near or below their thermal bleaching threshold. In this case, GFP-like proteins could be applied as a reef-scale indicator for monitoring and management purposes. Considered the importance of managing local stressors to promote resilience and adaptation of corals to environmental change (Wooldridge and Done, 2009; D'Angelo and Wiedenmann, 2014; Hume *et al.*, 2016), this would be a valuable addition to the community-based assessment "toolbox" (Risk *et al.*, 2001). This finding exemplifies how physiological studies of GFP-like protein regulation can yield potential biomarkers for application of the diagnostic method in the field (Downs *et al.*, 2005).

6.2.3 Future work

6.2.3.1 Effects of GFP-like proteins on symbiont photosynthesis *in hospite*

This thesis has complemented the existing body of research showing that the enhancement or reduction of light fluxes to benefit the symbiosis is a key function of GFP-like proteins in corals (Salih *et al.*, 2000; Smith *et al.*, 2013, 2017; Lyndby *et al.*, 2016). However, the benefit for the symbiosis has mostly been assessed indirectly, rather than directly quantified. In order to gain a more comprehensive understanding of how GFP-like proteins modify light fluxes inside coral tissue, and of what effect this has on symbiont photosynthesis, future studies should focus on characterising these processes *in hospite* on the microscale. By characterising the light microenvironment inside coral tissue, it is possible to directly assess of how changes in pigment absorption affect symbiont photosynthesis (Wangpraseurt *et al.*, 2017). With a similar method, the effects of GFP-like proteins on light fluxes should be evaluated *in hospite* in a comprehensive study encompassing multiple proteins and species. The approach briefly described below could be adopted to build on the findings presented in this thesis.

First, microscale measurements of light fluxes and photosynthesis should be performed in corals undergoing bleaching and recovery in the presence or absence of high concentrations of GFP-like proteins. This would complement the data presented in chapter 4, and provide a quantification of the effect of GFP-like proteins on coral recovery in terms of *Symbiodinium* physiology. Conspecific colour morphs unable to express high levels of GFP-like proteins should be included in the analysis, in order to provide insights into the trade-offs associated with high-level expression and into potential alternative strategies to facilitate recovery (Quick *et al.*, 2018).

Second, the microscale light environment of pcRFP-containing corals acclimated to shallow and mesophotic light spectra should be considered. This would provide further evidence that higher penetration of coral tissue by orange-red wavelengths stimulates photosynthesis in deeper symbiont layers (Smith *et al.*, 2017). Furthermore, it would be possible to directly quantify the effects of wavelength transformation by a partially converted pcRFP pool on light penetration and on photosynthesis. This would verify the hypothesis that incomplete maturation of RFPs and pcRFPs has functional significance in corals.

6.2.3.2 Towards a mechanistic understanding of GFP-like protein regulation

The studies presented in this thesis used GFP-like protein biomarkers to detect the presence of a particular physiological response, and to assess the response timescale. However, further work done on model species might enable us to mathematically predict the response of specific GFP-like proteins or groups of proteins to environmental conditions. A mechanistic model of GFP-like protein regulation could be used in conjunction with optical tissue models (Enríquez *et al.*, 2005; Wangpraseurt *et al.*, 2016) to assess how GFP-like protein regulation interacts with other processes, such as bleaching. This would provide a valuable tool for testing hypotheses *in vivo*; for example, downregulation of GFP-like proteins caused by heat stress (Smith-Keune and Dove, 2008) could be detected as a deviation from the modelled response.

In this context, a future study should also elucidate the cellular signalling pathway leading to the expression pattern observed in response to blue light (D'Angelo *et al.*, 2008). Light-sensing in corals has mostly been studied in relation to synchronous spawning events (Levy *et al.*, 2007; Kaniewska *et al.*, 2015). Cryptochromes, opsins, and g-protein-coupled receptors have been identified as potential parts of a light signal transduction mechanism (Levy *et al.*, 2007; Mason *et al.*, 2012; Kaniewska *et al.*, 2015), but no pathway has been clearly demonstrated. Knowledge of the cellular basis of GFP-like proteins regulation would enable identification of which parts of the pathway are affected by environmental stress, therefore potentially involved in deviations from the modelled response. For example, a light-induced signalling pathway involving cytoplasmic calcium (Hilton *et al.*, 2012) could be disrupted during heat stress (Desalvo *et al.*, 2008), resulting in the observed downregulation.

6.2.3.3 Multi-excitation fluorescence imaging in the field

The multi-excitation fluorescence imaging system presented in chapter 5 provides a stepping stone towards transferring the application of fluorescence as a biomarker from the laboratory to the field. The next development in this direction is the realisation of a

prototype imaging system for *in situ* testing. Chapter 5 has already highlighted some of the challenges and limitations associated with field applications of multi-excitation fluorescence imaging; these include image registration in a dynamic environment, need for high-power illumination, presence of ambient light, and low quantum yield of chlorophyll fluorescence *in vivo* (Mazel, 2005; Treibitz *et al.*, 2015; Beijbom *et al.*, 2016). Future studies should focus on providing solutions to each of these issues. The prototype designed should use off-the-shelf components in order to contain costs and make the system more widely accessible. The imaging system could then be used to obtain an *in situ* dataset for testing of different image annotation approaches, particularly machine learning techniques.

While the two wavebands (450 nm and 530 nm) used in chapter 5 are ideally suited to discriminate between the accessory pigments of different groups of algae, further studies could also consider the use of different wavebands to target specific fluorescence-based biomarkers. For example, a violet excitation light would enable imaging of CFPs, and allow assessments of the relative proportions of high and low induction threshold GFP-like proteins in model species.

One potentially valuable development of *in situ* multi-excitation imaging is the application of the technique to 3D reconstruction of benthic assemblages via photogrammetry. With photogrammetry, 3D models of coral reefs are produced from sets of overlapping 2D photographs taken from a number of angles (Bythell *et al.*, 2001). These models can then be used to perform measurements of surface area, volume and structural complexity (Burns *et al.*, 2015; Anelli *et al.*, 2017). Fluorescence provides an ideal signal for 3D reconstruction, particularly in strongly scattering conditions such as waters with high suspended particle load (Sato *et al.*, 2012; Treibitz *et al.*, 2012; Murez *et al.*, 2015). Therefore, models built from fluorescence images might not only provide better discrimination of benthic groups (Treibitz *et al.*, 2015), but they might also enable a more accurate shape reconstruction compared to reflectance ones. Preliminary work shows that fluorescence imaging is indeed a suitable approach to photogrammetry (Fig. 6.1). Models made with different excitation bands could be registered together using fluorescent markers, to provide a single multi-excitation model. As well as allowing functional classification of algal groups as shown for 2D imaging in chapter 5, multi-excitation photogrammetry could be used to reveal information on the 3D spatial distribution of GFP-like proteins on coral reefs, providing new insights into the function and regulation of these proteins for biomarker development.

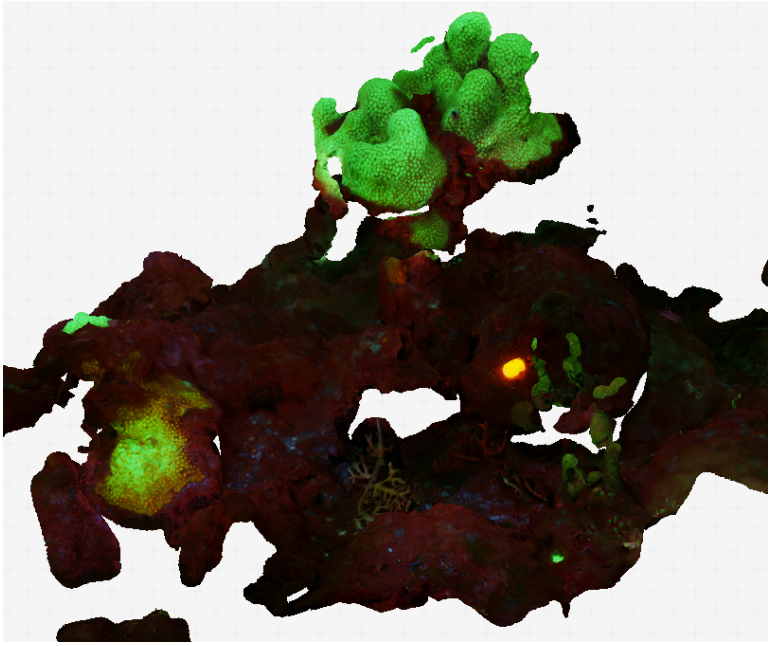

Figure 6.1 Fluorescence photogrammetry of a coral reef assemblage

Perspective view of a 3D model of a Caribbean coral reef, realised with fluorescence images (excitation = 450 nm). Courtesy of Dr A. Mogg (Scottish Association for Marine Science).

6.3 Concluding remarks

GFP-like proteins constitute a remarkable adaptation to the highly variable light environment experienced by reef-building corals. Fluorescence-based biomarkers can be used to understand and monitor how coral reef organisms respond to change, but knowledge of the diverse fundamental process controlling the regulation of these biomarkers in is key to future development and application. In light of the global crisis faced by coral reefs, it is hoped that the findings presented and the tools developed in this thesis will contribute to the ongoing effort to manage these ecosystems and conserve their vital resources for future generations.

List of References

Adam, V., Mizuno, H., Grichine, A., Hotta, J., Yamagata, Y., Moeyaert, B., Nienhaus, G. U., Miyawaki, A., Bourgeois, D. and Hofkens, J. (2010) 'Data storage based on photochromic and photoconvertible fluorescent proteins', *Journal of Biotechnology*, 149(4), 289–298.

Al-Horani, F. A., Al-Moghrabi, S. M. and de Beer, D. (2003) 'Microsensor study of photosynthesis and calcification in the scleractinian coral, *Galaxea fascicularis*: active internal carbon cycle', *Journal of Experimental Marine Biology and Ecology*, 288(1), 1–15.

Albins, M. A. and Hixon, M. A. (2011) 'Worst case scenario: potential long-term effects of invasive predatory lionfish *Pterois volitans* on Atlantic and Caribbean coral-reef communities', *Environmental Biology of Fishes*, 96(10-11), 1151–1157.

Alieva, N. O., Konzen, K. A., Field, S. F., Meleshkevitch, E. A., Hunt, M. E., Beltran-Ramirez, V., Miller, D. J., Wiedenmann, J., Salih, A. and Matz, M. V (2008) 'Diversity and evolution of coral fluorescent proteins', *PLoS ONE*, 3(7), e2680.

Ando, R., Hama, H., Yamamoto-Hino, M., Mizuno, H. and Miyawaki, A. (2002) 'An optical marker based on the UV-induced green-to-red photoconversion of a fluorescent protein', *Proceedings of the National Academy of Sciences*, 99(20), 12651–12656.

Andréfouët, S., Payri, C., Hochberg, E., Hu, C., Atkinson, M. and Muller-Karger, F. (2004) 'Use of *in situ* and airborne reflectance for scaling-up spectral discrimination of coral reef macroalgae from species to communities', *Marine Ecology Progress Series*, 283, 161–177.

Anelli, M., Julitta, T., Fallati, L., Galli, P., Rossini, M. and Colombo, R. (2017) 'Towards new applications of underwater photogrammetry for investigating coral reef morphology and habitat complexity in the Myeik Archipelago, Myanmar', *Geocarto International*, DOI: 10.1080/10106049.2017.1408703

Anthony, K. R. N., Hoogenboom, M. O. and Connolly, S. R. (2005) 'Adaptive variation in coral geometry and the optimization of internal colony light climates', *Functional Ecology*, 19(1), 17–26.

Anthony, K. R. N., Kline, D. I., Diaz-Pulido, G., Dove, S. and Hoegh-Guldberg, O. (2008) 'Ocean acidification causes bleaching and productivity loss in coral reef builders', *Proceedings of the National Academy of Sciences*, 105(45), 17442–17446.

Baird, G. S., Zacharias, D. A. and Tsien, R. Y. (2000) 'Biochemistry, mutagenesis, and oligomerization of DsRed, a red fluorescent protein from coral', *Proceedings of the National Academy of Sciences*, 97(22), 11984–11989.

Bak, R. P. M. (1976) 'The growth of coral colonies and the importance of crustose coralline algae and burrowing sponges in relation with carbonate accumulation', *Netherlands Journal of Sea Research*, 10(3), 285–337.

Barott, K., Smith, J., Dinsdale, E., Hatay, M., Sandin, S. and Rohwer, F. (2009) 'Hyperspectral and physiological analyses of coral-algal interactions', *PLoS ONE*, 4(11):e8043.

Beijbom, O., Edmunds, P. J., Kline, D. I., Mitchell, B. G. and Kriegman, D. (2012) 'Automated annotation of coral reef survey images', in *2012 IEEE Conference on Computer Vision and Pattern Recognition*. Providence, RI, 1170–1177.

Beijbom, O., Edmunds, P. J., Roelfsema, C., Smith, J., Kline, D. I., Neal, B. P., Dunlap, M. J., Moriarty, V., Fan, T. Y., Tan, C. J., Chan, S., Treibitz, T., Gamst, A., Mitchell, B. G. and Kriegman, D. (2015) 'Towards automated annotation of benthic survey images: Variability of human experts and operational modes of automation', *PLoS ONE*, 10(7), e0130312.

Beijbom, O., Treibitz, T., Kline, D. I., Eyal, G., Khen, A., Neal, B., Loya, Y., Mitchell, B. G. and Kriegman, D. (2016) 'Improving automated annotation of benthic survey images using wide-band fluorescence', *Scientific Reports*, 6, 23166.

Bollati, E., Plimmer, D., D'Angelo, C. and Wiedenmann, J. (2017) 'FRET-mediated long-range wavelength transformation by photoconvertible fluorescent proteins as an efficient mechanism to generate orange-red light in symbiotic deep water corals', *International Journal of Molecular Sciences*.,18(7), 1174.

Bongaerts, P., Ridgway, T., Sampayo, E. M. and Hoegh-Guldberg, O. (2010) 'Assessing the "deep reef refugia" hypothesis: focus on Caribbean reefs', *Coral Reefs*, 29(2), 309–327.

Bou-Abdallah, F., Chasteen, N. D. and Lesser, M. P. (2006) 'Quenching of superoxide radicals by green fluorescent protein', *Biochimica et Biophysica Acta (BBA) - General Subjects*, 1760(11), 1690–1695.

Bradley, P., Fisher, W. S., Bell, H., Davis, W., Chan, V., LoBue, C. and Wiltse, W. (2009) 'Development and implementation of coral reef biocriteria in U.S. jurisdictions', *Environmental Monitoring and Assessment*, 150, 43–51.

Bruno, J. F. and Selig, E. R. (2007) 'Regional decline of coral cover in the Indo-Pacific: Timing, extent, and subregional comparisons', *PLoS ONE*, 2(8), e711.

Burke, L., Reytar, K., Spalding, M. and Perry, A. (2011) *Reefs at Risk Revisited*. Washington, DC: World Resources Institute.

Burns, J., Delparte, D., Gates, R. and Takabayashi, M. (2015) 'Integrating structure-from-motion photogrammetry with geospatial software as a novel technique for quantifying 3D ecological characteristics of coral reefs', *PeerJ*, 3, e1077.

Bythell, J., Pan, P. and Lee, J. (2001) 'Three-dimensional morphometric measurements of reef corals using underwater photogrammetry techniques', *Coral Reefs*, 20(3), 193–199.

Chalfie, M., Tu, Y., Euskirchen, G., Ward, W. W. and Prasher, D. C. (1994) 'Green fluorescent protein as a marker for gene expression', *Science*, 263(5148), 802–805.

Chattoraj, M., King, B. A., Bublitz, G. U. and Boxer, S. G. (1996) 'Ultra-fast excited state dynamics in green fluorescent protein: multiple states and proton transfer.', *Proceedings of the National Academy of Sciences*, 93(16), 8362–8367.

Chennu, A., Färber, P., De'ath, G., de Beer, D. and Fabricius, K. E. (2017) 'A diver-operated hyperspectral imaging and topographic surveying system for automated mapping of benthic habitats', *Scientific Reports*, 7(1), 7122.

Chishima, T., Miyagi, Y., Wang, X., Yamaoka, H., Shimada, H., Moossa, A. R. and Hoffman, R. M. (1997) 'Cancer invasion and micrometastasis visualized in live tissue by green fluorescent protein expression', *Cancer research*, 57(10), 2042–2047.

Chudakov, D. M., Feofanov, A. V, Mudrik, N. N., Lukyanov, S. and Lukyanov, K. A. (2003) 'Chromophore environment provides clue to "kindling fluorescent protein" riddle', *Journal of Biological Chemistry*, 278(9), 7215–7219.

List of References

Clarke, G. L. and James, H. L. (1939) 'Laboratory analysis of the selective absorption of light by sea water', *Journal of the Optical Society of America*, 29(2), 43–55.

Cody, C. W., Prasher, D. C., Westler, W. M., Prendergast, F. G. and Ward, W. W. (1993) 'Chemical structure of the hexapeptide chromophore of the *Aequorea* green-fluorescent protein', *Biochemistry*, 32(5), 1212–1218.

Cooper, T. F., Gilmour, J. P. and Fabricius, K. E. (2009) 'Bioindicators of changes in water quality on coral reefs: review and recommendations for monitoring programmes', *Coral Reefs*, 28(3), 589–606.

Cox, G., Matz, M. and Salih, A. (2007) 'Fluorescence lifetime imaging of coral fluorescent proteins', *Microscopy Research and Technique*, 70(3), 243–251.

Crosby, M. P. and Reese, E. S. (1996) *A manual for monitoring coral reefs with indicator species: Butterflyfishes as indicators of change on Indo Pacific reefs*. Silver Spring: National Oceanic and Atmospheric Administration.

D'Angelo, C. and Wiedenmann, J. (2012) 'An experimental mesocosm for long-term studies of reef corals', *Journal of the Marine Biological Association of the United Kingdom*, 92(Special Issue 04), 769–775.

D'Angelo, C. and Wiedenmann, J. (2014) 'Impacts of nutrient enrichment on coral reefs: new perspectives and implications for coastal management and reef survival', *Current Opinion in Environmental Sustainability*, 7, 82–93.

D'Angelo, C., Denzel, A., Vogt, A., Matz, M., Oswald, F., Salih, A., Nienhaus, G. and Wiedenmann, J. (2008) 'Blue light regulation of host pigment in reef-building corals', *Marine Ecology Progress Series*, 364, 97–106.

D'Angelo, C., Smith, E. G., Oswald, F., Burt, J., Tchernov, D. and Wiedenmann, J. (2012) 'Locally accelerated growth is part of the innate immune response and repair mechanisms in reef-building corals as detected by green fluorescent protein (GFP)-like pigments', *Coral Reefs*, 31(4), 1045–1056.

De'ath, G., Lough, J. M. and Fabricius, K. E. (2009) 'Declining coral calcification on the Great Barrier Reef', *Science*, 323(5910), 116–119.

De'ath, G., Fabricius, K. E., Sweatman, H. and Puotinen, M. (2012) 'The 27-year decline of coral cover on the Great Barrier Reef and its causes.', *Proceedings of the National Academy of Sciences*, 109(44), 17995–17999.

Desalvo, M. K., Voolstra, C. R., Sunagawa, S., Schwarz, J. A., Stillman, J. H., Coffroth, M. A., Szmant, A. M. and Medina, M. (2008) 'Differential gene expression during thermal stress and bleaching in the Caribbean coral *Montastraea faveolata*', *Molecular Ecology*, 17(17), 3952–3971.

Diaz-Pulido, G., McCook, L. J., Dove, S., Berkelmans, R., Roff, G., Kline, D. I., Weeks, S., Evans, R. D., Williamson, D. H., Hoegh-Guldberg, O. (2009) 'Doom and boom on a resilient reef: climate change, algal overgrowth and coral recovery', *PLoS ONE*, 4(4):e5239.

Dove, S. G., Takabayashi, M. and Hoegh-Guldberg, O. (1995) 'Isolation and partial characterization of the pink and blue pigments of pocilloporid and acroporid corals', *The Biological Bulletin*, 189(3), 288–297.

Dove, S. G., Hoegh-Guldberg, O. and Ranganathan, S. (2001) 'Major colour patterns of reef-building corals are due to a family of GFP-like proteins', *Coral Reefs*, 19(3), 197–204.

Dove, S., Ortiz, J. C., Enríquez, S., Fine, M., Fisher, P., Iglesias-Prieto, R., Thornhill, D. and Hoegh-Guldberg, O. (2006) 'Response of holosymbiont pigments from the scleractinian coral *Montipora monasteriata* to short-term heat stress', *Limnology and Oceanography*, 51(2), 1149–1158.

Downs, C. A., Woodley, C. M., Richmond, R. H., Lanning, L. L. and Owen, R. (2005) 'Shifting the paradigm of coral-reef "health" assessment', *Marine Pollution Bulletin*, 51(5–7), 486–494.

Downs, C. A., Ostrander, G. K., Rougee, L., Rongo, T., Knutson, S., Williams, D. E., Mendiola, W., Holbrook, J. and Richmond, R. H. (2012) 'The use of cellular diagnostics for identifying sub-lethal stress in reef corals', *Ecotoxicology*, 21(3), 768–782.

Dubinsky, Z. and Jokiel, P. L. (1994) 'Ratio of energy and nutrient fluxes regulates symbiosis between zooxanthellae and corals', *Pacific Science*, 48(3), 313–324.

Edge, S. E., Morgan, M. B., Gleason, D. F. and Snell, T. W. (2005) 'Development of a coral cDNA array to examine gene expression profiles in *Montastraea faveolata* exposed to environmental stress', *Marine Pollution Bulletin*, 51(5–7), 507–523.

Einbinder, S., Mass, T., Brokovich, E., Dubinsky, Z., Erez, J. and Tchernov, D. (2009) 'Changes in morphology and diet of the coral *Stylophora pistillata* along a depth gradient', *Marine Ecology Progress Series*, 381, 167–174.

Enríquez, S., Méndez, E. R. and -Prieto, R. I. (2005) 'Multiple scattering on coral skeletons enhances light absorption by symbiotic algae', *Limnology and Oceanography*, 50(4), 1025–1032.

Enríquez, S., Méndez, E. R., Hoegh-Guldberg, O. and Iglesias-Prieto, R. (2017) 'Key functional role of the optical properties of coral skeletons in coral ecology and evolution', *Proceedings of the Royal Society of London B*, 284, 1853.

Eyal, G., Wiedenmann, J., Grinblat, M., D'Angelo, C., Kramarsky-Winter, E., Treibitz, T., Ben-Zvi, O., Shaked, Y., Smith, T. B., Harii, S., Denis, V., Noyes, T., Tamir, R. and Loya, Y. (2015) 'Spectral diversity and regulation of coral fluorescence in a mesophotic reef habitat in the Red Sea', *PLoS ONE*, 10(6), e0128697.

Fabricius, K. E. (2005) 'Effects of terrestrial runoff on the ecology of corals and coral reefs: review and synthesis', *Marine Pollution Bulletin*, 50(2), 125–146.

Fabricius, K. and De'ath, G. (2001) 'Environmental factors associated with the spatial distribution of crustose coralline algae on the Great Barrier Reef', *Coral Reefs*, 19(4), 303–309.

Fabricius, K., De'ath, G., McCook, L., Turak, E. and Williams, D. M. B. (2005) 'Changes in algal, coral and fish assemblages along water quality gradients on the inshore Great Barrier Reef', *Marine Pollution Bulletin*, 51(1-4), 384–398.

Falkowski, P. and Kiefer, D. A. (1985) 'Chlorophyll a fluorescence in phytoplankton: Relationship to photosynthesis and biomass', *Journal of Plankton Research*, 7(5), 715–731.

Ferrario, F., Beck, M. W., Storlazzi, C. D., Micheli, F., Shepard, C. C. and Airoldi, L. (2014) 'The effectiveness of coral reefs for coastal hazard risk reduction and adaptation'. *Nature Communications*, 5, 3794.

Field, S. F. and Matz, M. V (2010) 'Retracing evolution of red fluorescence in GFP-like proteins from Faviina corals', *Molecular Biology and Evolution*, 27(2), 225–233.

List of References

Field, S., Bulina, M., Kelmanson, I., Bielawski, J. and Matz, M. (2006) 'Adaptive evolution of multicolored fluorescent proteins in reef-building corals', *Journal of Molecular Evolution*, 62(3), 332–339.

Fisher, W. S., Fore, L. S., Hutchins, A., Quarles, R. L., Campbell, J. G., LoBue, C. and Davis, W. S. (2008) 'Evaluation of stony coral indicators for coral reef management', *Marine Pollution Bulletin*, 56(10), 1737–1745.

Förster, T. (1960) 'Transfer mechanisms of electronic excitation energy', *Radiation Research Supplement*, 2, 326-339.

French, C. S. and Young, V. K. (1952) 'The fluorescence spectra of red algae and the transfer of energy from phycoerythrin to phycocyanin and chlorophyll', *The Journal of General Physiology*, 35(6), 873–90.

Garcia, R. A., Lee, Z. and Hochberg, E. J. (2018) 'Hyperspectral shallow-water remote sensing with an enhanced benthic classifier', *Remote Sensing*, 10(1), 147.

Gardner, T. A., Côté, I. M., Gill, J. A., Grant, A. and Watkinson, A. R. (2003) 'Long-term region-wide declines in Caribbean corals', *Science*, 301(5635), 958–960.

Gayler, K., Sandall, D., Greening, D., Keays, D., Polidano, M., Livett, B., Down, J., Satkunanathan, N. and Khalil, Z. (2005) 'Molecular prospecting for drugs from the sea', *IEEE Engineering in Medicine and Biology Magazine*, 24(2), 79–84.

Giepmans, B. N. G., Adams, S. R., Ellisman, M. H. and Tsien, R. Y. (2006) 'The fluorescent toolbox for assessing protein location and function', *Science*, 312(5771), 217–224.

Gilmore, A. M., Larkum, A. W. D., Salih, A., Itoh, S., Shibata, Y., Bena, C., Yamasaki, H., Papina, M. and Van Woesik, R. (2003) 'Simultaneous time resolution of the emission spectra of fluorescent proteins and zooxanthellar chlorophyll in reef-building corals', *Photochemistry and Photobiology*, 77(5), 515–523.

Gittins, J. R., D'Angelo, C., Oswald, F., Edwards, R. J. and Wiedenmann, J. (2015) 'Fluorescent protein-mediated colour polymorphism in reef corals: multicopy genes extend the adaptation/acclimatization potential to variable light environments', *Molecular ecology*, 24(2), 453–465.

Gleason, A. C. R., Reid, R. P. and Voss, K. J. (2007) 'Automated classification of underwater multispectral imagery for coral reef monitoring', in *OCEANS 2007*. Vancouver, BC, 1–8.

Gleason, D. F. and Wellington, G. M. (1993) 'Ultraviolet radiation and coral bleaching', *Nature*, 365(6449), 836–838.

Glynn, P. W. (1996) 'Coral reef bleaching: facts, hypotheses and implications', *Global Change Biology*, 2(6), 495–509.

González-Rivero, M., Bongaerts, P., Beijbom, O., Pizarro, O., Friedman, A., Rodriguez-Ramirez, A., Upcroft, B., Laffoley, D., Kline, D., Bailhache, C., Vevers, R. and Hoegh-Guldberg, O. (2014) 'The Catlin Seaview Survey - kilometre-scale seascape assessment, and monitoring of coral reef ecosystems', *Aquatic Conservation: Marine and Freshwater Ecosystems*, 24(S2), 184–198.

Gordon, G. W., Berry, G., Liang, X. H., Levine, B. and Herman, B. (1998) 'Quantitative fluorescence resonance energy transfer measurements using fluorescence microscopy', *Biophysical Journal*, 74(5), 2702–2713.

Goreau, T. F. (1963) ‘Calcium carbonate deposition by coralline algae and corals in relation to their roles as reef-builders’, *Annals of the New York Academy of Sciences*, 109(1), 127–167.

Graham, N. A. J., Wilson, S. K., Jennings, S., Polunin, N. V. C., Robinson, J., Bijoux, J. P. and Daw, T. M. (2007) ‘Lag effects in the impacts of mass coral bleaching on coral reef fish, fisheries, and ecosystems’, *Conservation Biology*, 21(5), 1291–1300.

Gross, L. A., Baird, G. S., Hoffman, R. C., Baldridge, K. K. and Tsien, R. Y. (2000) ‘The structure of the chromophore within DsRed, a red fluorescent protein from coral’, *Proceedings of the National Academy of Sciences*, 97(22), 11990–11995.

Gruber, D. F., Kao, H.-T., Janoschka, S., Tsai, J. and Pieribone, V. A. (2008) ‘Patterns of fluorescent protein expression in scleractinian corals’, *The Biological Bulletin*, 215(2), 143–154.

Hardy, J. T., Hoge, F. E., Yungel, J. K. and Dodge, R. E. (1992) ‘Remote detection of coral “bleaching” using pulsed-laser fluorescence spectroscopy.’, *Marine Ecology Progress Series*, 88, 247–255.

Hedley, J. D. and Mumby, P. J. (2002) ‘Biological and remote sensing perspectives of pigmentation in coral reef organisms’, *Advances in Marine Biology*, 43, 277–317.

Hedley, J. D., Mumby, P. J., Joyce, K. E. and Phinn, S. R. (2004) ‘Spectral unmixing of coral reef benthos under ideal conditions’, *Coral Reefs*, 23(1), 60–73.

Heikal, A. A., Hess, S. T., Baird, G. S., Tsien, R. Y. and Webb, W. W. (2000) ‘Molecular spectroscopy and dynamics of intrinsically fluorescent proteins: Coral red (dsRed) and yellow (Citrine)’, *Proceedings of the National Academy of Sciences*, 97(22), 11996–12001.

Heim, R., Prasher, D. C. and Tsien, R. Y. (1994) ‘Wavelength mutations and posttranslational autoxidation of green fluorescent protein’, *Proceedings of the National Academy of Sciences*, 91(26), 12501–12504.

Hempson, T. N., Graham, N. A. J., MacNeil, M. A., Williamson, D. H., Jones, G. P. and Almany, G. R. (2017) ‘Coral reef mesopredators switch prey, shortening food chains, in response to habitat degradation’, *Ecology and Evolution*, 7(8), 2626–2635.

Henderson, J. N. and Remington, S. J. (2005) ‘Crystal structures and mutational analysis of amFP486, a cyan fluorescent protein from *Anemonia majano*’, *Proceedings of the National Academy of Sciences*, 102(36), 12712–12717.

Heyward, A. J. and Negri, A. P. (1999) ‘Natural inducers for coral larval metamorphosis’, *Coral Reefs*, 18(3), 273–279.

Hilton, J. D., Brady, A. K., Spaho, S. A. and Vize, P. D. (2012) ‘Photoreception and signal transduction in corals: proteomic and behavioral evidence for cytoplasmic calcium as a mediator of light responsivity’, *The Biological Bulletin*, 223(3), 291–299.

Hochberg, E. J., Atkinson, M. J. and Andréfouët, S. (2003) ‘Spectral reflectance of coral reef bottom-types worldwide and implications for coral reef remote sensing’, *Remote Sensing of Environment*, 85(2), 159–173.

Hochberg, E., Atkinson, M., Apprill, A. and Andréfouët, S. (2004) ‘Spectral reflectance of coral’, *Coral Reefs*, 23(1), 84–95.

Hochstrasser, R. M. and Porter, G. B. (1960) ‘Primary processes in photo-oxidation’, *Quarterly Reviews, Chemical Society*, 14(2), 146–173.

Hodgson, G. (1999) 'A global assessment of human effects on coral reefs', *Marine Pollution Bulletin*, 38(5), 345–355.

Hoegh-Guldberg, O. and Jones, R. J. (1999) 'Photoinhibition and photoprotection in symbiotic dinoflagellates from reef-buiding corals', *Marine Ecology Progress Series*, 183:73–86.

Hoegh-Guldberg, O., Poloczanska, E. S., Skirving, W. and Dove, S. (2017) 'Coral reef ecosystems under climate change and ocean acidification', *Frontiers in Marine Science*, 4, 158.

Hoppe, A., Christensen, K. and Swanson, J. A. (2002) 'Fluorescence Resonance Energy Transfer-based stoichiometry in living cells', *Biophysical Journal*, 83(6), 3652–3664.

Hosoi, H., Mizuno, H., Miyawaki, A. and Tahara, T. (2006) 'Competition between energy and proton transfer in ultrafast excited-state dynamics of an oligomeric fluorescent protein red Kaede', *The Journal of Physical Chemistry B*, 110(45), 22853–22860.

Hughes, T. P., Baird, A. H., Bellwood, D. R., Card, M., Connolly, S. R., Folke, C., Grosberg, R., Hoegh-Guldberg, O., Jackson, J. B. C., Kleypas, J., Lough, J. M., Marshall, P., Nyström, M., Palumbi, S. R., Pandolfi, J. M., Rosen, B. and Roughgarden, J. (2003) 'Climate change, human impacts, and the resilience of coral reefs', *Science*, 301(5635), 929–933.

Hughes, T. P., Rodrigues, M. J., Bellwood, D. R., Ceccarelli, D., Hoegh-Guldberg, O., McCook, L., Moltschaniwskyj, N., Pratchett, M. S., Steneck, R. S. and Willis, B. (2007) 'Phase shifts, herbivory, and the resilience of coral reefs to climate change', *Current Biology*, 17(4), 360–365.

Hughes, T. P., Kerry, J. T., Álvarez-Noriega, M., Álvarez-Romero, J. G., Anderson, K. D., Baird, A. H., Babcock, R. C., Beger, M., Bellwood, D. R., Berkelmans, R., Bridge, T. C., Butler, I. R., Byrne, M., Cantin, N. E., Comeau, S., Connolly, S. R., Cumming, G. S., Dalton, S. J., Diaz-Pulido, G., Eakin, C. M., Figueira, W. F., Gilmour, J. P., Harrison, H. B., Heron, S. F., Hoey, A. S., Hobbs, J. A., Hoogenboom, M. O., Kennedy, E. V., Kuo, C., Lough, J. M., Lowe, R. J., Liu, G., McCulloch, M. T., Malcolm, H. A., McWilliam, M. J., Pandolfi, J. M., Pears, R. J., Pratchett, M. S., Schoepf, V., Simpson, T., Skirving, W. J., Sommer, B., Torda, G., Wachenfeld, D. R., Willis, B. L. and Wilson, S. K. (2017) 'Global warming and recurrent mass bleaching of corals', *Nature*, 543(7645), 373–377.

Hughes, T. P., Anderson, K. D., Connolly, S. R., Heron, S. F., Kerry, J. T., Lough, J. M., Baird, A. H., Baum, J. K., Berumen, M. L., Bridge, T. C., Claar, D. C., Eakin, C. M., Gilmour, J. P., Graham, N. A. J., Harrison, H., Hobbs, J.-P. A., Hoey, A. S., Hoogenboom, M., Lowe, R. J., McCulloch, M. T., Pandolfi, J. M., Pratchett, M., Schoepf, V., Torda, G. and Wilson, S. K. (2018) 'Spatial and temporal patterns of mass bleaching of corals in the Anthropocene.', *Science*, 359(6371), 80–83.

Hume, B., D'Angelo, C., Burt, J., Baker, A. C., Riegl, B. and Wiedenmann, J. (2013) 'Corals from the Persian/Arabian Gulf as models for thermotolerant reef-builders: Prevalence of clade C3 Symbiodinium, host fluorescence and *ex situ* temperature tolerance', *Marine Pollution Bulletin*, 72(2), 313–322.

Hume, B. C. C., Voolstra, C. R., Arif, C., D'Angelo, C., Burt, J. A., Eyal, G., Loya, Y. and Wiedenmann, J. (2016) 'Ancestral genetic diversity associated with the rapid spread of stress-tolerant coral symbionts in response to Holocene climate change.', *Proceedings of the National Academy of Sciences*, 113(16), 4416–21.

Inouye, S. and Tsuji, F. I. (1994) '*Aequorea* green fluorescent protein: Expression of the gene and fluorescence characteristics of the recombinant protein', *FEBS Letters*, 341(2–3), 277–280.

Jackson, J. B., Kirby, M. X., Berger, W. H., Bjorndal, K. A., Botsford, L. W., Bourque, B. J., Bradbury, R. H., Cooke, R., Erlandson, J., Estes, J. A., Hughes, T. P., Kidwell, S., Lange, C. B., Lenihan, H. S., Pandolfi, J. M., Peterson, C. H., Steneck, R. S., Tegner, M. J. and Warner, R. R. (2001) 'Historical overfishing and the recent collapse of coastal ecosystems.', *Science*, 293(5530), 629–37.

Jaffe, J. S. (2015) 'Underwater optical imaging: The past, the present, and the prospects', *IEEE Journal of Oceanic Engineering*, 40(3), 683–700.

Jameson, S. C., Erdmann, M. V, Gibson Jr, G. R. and Potts, K. W. (1998) *Development of biological criteria for coral reef ecosystem assessment*. Washington, DC: Unites States Environmental Protection Agency.

Jeffrey, S. W. and Haxo, F. T. (1968) 'Photosynthetic pigments of symbiotic dinoflagellates (zooxanthellae) from corals and clams', *The Biological Bulletin*, 135(1), 149–165.

Jerlov, N. G. (1976) *Marine Optics*. Amsterdam: Elsevier.

Jokiel, P., Rodgers, K., Kuffner, I., Andersson, A., Cox, E. and Mackenzie, F. (2008) 'Ocean acidification and calcifying reef organisms: a mesocosm investigation', *Coral Reefs*, 27(3), 473–483.

Jokiel, P. L., Rodgers, K. S., Brown, E. K., Kenyon, J. C., Aeby, G., Smith, W. R. and Farrell, F. (2015) 'Comparison of methods used to estimate coral cover in the Hawaiian Islands.', *PeerJ*, 3, e954.

Jones, R. J., Hoegh-Guldberg, O., Larkum, A. W. D. and Schreiber, U. (1998) 'Temperature-induced bleaching of corals begins with impairment of the CO_2 fixation mechanism in zooxanthellae', *Plant, Cell and Environment*, 21(12), 1219–1230.

Kahng, S. E., Hochberg, E. J., Apprill, A., Wagner, D., Luck, D. G., Perez, D. and Bidigare, R. R. (2012) 'Efficient light harvesting in deep-water zooxanthellate corals', *Marine Ecology Progress Series*, 455, 65–77.

Kaniewska, P., Campbell, P. R., Fine, M. and Hoegh-Guldberg, O. (2009) 'Phototropic growth in a reef flat acroporid branching coral species', *Journal of Experimental Biology*, 212(5), 662–667.

Kaniewska, P., Alon, S., Karako-Lampert, S., Hoegh-Guldberg, O. and Levy, O. (2015) 'Signaling cascades and the importance of moonlight in coral broadcast mass spawning', *eLife*, 4, e09991.

Kasha, M. (1950) 'Characterization of electronic transitions in complex molecules', *Discussions of the Faraday Society*, 9, 14–19.

Kautsky, H. and Hirsch, A. (1931) 'Neue Versuche zur Kohlensaureassimilation', *Naturwissenschafen*, 48(19), 964.

Kawaguti, S. (1944) 'On the physiology of reef corals. VI. Study of the pigments', *Palao tropical Biological Station Studies*, 2, 617–674.

Kawaguti, S. (1969) 'Effect of the green fluorescent pigment on the productivity of the reef corals', *Micronesica*, 5(2), 71–97.

Kelmanson, I. V and Matz, M. V (2003) 'Molecular basis and evolutionary origins of color diversity in great star coral *Montastraea cavernosa* (Scleractinia: Faviida)', *Molecular biology and evolution*, 20(7), 1125–1133.

Kim, J. K., Kraemer, G. P., Neefus, C. D., Chung, I. K. and Yarish, C. (2007) 'Effects of temperature and ammonium on growth, pigment production and nitrogen uptake by four species of *Porphyra* (Bangiales, Rhodophyta) native to the New England coast', *Journal of Applied Phycology*, 19(5), 431–440.

Kirk, J. T. O. (1994) *Light and photosynthesis in aquatic ecosystems*. Cambridge: Cambridge University Press.

Kittinger, J. N., Teneva, L. T., Koike, H., Stamoulis, K. A., Kittinger, D. S., Oleson, K. L. L., Conklin, E., Gomes, M., Wilcox, B. and Friedlander, A. M. (2015) 'From reef to table: Social and ecological factors affecting coral reef fisheries, artisanal seafood supply chains, and seafood security', *PLoS ONE*, 10(8), e0123856.

Kleypas, J. A., McManus, J. W. and Meñez, L. A. B. (1999a) 'Environmental limits to coral reef development: Where do we draw the line?', *American Zoologist*, 39(1), 146–159.

Kleypas, J. A., Buddemeier, R. W., Archer, D., Gattuso, J.-P., Langdon, C. and Opdyke, B. N. (1999b) 'Geochemical consequences of increased atmospheric carbon dioxide on coral reefs', *Science*, 284(5411), 118–120.

Knowlton, N. (2010) 'Coral reef biodiversity', in McIntyre, A. D. (ed.) *Life in the World's Oceans: Diversity, Distribution, and Abundance*. Chichester, UK: Wiley-Blackwell, 65–77.

Kuffner, I. B., Walters, L. J., Becerro, M. A., Paul, V. J., Ritson-Williams, R. and Beach, K. S. (2006) 'Inhibition of coral recruitment by macroalgae and cyanobacteria', *Marine Ecology Progress Series*, 107–117.

Kuffner, I. B., Andersson, A. J., Jokiel, P. L., Rodgers, K. S. and Mackenzie, F. T. (2008) 'Decreased abundance of crustose coralline algae due to ocean acidification', *Nature Geoscience*, 1(2), 114–117.

Kuguru, B., Chadwick, N. E., Achituv, Y., Zandbank, K. and Tchernov, D. (2008) 'Mechanisms of habitat segregation between corallimorpharians: photosynthetic parameters and *Symbiodinium* types', *Marine Ecology Progress Series*, 369, 115–129.

Kühl, M., Cohen, Y., Dalsgaard, T., Jorgensen, B. B. and Revsbech, N. P. (1995) 'Microenvironment and photosynthesis of zooxanthellae in scleractinian corals studied with microsensors for 0_2, pH and light', *Marine Ecology Progress Series*, 117, 159–172.

Kutser, T., Miller, I. and Jupp, D. L. B. (2006) 'Mapping coral reef benthic substrates using hyperspectral space-borne images and spectral libraries', *Estuarine, Coastal and Shelf Science*, 70(3), 449–460.

Labas, Y. A., Gurskaya, N. G., Yanushevich, Y. G., Fradkov, A. F., Lukyanov, K. A., Lukyanov, S. A. and Matz, M. V (2002) 'Diversity and evolution of the green fluorescent protein family', *Proceedings of the National Academy of Sciences*, 99(7), 4256–4261.

Lelimousin, M., Adam, V., Nienhaus, G. U., Bourgeois, D. and Field, M. J. (2009) 'Photoconversion of the fluorescent protein EosFP: A hybrid potential simulation study reveals intersystem crossings', *Journal of the American Chemical Society*, 131(46), 16814–16823.

Lesser, M. P. (1997) 'Oxidative stress causes coral bleaching during exposure to elevated temperatures', *Coral Reefs*, 16(3), 187–192.

Leutenegger, A., D'Angelo, C., Matz, M. V, Denzel, A., Oswald, F., Salih, A., Nienhaus, G. U. and Wiedenmann, J. (2007a) 'It's cheap to be colorful', *FEBS Journal*, 274(10), 2496–2505.

Leutenegger, A., Kredel, S., Gundel, S., D'Angelo, C., Salih, A. and Wiedenmann, J. (2007b) 'Analysis of fluorescent and non-fluorescent sea anemones from the Mediterranean Sea during a bleaching event', *Journal of Experimental Marine Biology and Ecology*, 353(2), 221–234.

Levy, O., Appelbaum, L., Leggat, W., Gothlif, Y., Hayward, D. C., Miller, D. J. and Hoegh-Guldberg, O. (2007) 'Light-responsive cryptochromes from a simple multicellular animal, the coral *Acropora millepora*', *Science*, 318(5849), 467–470.

Liu, G., Heron, S. F., Mark Eakin, C., Muller-Karger, F. E., Vega-Rodriguez, M., Guild, L. S., de la Cour, J. L., Geiger, E. F., Skirving, W. J., Burgess, T. F. R., Strong, A. E., Harris, A., Maturi, E., Ignatov, A., Sapper, J., Li, J. and Lynds, S. (2014) 'Reef-scale thermal stress monitoring of coral ecosystems: New 5-km global products from NOAA coral reef watch', *Remote Sensing*, 6(11), 11579–11606.

Loya, Y. (2004) 'The coral reefs of Eilat — Past, present and future: Three decades of coral community structure studies', in Rosenberg, E. and Loya, Y. (eds.) *Coral Health and Disease*. Berlin, Heidelberg: Springer, 1–34.

Lukyanov, K. A., Fradkov, A. F., Gurskaya, N. G., Matz, M. V, Labas, Y. A., Savitsky, A. P., Markelov, M. L., Zaraisky, A. G., Zhao, X., Fang, Y., Tan, W. and Lukyanov, S. A. (2000) 'Natural animal coloration can be determined by a nonfluorescent green fluorescent protein homolog', *Journal of Biological Chemistry*, 275(34), 25879–25882.

Lyndby, N. H., Kühl, M. and Wangpraseurt, D. (2016) 'Heat generation and light scattering of green fluorescent protein-like pigments in coral tissue', *Scientific Reports*, 6, 26599.

Mackinney, G. (1941) 'Absorption of light by chlorophyll', *Journal of Biological Chemistry*, 140, 315–322.

Mahmood, A., Bennamoun, M., An, S., Sohel, F., Boussaid, F., Hovey, R., Kendrick, G. and Fisher, R. B. (2016) 'Coral classification with hybrid feature representations', in *Proceedings - International Conference on Image Processing*. Phoenix, AZ, 519–523.

Marcelino, L. A., Westneat, M. W., Stoyneva, V., Henss, J., Rogers, J. D., Radosevich, A., Turzhitsky, V., Siple, M., Fang, A., Swain, T. D., Fung, J. and Backman, V. (2013) 'Modulation of light-enhancement to symbiotic algae by light-scattering in corals and evolutionary trends in bleaching', *PLoS ONE*, 8(4), e61492.

Mason, B., Schmale, M., Gibbs, P., Miller, M. W., Wang, Q., Levay, K., Shestopalov, V. and Slepak, V. Z. (2012) 'Evidence for multiple phototransduction pathways in a reef-building coral', *PLoS ONE*, 7(12), e50371.

Matz, M. V, Fradkov, A. F., Labas, Y. A., Savitsky, A. P., Zaraisky, A. G., Markelov, M. L. and Lukyanov, S. A. (1999) 'Fluorescent proteins from nonbioluminescent Anthozoa species', *Nature Biotechnology*, 17(10), 969–973.

Matz, M. V, Marshall, N. J. and Vorobyev, M. (2006) 'Are corals colorful?', *Photochemistry and Photobiology*, 82(2), 345–350.

List of References

Mazel, C. H. (1995) 'Spectral measurements of fluorescence emission in Caribbean cnidarians', *Marine Ecology Progress Series*, 120, 185–191.

Mazel, C. H., Strand, M. P., Lesser, M. P., Crosby, M. P., Coles, B. and Nevis, A. J. (2003a) 'High resolution determination of coral reef bottom cover from multispectral fluorescence laser line scan imagery', *Limnology and Oceanography*, 48(1, part 2), 522–534.

Mazel, C. H., Lesser, M. P., Gorbunov, M. Y., Barry, T. M., Farrell, J. H., Wyman, K. D. and Falkowski, P. G. (2003b) 'Green-fluorescent proteins in Caribbean corals', *Limnology and Oceanography*, 48(1, part 2), 402–411.

Mazel, C. H. (2005) 'Underwater fluorescence photography in the presence of ambient light', *Limnology and Oceanography: Methods*, 3(11), 499–510.

McManus, J. W., Reyes, R. B. and Nañola, C. L. (1997) 'Effects of some destructive fishing methods on coral cover and potential rates of recovery', *Environmental Management*, 21(1), 69–78.

Mehbub, M. F., Lei, J., Franco, C. and Zhang, W. (2014) 'Marine sponge derived natural products between 2001 and 2010: Trends and opportunities for discovery of bioactives', *Marine Drugs*, 4539–4577.

Mehta, A., Ribeiro, E., Gilner, J. and Woesik, R. Van (2007) 'Coral reef texture classification using support vector machines.', in *Proceedings of the Second International Conference on Computer Vision Theory and Applications*. Barcelona, 2.

Mizuno, H., Mal, T. K., Tong, K. I., Ando, R., Furuta, T., Ikura, M. and Miyawaki, A. (2003) 'Photo-induced peptide cleavage in the green-to-red conversion of a fluorescent protein', *Molecular Cell*, 12(4), 1051–1058.

Morin, J. G. and Hastings, J. W. (1971) 'Energy transfer in a bioluminescent system', *Journal of Cellular Physiology*, 77(3), 313–318.

Morise, H., Shimomura, O., Johnson, F. H. and Winant, J. (1974) 'Intermolecular energy transfer in the bioluminescent system of *Aequorea*', *Biochemistry*, 13(12), 2656–2662.

Morse, D. E., Hooker, N., Morse, A. N. C. and Jensen, R. A. (1988) 'Control of larval metamorphosis and recruitment in sympatric agariciid corals', *Journal of Experimental Marine Biology and Ecology*, 116(3), 193–217.

Muir, P. R., Wallace, C. C., Done, T. and Aguirre, J. D. (2015) 'Limited scope for latitudinal extension of reef corals', *Science*, 348(6239), 1135–1138.

Muko, S., Kawasaki, K., Sakai, K., Takasu, F. and Shigesada, N. (2000) 'Morphological plasticity in the coral *Porites sillimaniani* and its adaptive significance', *Bulletin of Marine Science*, 66(1), 225–239.

Müller, S. M., Galliardt, H., Schneider, J., Barisas, B. G. and Seidel, T. (2013) 'Quantification of Förster resonance energy transfer by monitoring sensitized emission in living plant cells', *Frontiers in Plant Science*, 4, 413.

Mumby, P. J., Skirving, W., Strong, A. E., Hardy, J. T., LeDrew, E. F., Hochberg, E. J., Stumpf, R. P. and David, L. T. (2004) 'Remote sensing of coral reefs and their physical environment', *Marine Pollution Bulletin*, 219–228.

Murez, Z., Treibitz, T., Ramamoorthi, R. and Kriegman, D. (2015) 'Photometric stereo in a scattering medium', in *IEEE Transactions on Pattern Analysis and Machine Intelligence*, 39(9), 3415–3423.

Muscatine, L. (1990) 'The role of sybiotic algae in carbon and energy flux in coral reefs', in Dubinsky, Z. (ed.) *Ecosystems of the World, 25. Coral Reefs*. Amsterdam: Elsevier, 75–87.

Nienhaus, G. U. and Wiedenmann, J. (2009) 'Structure, dynamics and optical properties of fluorescent proteins: perspectives for marker development', *ChemPhysChem*, 10(9–10), 1369–1379.

Nienhaus, K., Nienhaus, G. U., Wiedenmann, J. and Nar, H. (2005) 'Structural basis for photo-induced protein cleavage and green-to-red conversion of fluorescent protein EosFP', *Proceedings of the National Academy of Sciences*, 102(26), 9156–9159.

Nienhaus, K., Renzi, F., Vallone, B., Wiedenmann, J. and Nienhaus, G. U. (2006a) 'Chromophore-protein interactions in the anthozoan green fluorescent protein asFP499.', *Biophysical journal*, 91(11), 4210–4220.

Nienhaus, G. U., Nienhaus, K., Hölzle, A., Ivanchenko, S., Renzi, F., Oswald, F., Wolff, M., Schmitt, F., Röcker, C. and Vallone, B. (2006b) 'Photoconvertible fluorescent protein EosFP: biophysical properties and cell biology applications', *Photochemistry and photobiology*, 82(2), pp. 351–358.

Ninio, R., Delean, S., Osborne, K. and Sweatman, H. (2003) 'Estimating cover of benthic organisms from underwater video images: variability associated with multiple observers', *Marine Ecology Progress Series*, 265, 107–116.

Van Oppen, M. J. H. and Gates, R. D. (2006) 'Conservation genetics and the resilience of reef-building corals', *Molecular Ecology*, 15(13), 3863–3883.

Orm, M., Cubitt, A. B., Kallio, K., Gross, L. A., Tsien, R. Y. and Remington, S. J. (1996) 'Crystal structure of the *Aequorea victoria* green fluorescent protein', *Science*, 273(5280), 1392–1395.

Orr, J. C., Fabry, V. J., Aumont, O., Bopp, L., Doney, S. C., Feely, R. A., Gnanadesikan, A., Gruber, N., Ishida, A., Joos, F., Key, R. M., Lindsay, K., Maier-Reimer, E., Matear, R., Monfray, P., Mouchet, A., Najjar, R. G., Plattner, G.-K., Rodgers, K. B., Sabine, C. L., Sarmiento, J. L., Schlitzer, R., Slater, R. D., Totterdell, I. J., Weirig, M.-F., Yamanaka, Y. and Yool, A. (2005) 'Anthropogenic ocean acidification over the twenty-first century and its impact on calcifying organisms', *Nature*, 437(7059), 681–686.

Oswald, F., Schmitt, F., Leutenegger, A., Ivanchenko, S., D'Angelo, C., Salih, A., Maslakova, S., Bulina, M., Schirmbeck, R., Nienhaus, G. U., Matz, M. V and Wiedenmann, J. (2007) 'Contributions of host and symbiont pigments to the coloration of reef corals', *FEBS Journal*, 274(4), 1102–1122.

Pandolfi, J. M., Bradbury, R. H., Sala, E., Hughes, T. P., Bjorndal, K. A., Cooke, R. G., McArdle, D., McClenachan, L., Newman, M. J. H., Paredes, G., Warner, R. R. and Jackson, J. B. C. (2003) 'Global trajectories of the long-term of coral reef ecosystems', *Science*, 301(5635), 955–958.

Payri, C. E., Maritorena, S., Bizeau, C. and Rodière, M. (2001) 'Photoacclimation in the tropical coralline alga *Hydrolithon onkodes* (Rhodophyta, Corallinaceae) from a French Polynesian reef', *Journal of Phycology*, 37(2), 223–234.

Pizarro, O., Rigby, P., Johnson-Roberson, M., Williams, S. B. and Colquhoun, J. (2008) 'Towards image-based marine habitat classification', in *OCEANS 2008*. Quebec City, QC, 1–7.

Prasher, D. C., Eckenrode, V. K., Ward, W. W., Prendergast, F. G. and Cormier, M. J. (1992) 'Primary structure of the *Aequorea victoria* green-fluorescent protein', *Gene*, 111(2), 229–233.

Prescott, M., Ling, M., Beddoe, T., Oakley, A. J., Dove, S., Hoegh-Guldberg, O., Devenish, R. J. and Rossjohn, J. (2003) 'The 2.2 Å crystal structure of a pocilloporin pigment reveals a nonplanar chromophore conformation', *Structure*, 11(3), 275–284.

Quick, C., D'Angelo, C. and Wiedenmann, J. (2018) 'Trade-offs associated with photoprotective green fluorescent protein expression as potential drivers of balancing selection for colour polymorphism in reef corals', *Frontiers in Marine Science*, 5, 11.

Rabinowitch, E. (1944) 'Spectra of porphyrins and chlorophyll', *Reviews of Modern Physics*, 16(3–4), 226–235.

Risk, M. J. (1972) 'Fish diversity on a coral reef in the Virgin Islands', *Atoll Research Bulletin*, (193), 1–6.

Risk, M. J., Heikoop, J. M., Edinger, E. N. and Erdmann, M. V (2001) 'The assessment "toolbox": Community-based reef evaluation methods coupled with geochemical techniques to identify sources of stress', *Bulletin of Marine Science*, 69(2), 443–458.

Rodríguez-Román, A., Hernández-Pech, X., Thomé, P. E., Enríquez, S. and Iglesias-Prieto, R. (2006) 'Photosynthesis and light utilization in the Caribbean coral *Montastraea faveolata* recovering from a bleaching event', *Limnology and Oceanography*, 51(6), 2702–2710.

Rosic, N., Kaniewska, P., Chan, C.-K., Ling, E. Y., Edwards, D., Dove, S. and Hoegh-Guldberg, O. (2014) 'Early transcriptional changes in the reef-building coral *Acropora aspera* in response to thermal and nutrient stress', *BMC Genomics*, 15, 1052.

Rosset, S., Wiedenmann, J., Reed, A. J. and D'Angelo, C. (2017) 'Phosphate deficiency promotes coral bleaching and is reflected by the ultrastructure of symbiotic dinoflagellates', *Marine Pollution Bulletin*, 118(1–2), 180–187.

Roth, M. S. and Deheyn, D. D. (2013) 'Effects of cold stress and heat stress on coral fluorescence in reef-building corals', *Scientific Reports*, 3, 1421.

Roth, M. S., Latz, M. I., Goericke, R. and Deheyn, D. D. (2010) 'Green fluorescent protein regulation in the coral *Acropora yongei* during photoacclimation', *The Journal of Experimental Biology*, 213(21), 3644–3655.

Roth, M. S., Padilla-Gamiño, J. L., Pochon, X., Bidigare, R. R., Gates, R. D., Smith, C. M. and Spalding, H. L. (2015) 'Fluorescent proteins in dominant mesophotic reef-building corals', *Marine Ecology Progress Series*, 521, 63–79.

Salih, A., Larkum, A., Cox, G., Kühl, M. and Hoegh-Guldberg, O. (2000) 'Fluorescent pigments in corals are photoprotective', *Nature*, 408(6814), 850–853.

Salih, A., Cox, G. and Larkum, A. W. D. (2003) 'Cellular organisation and spectral diversity of GFP-like proteins in live coral cells studied by single and multi-photon imaging and microspectroscopy', *Proceedings of SPIE*, 4963, 194–200.

Salih, A., Wiedenmann, J., Matz, M., Larkum, A. W. and Cox, G. (2006) 'Photoinduced activation of GFP-like proteins in tissues of reef corals', *Proceedings of SPIE*, 60980B.

Sato, I., Okabe, T. and Sato, Y. (2012) 'Bispectral photometric stereo based on fluorescence', in *Proceedings of the IEEE Computer Society Conference on Computer Vision and Pattern Recognition*. Providence, RI, 270–277.

Schindelin, J., Arganda-Carreras, I., Frise, E., Kaynig, V., Longair, M., Pietzsch, T., Preibisch, S., Rueden, C., Saalfeld, S., Schmid, B., Tinevez, J.-Y., White, D. J., Hartenstein, V., Eliceiri, K., Tomancak, P. and Cardona, A. (2012) 'Fiji: an open-source platform for biological-image analysis', *Nature Methods*. 9(7), 676–682.

Schlichter, D., Fricke, H. W. and Weber, W. (1986) 'Light harvesting by wavelength transformation in a symbiotic coral of the Red Sea twilight zone', *Marine Biology*, 91(3), 403–407.

Schüttrigkeit, T. A., Zachariae, U., von Feilitzsch, T., Wiehler, J., von Hummel, J., Steipe, B. and Michel-Beyerle, M. E. (2001) 'Picosecond time-resolved FRET in the fluorescent protein from *Discosoma* Red (wt-DsRed)', *ChemPhysChem*, 2(5), 325–328.

Seneca, F., Forêt, S., Ball, E., Smith-Keune, C., Miller, D. and Oppen, M. H. (2010) 'Patterns of gene expression in a scleractinian coral undergoing natural bleaching', *Marine Biotechnology*, 12(5), 594–604.

Seppala, J. and Balode, M. (1998) 'The use of spectral fluorescence methods to detect changes in the phytoplankton community', *Hydrobiologia*, 363(207), 207–217.

Shagin, D. A., Barsova, E. V, Yanushevich, Y. G., Fradkov, A. F., Lukyanov, K. A., Labas, Y. A., Semenova, T. N., Ugalde, J. A., Meyers, A., Nunez, J. M., Widder, E. A., Lukyanov, S. A. and Matz, M. V (2004) 'GFP-like proteins as ubiquitous metazoan superfamily: evolution of functional features and structural complexity', *Molecular Biology and Evolution*, 21(5), 841–850.

Shihavuddin, A. S. M., Gracias, N., Garcia, R., Gleason, A. C. R. and Gintert, B. (2013) 'Image-based coral reef classification and thematic mapping', *Remote Sensing*, 5(4), 1809–1841.

Shikina, S., Chiu, Y. L., Chung, Y. J., Chen, C. J., Lee, Y. H. and Chang, C. F. (2016) 'Oocytes express an endogenous red fluorescent protein in a stony coral, *Euphyllia ancora*: A potential involvement in coral oogenesis', *Scientific Reports*, 6(1), 25868.

Shimomura, O. (1979) 'Structure of the chromophore of *Aequorea* green fluorescent protein', *FEBS Letters*, 104(2), 220–222.

Shimomura, O., Johnson, F. H. and Saiga, Y. (1962) 'Extraction, purification and properties of aequorin, a bioluminescent protein from the luminous hydromedusan, *Aequorea*', *Journal of cellular and comparative physiology*, 59(3), 223–239.

Smith-Keune, C. and Dove, S. (2008) 'Gene expression of a green fluorescent protein homolog as a host-specific biomarker of heat stress within a reef-building coral', *Marine Biotechnology*, 10(2), 166–180.

Smith, J. E., Shaw, M., Edwards, R. A., Obura, D., Pantos, O., Sala, E., Sandin, S. A., Smirga, S., Hatay, M. and Rowher, F. (2006) 'Indirect effects of algae on coral: algae-mediated, microbe-induced coral mortality', *Ecology Letters*, 9(7):835–845.

Smith, E. G., D'Angelo, C., Salih, A. and Wiedenmann, J. (2013) 'Screening by coral green fluorescent protein (GFP)-like chromoproteins supports a role in photoprotection of zooxanthellae', *Coral Reefs*, 32(2), 463–474.

Smith, E. G., D'Angelo, C., Sharon, Y., Tchernov, D. and Wiedenmann, J. (2017) 'Acclimatization of symbiotic corals to mesophotic light environments through wavelength transformation by fluorescent protein pigments', *Proceedings of the Royal Society of London B*, 284, 20170320.

Soriano, M., Marcos, S., Saloma, C., Quibilan, M. and Alino, P. (2001) 'Image classification of coral reef components from underwater color video', in *Oceans 2001*. Honolulu, HI, 1008–1013.

Spalding, M., Ravilious, C. and Green, E. P. (2001) *World atlas of coral reefs*. University of California Press.

Spalding, M., Burke, L., Wood, S. A., Ashpole, J., Hutchison, J. and zu Ermgassen, P. (2017) 'Mapping the global value and distribution of coral reef tourism', *Marine Policy*, 82, 104–113.

Stambler, N. and Dubinsky, Z. (2005) 'Corals as light collectors: an integrating sphere approach', *Coral Reefs*, 24(1), 1–9.

Stokes, G. G. (1852) 'On the change of refrangibility of light', *Philosophical Transactions of the Royal Society of London*, 142, 463–562.

Stokes, M. D. and Deane, G. B. (2009) 'Automated processing of coral reef benthic images', *Limnology and Oceanography: Methods*, 7(2), 157–168.

Strack, R. L., Strongin, D. E., Mets, L., Glick, B. S. and Keenan, R. J. (2010) 'Chromophore formation in DsRed occurs by a branched pathway', *Journal of the American Chemical Society*, 132(24), 8496–8505.

Strand, M. P., Coles, B. W., Nevis, A. J. and Regan, R. F. (1997) 'Laser line-scan fluorescence and multispectral imaging of coral reef environments', *Proceedings of SPIE*, 2963, 790–795.

Suggett, D. J., Moore, C. M., Hickman, A. E. and Geider, R. J. (2009) 'Interpretation of fast repetition rate (FRR) fluorescence: Signatures of phytoplankton community structure versus physiological state', *Marine Ecology Progress Series*, 376, 1–19.

Sussman, M., Bourne, D. G. and Willis, B. L. (2006) 'A single cyanobacterial ribotype is associated with both red and black bands on diseased corals from Palau', *Marine Ecology Progress Series*, 69(1):111–118.

Swain, T. D., DuBois, E., Gomes, A., Stoyneva, V. P., Radosevich, A. J., Henss, J., Wagner, M. E., Derbas, J., Grooms, H. W., Velazquez, E. M., Traub, J., Kennedy, B. J., Grigorescu, A. A., Westneat, M. W., Sanborn, K., Levine, S., Schick, M., Parsons, G., Biggs, B. C., Rogers, J. D., Backman, V. and Marcelino, L. A. (2016) 'Skeletal light-scattering accelerates bleaching response in reef-building corals', *BMC Ecology*, 16(1), 10.

Tchernov, D., Gorbunov, M. Y., de Vargas, C., Narayan Yadav, S., Milligan, A. J., Häggblom, M. and Falkowski, P. G. (2004) 'Membrane lipids of symbiotic algae are diagnostic of sensitivity to thermal bleaching in corals', *Proceedings of the National Academy of Sciences*, 101(37), 13531–13535.

Teh, L. S. L., Teh, L. C. L., Sumaila, U. R., Tapia, W. and Maina, J. (2013) 'A global estimate of the number of coral reef fishers', *PLoS ONE*, 8(6), e65397.

Terán, E., Méndez, E. R., Enríquez, S. and Iglesias-Prieto, R. (2010) 'Multiple light scattering and absorption in reef-building corals', *Applied Optics*, 49(27), 5032–5042.

Thévenaz, P., Ruttimann, U. E. and Unser, M. (1998) 'A pyramid approach to subpixel registration based on intensity', *IEEE Transactions on Image Processing*, 7(1), 27–41.

Thornber, J. P. (1975) 'Chlorophyll-proteins: Light-harvesting and reaction center components of plants', *Annual Review of Plant Physiology*, 26(1), 127–158.

Topinka, J. A., Korjeff Bellows, W. and Yentsch, C. S. (1990) 'Characterization of marine macroalgae by fluorescence signatures', *International Journal of Remote Sensing*, 11(12), 2329–2335.

Tracey, J. I., Ladd, H. S. and Hoffmeister, J. E. (1948) 'Reefs of Bikini, Marshall Islands', *Bulletin of the Geological Society of America*, 59(9), 861–878.

Treibitz, T., Murez, Z., Mitchell, B. G. and Kriegman, D. (2012) 'Shape from fluorescence', in Fitzgibbon, A., Lazebnik, S., Perona, P., Sato, Y. and Schmid, C. (eds.), *Lecture Notes in Computer Science*. Berlin, Heidelberg: Springer, 292–306.

Treibitz, T., Neal, B. P., Kline, D. I., Beijbom, O., Roberts, P. L. D., Mitchell, B. G. and Kriegman, D. (2015) 'Wide field-of-view fluorescence imaging of coral reefs', *Scientific Reports*, 5, 7694.

Trench, R. K. (1993) 'Microalgal-invertebrate symbioses – a review', *Endocytobiosis Cell Research*, 9, 135–175.

Valeur, B. and Berberan-Santos, M. N. (2013) *Molecular Fluorescence : principles and applications*. Weinheim: Wiley-VCH.

Vandermeulen, J. H. (1975) 'Studies on reef corals. III. Fine structural changes of calicoblast cells in *Pocillopora damicornis* during settling and calcification', *Marine Biology*, 31(1), 69–77.

Vogt, A., D'Angelo, C., Oswald, F., Denzel, A., Mazel, C. H., Matz, M. V, Ivanchenko, S., Nienhaus, G. U. and Wiedenmann, J. (2008) 'A green fluorescent protein with photoswitchable emission from the deep sea', *PLoS ONE*, 3(11), e3766.

Wacker, S. A., Oswald, F., Wiedenmann, J. and Knöchel, W. (2007) 'A green to red photoconvertible protein as an analyzing tool for early vertebrate development', *Developmental Dynamics*, 236(2), 473–480.

Wall, M. A., Socolich, M. and Ranganathan, R. (2000) 'The structural basis for red fluorescence in the tetrameric GFP homolog DsRed', *Nature Structural Biology*, 7(12), 1133–1138.

Wangpraseurt, D., Larkum, A. W. D., Ralph, P. J. and Kühl, M. (2012) 'Light gradients and optical microniches in coral tissues', *Frontiers in Microbiology*, 3, 316.

Wangpraseurt, D., Larkum, A. W. D., Franklin, J., Szabó, M., Ralph, P. J. and Kühl, M. (2014) 'Lateral light transfer ensures efficient resource distribution in symbiont-bearing corals', *The Journal of Experimental Biology*, 217, 489–98.

Wangpraseurt, D., Jacques, S. L., Petrie, T. and Kühl, M. (2016) 'Monte Carlo modeling of photon propagation reveals highly scattering coral tissue', *Frontiers in Plant Science*, 7, 1404.

Wangpraseurt, D., Holm, J. B., Larkum, A. W. D., Pernice, M., Ralph, P. J., Suggett, D. J. and Kühl, M. (2017) '*In vivo* microscale measurements of light and photosynthesis during coral bleaching: Evidence for the optical feedback loop?', *Frontiers in Microbiology*, 8, 59.

Ward, W. W., Prentice, H. J., Roth, A. F., Cody, C. W. and Reeves, S. C. (1982) 'Spectral perturbations of the *Aequorea* green-fluorescent protein', *Photochemistry and Photobiology*, 35(6), 803–808.

Warner, M. E., Fitt, W. K. and Schmidt, G. W. (1999) 'Damage to photosystem II in symbiotic dinoflagellates: a determinant of coral bleaching.', *Proceedings of the National Academy of Sciences*, 96(14), 8007–8012.

Warner, M. E., Lesser, M. P. and Ralph, P. J. (2010) 'Chlorophyll fluorescence in reef building corals', in Suggett, D., Prášil, O. and Borowitzka, M. (eds.), *Chlorophyll a Fluorescence in Aquatic Sciences: Methods and Applications*. Dordrecht: Springer Netherlands, 209–222.

Weis, V. M. (2008) 'Cellular mechanisms of Cnidarian bleaching: stress causes the collapse of symbiosis', *Journal of Experimental Biology*, 211(19), 3059–3066.

Wiedenmann, J. (1997) 'The application of an orange fluorescent protein and further colored proteins and the corresponding genes from the species group *Anemonia* sp. (*sulcata*) Pennant, (Cnidaria, Anthozoa, Actinaria) in gene technology and molecular biology'. Germany: Deutsches Patent und Markenamt.

Wiedenmann, J. and D'Angelo, C. (2015) 'Revealed: why some corals are more colourful than others', *The Conversation*.

Wiedenmann, J., Röcker, C. and Funke, W. (1999) 'The morphs of *Anemonia* aff. *sulcata* (Cnidaria, Anthozoa) in particular consideration of the ectodermal pigments.', in Pfadenhauer, J. (ed.), *Verhandlungen der Gesellschaft für Ökologie*. Heidelberg: Spektrum Akademischer Verlag, 497–503.

Wiedenmann, J., Elke, C., Spindler, K.-D. and Funke, W. (2000) 'Cracks in the β-can: Fluorescent proteins from *Anemonia sulcata* (Anthozoa, Actinaria)', *Proceedings of the National Academy of Sciences*, 97(26), 14091–14096.

Wiedenmann, J., Schenk, A., Röcker, C., Girod, A., Spindler, K.-D. and Nienhaus, G. U. (2002) 'A far-red fluorescent protein with fast maturation and reduced oligomerization tendency from *Entacmaea quadricolor* (Anthozoa, Actinaria)', *Proceedings of the National Academy of Sciences*, 99(18), 11646–11651.

Wiedenmann, J., Ivanchenko, S., Oswald, F., Schmitt, F., Röcker, C., Salih, A., Spindler, K.-D. and Nienhaus, G. U. (2004a) 'EosFP, a fluorescent marker protein with UV-inducible green-to-red fluorescence conversion', *Proceedings of the National Academy of Sciences*, 101(45), 15905–15910.

Wiedenmann, J., Ivanchenko, S., Oswald, F. and Nienhaus, G. U. (2004b) 'Identification of GFP-like proteins in nonbioluminescent, azooxanthellate Anthozoa opens new perspectives for bioprospecting', *Marine Biotechnology*, 6(3), 270–277.

Wiedenmann, J., Oswald, F. and Nienhaus, G. U. (2009) 'Fluorescent proteins for live cell imaging: Opportunities, limitations, and challenges', *IUBMB Life*, 61(11), 1029–1042.

Wiedenmann, J., D'Angelo, C., Smith, E. G., Hunt, A. N., Legiret, F.-E., Postle, A. D. and Achterberg, E. P. (2013) 'Nutrient enrichment can increase the susceptibility of reef corals to bleaching', *Nature Climate Change*, 3(2), 160–164.

Wijgerde, T., van Melis, A., Silva, C. I. F., Leal, M. C., Vogels, L., Mutter, C. and Osinga, R. (2014) 'Red light represses the photophysiology of the scleractinian coral *Stylophora pistillata*', *PLoS ONE*, 9(3), e92781.

Williams, E. H. and Bunkley-Williams, L. (1990) 'The world-wide coral reef bleaching cycle and related sources of coral mortality', *Atoll Research Bulletin*, 335(1), 67.

Wolf, H., Barisas, B. G., Dietz, K.-J. and Seidel, T. (2013) 'Kaede for detection of protein oligomerization', *Molecular Plant*, 6(5), 1453–1462.

Wooldridge, S. A. and Done, T. J. (2009) 'Improved water quality can ameliorate effects of climate change on corals', *Ecological Applications*, 19(6), 1492–1499.

Yang, F., Moss, L. G. and Phillips, G. N. (1996) 'The molecular structure of green fluorescent protein', *Nature Biotechnology*, 14(10), 1246–1251.

Yentsch, C. S. and Phinney, D. A. (1985) 'Spectral fluorescence: An ataxonomic tool for studying the structure of phytoplankton populations', *Journal of Plankton Research*, 7(5), 617–632.

Zawada, D. G. and Jaffe, J. S. (2003) 'Changes in the fluorescence of the Caribbean coral *Montastraea faveolata* during heat-induced bleaching', *Limnology and oceanography*, 48(1), 412–425.

Zawada, D. G. and Mazel, C. H. (2014) 'Fluorescence-based classification of Caribbean coral reef organisms and substrates', *PLoS ONE*, 9(1), e84570.

Zweifler, A., Akkaynak, D., Mass, T. and Treibitz, T. (2017) '*In situ* analysis of coral recruits using fluorescence imaging', *Frontiers in Marine Science*, 4, 273